https://doi.org/10.5194/egusphere-2026-467
Preprint. Discussion started: 29 January 2026

Plant belowground traits indicate increased plant-mediated methane transport along a peatland permafrost thaw gradient

Tiia Määttä[1], Samantha Bosman[2], Jeffrey Chanton[3], Patrick Crill[4], Suzanne Hodgkins[5], Jalisha Theanutti Kallingal[6], Rachel Wilson[3], Ruth Varner[4,7], and Avni Malhotra[1,8]

1 Department of Geography, Faculty of Science, University of Zürich, Winterthurerstrasse 190, 8057 Zürich, Switzerland
2 Department of Oceanography, Dalhousie University, Halifax, NS, Canada
3 Department of Earth Ocean and Atmospheric Sciences, Florida State University, Tallahassee, Fl 32301, USA
4 Department of Geological Sciences and Bolin Centre for Climate Research, Stockholm University, Sweden
5 Department of Microbiology, The Ohio State University, Columbus, OH, USA
6 Department of Physical Geography and Ecosystem Science, Lund University, Lund, 223 62, Sweden
7 Department of Earth Sciences and Institute for the Study of Earth, Oceans and Space, University of New Hampshire, Durham, NH, USA
8 Biological Sciences Division, Pacific Northwest National Laboratory, 902 Battelle Boulevard, Richland, WA, USA

Correspondence to: Tiia Määttä (tiia.maatta@geo.uzh.ch)

Abstract. Permafrost thaw in subarctic peatlands alters ecosystem methane (CH_4) fluxes. Collapsing permafrost palsas change hydrology, interstitial oxygen availability, and vegetation composition, and each of these factors contribute to net CH_4 flux by influencing CH_4 production, consumption and transport. However, changes in plant-mediated CH_4 fluxes have mostly been estimated using aboveground characteristics, such as biomass and leaf area, leaving belowground parts (roots and rhizomes) understudied despite their direct contact to depth-dependent CH_4 flux processes. Here, we explored the potential of using root and rhizome traits as proxies for plant-mediated CH_4 cycling along a peatland permafrost thaw gradient in subarctic Sweden. We investigated changes in root and rhizome biomass, surface area (SA), diameter, tissue density (TD), and specific root length (SRL) along the permafrost thaw gradient, and how these traits relate to early-, middle-, peak- and season median CH_4 fluxes. We utilized chamber CH_4 flux and pore water CH_4 concentration and isotopic measurements during the productive season. Shrub SRL, diameter and isotopic data suggested increased plant-mediated carbon substrates available for acetoclastic methanogenesis across the thaw gradient. Root TD, proxy for root porosity, decreased with thaw and had negative correlations with CH_4 fluxes throughout the season. Simultaneously, herbaceous rhizome SA-CH_4 flux correlations were positive and pore water CH_4 concentrations were lowest in the fully thawed stage. These results indicated increasing herbaceous plant-mediated transport of acetoclastically-produced CH_4 with thaw. Our study demonstrates that integrating plant belowground traits with environmental and biogeochemical data can help improve CH_4 flux predictions in thawing landscapes and revealed key mechanistic insights regarding the interplay between substrate availability for methanogenesis and gas transport.

https://doi.org/10.5194/egusphere-2026-467
Preprint. Discussion started: 29 January 2026

1 Introduction

Northern peatlands are significant net methane (CH_4) emitters primarily due to the predominance of anoxia throughout the peat depth profile (Gorham, 1991; McGuire et al., 2009; Zhuang et al., 2004). Owing to high organic carbon accumulation, high-latitude peatlands store approximately a third of the global carbon stock (Gorham, 1991), with a substantial fraction preserved in and beneath permafrost (Schuur et al., 2008). In the high latitudes, increasing air temperatures drive permafrost thaw, which can expose the previously frozen organic matter to soil decomposers, including methanogens. Together with altered hydrological and thermal conditions, these processes may increase CH_4 emissions and lead to positive climate feedback (Olefeldt et al., 2013; Schuur et al., 2008). Palsa mires with permafrost plateaus (palsas) are especially vulnerable to increasing temperatures and changes in precipitation. In northern Fennoscandia, permafrost thaw has formed transitional gradients from frozen palsas and peat plateau to permafrost-free bogs and fens (Luoto et al., 2004; Olvmo et al., 2020; Swindles et al., 2015). Almost all arctic permafrost has been estimated to degrade and result in 120 ± 85 Gt of carbon emissions by 2100 (Lawrence et al., 2008; Schaefer et al., 2014). Together with the inevitable disappearance of palsa mires (Luoto et al., 2004; Olvmo et al., 2020), this highlights the urgent need to investigate the network of CH_4 flux controls in thawing palsa mires.

One of the key biotic CH_4 flux drivers in permafrost peatlands are wetland plants and the traits reflecting their adaptive and resource acquisition strategies. In general, plants contribute to CH_4 fluxes by mediating gas transport, providing carbon substrates for methanogens, and modifying the physicochemical properties of the rhizosphere (Chanton & Dacey, 1991; Gerard & Chanton, 1993; Joabsson et al., 1999; Laanbroek, 2010; Määttä & Malhotra, 2024; Noyce et al., 2014). As an adaptive strategy to anoxia, many wetland plant species develop aerenchyma which are air spaces within the plant stem, roots and rhizomes that transport oxygen (O_2) from the atmosphere to the roots and the surrounding soil (Armstrong et al., 1991; Končalová, 1990; Vroom et al., 2022). This plant-mediated gas transport mechanism enhances rhizosphere oxygenation and CH_4 consumption, but also simultaneously increases CH_4 transport from anoxic peat to the atmosphere (Laanbroek, 2010; Noyce et al., 2014; Ström et al., 2005). While peatlands store vast quantities of carbon, much of it is too recalcitrant to be directly utilized by methanogens particularly in deep peat (Christensen et al., 1999; Frolking et al., 2010; Hogg, 1993; Ström et al., 2005). The release of labile carbon substrates such as acetate and other organic acids by plant roots stimulates CH_4 production and emission (Joabsson & Christensen, 2001; Ström et al., 2003).

Studies using plant functional traits to predict CH_4 fluxes have primarily focused on aboveground features, such as plant green area, even though plant belowground biomass can exceed that aboveground especially in (sub)arctic ecosystems (Iversen et al., 2015; Malhotra & Roulet, 2015). Often, the aboveground traits have been used to estimate belowground characteristics, such as root porosity, based on the plant species or functional type (PFT) (Bouchard et al., 2007; Greenup et al., 2000; Iversen et al., 2015; Riutta et al., 2007). However, above- and belowground plant traits and the functional connections between them have not been adequately studied in relation to carbon cycling and the use of aboveground traits

https://doi.org/10.5194/egusphere-2026-467
Preprint. Discussion started: 29 January 2026

as proxies for plant-mediated belowground carbon functioning remains unresolved (Iversen et al., 2015; Määttä & Malhotra, 2024).

Many studies have used above- and/or belowground biomass as CH_4 flux predictors but the direction of the relationship varies strongly between studies, species, and PFTs (e.g., Chanton et al., 1997; Greenup et al., 2000; Joabsson & Christensen, 2001; Koelbener et al., 2010; Ström et al., 2005). While above and belowground biomass may reflect plant productivity, quantification of plant-mediated CH_4 fluxes may be better served by a knowledge of belowground traits more directly related to CH_4 production, consumption and transport. For example, root exudation in some instances can explain CH_4 flux variation better than biomass (Ström et al., 2005; Waldo et al., 2019). Because belowground traits, such as rooting depth, change with a deepening active layer (Blume-Werry et al., 2016; Iversen et al., 2015), assessing these trait variations and their effects on CH_4 fluxes along permafrost thaw gradients is essential.

Wetland CH_4 fluxes can be driven by plant-mediated carbon release and CH_4 and O_2 transport (Knox et al., 2021), which can be reflected in root and rhizome traits. Increases in root and rhizome tissue porosity (i.e., lower tissue density and larger diameter; Freschet et al., 2021a; Purnobasuki & Suzuki, 2004; Visser et al., 2000) can enhance plant-mediated gas transport and, depending on species and environmental conditions (e.g., water table level), can lead to increased CH_4 transport and net flux (Bhullar et al., 2013; Henneberg et al., 2012, 2016; van den Berg et al., 2020) or rhizospheric CH_4 oxidation and decreased net CH_4 flux (Dullo et al., 2017; Fritz et al., 2011; Noyce et al., 2023). CH_4 production can be stimulated by increased labile carbon provision particularly from root exudation (Ström et al., 2003, 2012; Waldo et al., 2019) but also from rhizome and root decomposition (Hackney & De La Cruz, 1980; Scheffer & Aerts, 2000). Specific root length (SRL), the relationship between root length and dry mass, could be a proxy for carbon substrate provision, as high SRL is associated with low tissue density, shorter lifespan, high turnover rates (Bergmann et al., 2020; Eissenstat et al., 2000), and root exudation (Wen et al., 2022). However, studies on the relationships between different root traits, especially SRL and tissue density, in wetlands are rare (Iversen et al., 2015; Pan et al., 2019).

Here, we investigated 1) how root (biomass, surface area, diameter, tissue density, and SRL) and rhizome (biomass, surface area, diameter, and tissue density) traits vary along a peatland permafrost thaw gradient, 2) the correlation of these belowground traits with CH_4 fluxes, and 3) whether root and rhizome traits are strong predictors of CH_4 flux during early, middle and peak CH_4 flux during the productive season. We expected that root biomass, surface area and SRL would be highest at the intact and partly thawed permafrost stages due to lower soil moisture and high species diversity (Hough et al., 2022; Iversen et al., 2015; Keuper et al., 2017). We hypothesized that shrub rhizomes would be most abundant in the intact permafrost stage, whereas most herbaceous rhizome biomass would be found in the more thawed permafrost stage (Hough et al., 2022). We hypothesized that root and rhizome tissue density would decrease from intact to fully thawed permafrost due to increased soil moisture. We also expected that SRL would increase CH_4 flux (Saarnio et al., 2004; Ström & Christensen, 2007; Wen et al., 2022), while tissue density would have negative relationships with CH_4 fluxes throughout the productive

https://doi.org/10.5194/egusphere-2026-467
Preprint. Discussion started: 29 January 2026

season. We expected the trait-CH_4 flux relationships to be stronger for herbaceous plants than for shrubs at the middle and peak CH_4 flux periods, because herbaceous plants increase root biomass throughout the growing season in the tundra (Billings et al., 1978; Kummerow & Russell, 1980; Wang et al., 2016) whereas shrub root biomass can remain relatively constant (Wang et al., 2016).

2 Materials and methods

2.1 Study area

The study area is the Stordalen mire in northern Sweden (68° 22' N 19° 03' E; Fig. 1). The mean annual temperature of the area was -0.5 °C and mean annual precipitation sum was 204 mm for period 1985-2023, based on measurements from a nearby meteorological station (Polarforskningssekretariatet & SMHI, 2025a, 2025b). The area contains a permafrost thaw gradient ranging from palsa with intact permafrost to partly and fully thawed permafrost, each of which includes hydrological conditions and vegetation compositions typical for each thaw stage. The permafrost is largely intact in drained palsa with ericaceous shrubs (e.g., *Empetrum nigrum*, *Andromeda polifolia*, *Rubus chamaemorus*), hummock-forming *Eriophorum vaginatum*, mosses (e.g., *Dicranum* sp.) and lichens (Holmes et al., 2022; Hough et al., 2021; Malhotra & Roulet, 2015). In the partly thawed hydrologically perched stage, the vegetation is dominated by *Sphagnum* spp. and feather mosses as well as sedges, such as *Eriophorum vaginatum* and *Carex rotundata*, typical for ombrotrophic bogs (Holmes et al., 2022; Malhotra & Roulet, 2015). The fully thawed stage includes wet minerotrophic fens that have generally higher pH and their dominant vegetation includes *Eriophorum angustifolium*, *Equisetum fluviatile* and *Carex rostrata* (Holmes et al., 2022; Johansson et al., 2006; Malhotra & Roulet, 2015). In general, moisture increases from intact to fully thawed permafrost stages, due to improved connections to the ground water (2007-2017 mean annual water table level ± standard deviation at partly thawed stage: 9.1 ± 4.6 cm below peat surface, fully thawed stage: 2.1 ± 4.4 cm above peat surface) (Crill et al., 2023; Holmes et al., 2022; Malhotra & Roulet, 2015). The peat depth reaches down to 3 m and is underlain by silt (Johansson et al., 2006).

https://doi.org/10.5194/egusphere-2026-467
Preprint. Discussion started: 29 January 2026

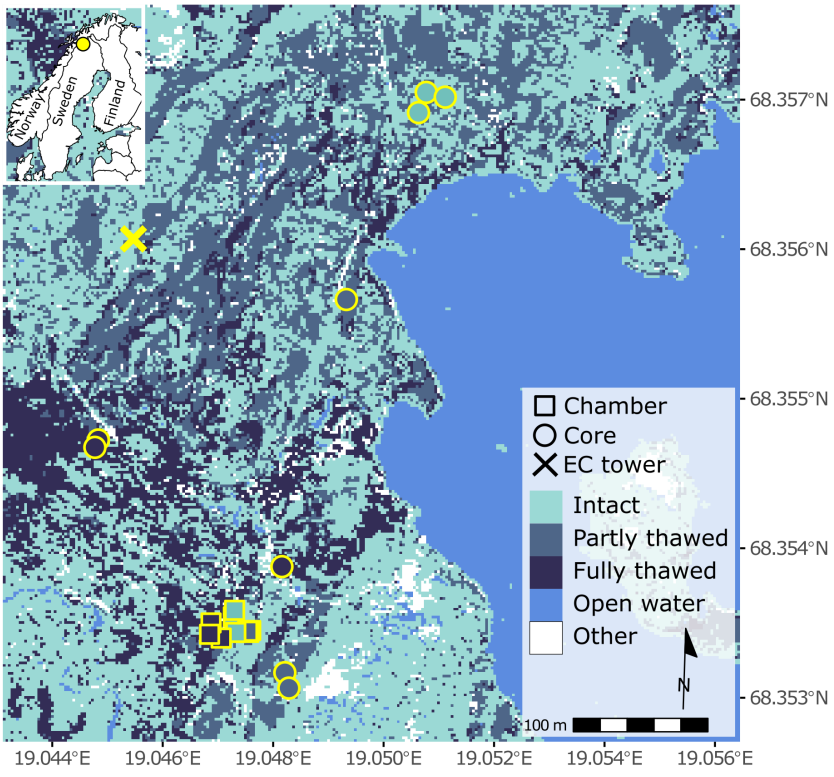

Figure 1: Location of the Stordalen mire and CH_4 flux and peat coring plots within the study area. Based on vegetation classification in 2014, the study area was classified into intact permafrost (tall shrub and hummock, in light blue), partly thawed permafrost (semi-wet and wet, in dark gray), fully thawed permafrost (tall graminoid, in dark blue), open water (bright blue) and other (rock and anthropogenic surfaces, in white) (Palace et al., 2018, 2022; Varner et al., 2022). Rectangles indicate automated chamber CH_4 flux measurement plots, circles indicate peat coring plots, and the cross represents the eddy covariance tower (ICOS: SE-Sto).

2.2 Peat cores

We took peat cores using a push corer (d=12 cm, length=45 cm) to obtain plant material for belowground trait measurements. Despite destructive sampling being restricted, we were able to obtain three cores per thaw stage (n=9 cores in total). In addition, peat coring was not possible next to the CH_4 flux chambers and within the eddy covariance footprint, so we estimated the vegetation composition (vascular plant and moss species) in the chamber collars with vegetation surveys (point intercept method; Text A1, Table C1) and found representative vegetation patches for each chamber outside of the footprint. In the plot selection, emphasis was put on vascular plant species and secondarily on moss species cover. The peat cores were collected on the 21st of July 2023. The tightly packed samples were put into a cooler with ice packs and stored

https://doi.org/10.5194/egusphere-2026-467
Preprint. Discussion started: 29 January 2026

frozen for four days. The samples were transported from Sweden to University of Zurich, Switzerland (11 h), and stored in a freezer in -20 °C until further processing.

2.3 Plant green area measurements

To compare the chamber and peat coring plots, and to provide a non-destructive aboveground plant trait comparison to the belowground traits, we estimated species-specific vascular plant green area (GA; Table 1 and C2). We randomly assigned three (peat coring plots) to five (chamber plots) subquadrats (16.8 x 16.8 cm) of the vegetation survey grid (Text A1) for GA measurements using the function sample in R (R Core Team, 2024). We measured green leaf and stem dimensions (leaf width and length, stem length and diameter) per species within each subquadrat. We measured 10 leaves per species per subquadrat, with the exception of fully thawed stage chamber plots where we measured all leaves and stems. For *E. nigrum*, we estimated the total number of leaves by counting all the leaves of three stems roughly representing the majority of the stems within the subquadrat. We calculated species-specific leaf and stem area (m^2) based on geometric formulae, and GA was estimated based on the average number of green leaves and stems per m^2 multiplied by green leaf and stem area per m^2 (Wilson et al., 2007). Since the leaves of *Rubus chamaemorus* did not fit into a simple geometric formula, we estimated their green area using photos taken above the survey grid and ImageJ.JS v0.5.8 (Ouyang et al., 2019; Schneider et al., 2012) (see mean GA per species in Table C2).

https://doi.org/10.5194/egusphere-2026-467
Preprint. Discussion started: 29 January 2026

Table 1: Vegetation characteristics at CH_4 flux chambers and corresponding peat coring plots at each permafrost thaw stage (intact, partly and fully thawed). "Core" refers to the plots where peat cores were taken for root and rhizome samples. "Species" includes the species encountered in the vegetation survey (Text A1), while vascular plant green area (GA) measurements also included species that were not included in the plant cover measurements. "Total" in GA is the mean vascular plant GA across plots per thaw stage. See vegetation coverage at the plot level in Table C1.

Thaw stage	Species	Mean plant cover (%)		Mean GA (m^2 m^{-2})	
		Chamber	Core	Chamber	Core
Intact	*Eriophorum vaginatum*	66	41		
	Andromeda polifolia	31	27		
	Vaccinium uliginosum	25	24		
	Empetrum nigrum	17	31		
	Rubus chamaemorus	10	15		
	Betula nana	8	20		
	Carex rotundata	4	0		
	Vaccinium vitis-idaea	0	4		
	Ptilium ciliare	48	20		
	Sphagnum balticum	32	0		
	Dicranum sp.	8	27		
	Polytrichum sp.	0	20		
	Herbaceous	45	41	0.01	0.01
	Shrub	83	104	0.04	0.02
				Total: 1.98	Total: 3.61
Partly thawed	*C. rotundata*	48	48		
	E. vaginatum	0	42		
	V. oxycoccos	32	28		
	A. polifolia	28	24		
	E. angustifolium	0	16		
	Drosera rotundifolia	0	4		
	S. capillifolium	96	89		
	P. ciliare	0	16		
	Herbaceous	48	72	0.004	0.007
	Shrub	31	27	0.001	0.002
				Total: 0.05	Total: 0.09
Fully thawed	*E. angustifolium*	92	95		
	Equisetum fluviatile	32	44		
	Comarum palustre	4	12		
	S. riparium	26	96		
	Herbaceous	115	128	0.02	0.03
	Shrub	0	0	0.002	0
				Total: 0.32	Total: 0.8

https://doi.org/10.5194/egusphere-2026-467
Preprint. Discussion started: 29 January 2026

2.4 Environmental variables

In order to compare the abiotic environmental characteristics of the peat coring plots with the chamber plots, we measured soil temperature (°C), pH, water table level (cm) and active layer depth (cm) at the individual plots (Table 2). Peat temperature was measured 2-3 times a day (8 AM, 12 PM, 5 PM) at 10 cm depth over a three-day period (July 23rd-25th 2023) using a soil temperature probe (Testo 720, SN 03679207, Testo, Titisee-Neustadt, Germany). Active layer depth was measured with a metal rod.

We measured pH on July 25th 2023. For the intact and partly thawed plots, we took ca. 8.5 g of peat from 0.5 m distance from the chamber collar at ca. 5 cm depth (intact) or 7-10 cm depth (partly thawed). The pH was measured using a pH meter (826 pH mobile, SN 1826001012160, Metrohm, Herisau, Switzerland) and pH electrode (Polyplast, Ref 238380, SN13208, Hamilton, Reno, USA) by mixing the peat sample with $CaCl_2$ solution (10 ml 0.01 mol/L $CaCl_2$ per sample). At fully thawed plots, pH was measured directly from open water at ca. 5 cm depth. The electrode was always kept in liquid and when not in measurement solution, it was kept in a protective tube with KCl.

Half-hourly peat temperature data was measured with thermocouples installed at each chamber and acquired with CR10x data logger (Campbell Scientific Inc., UT, USA) (Bäckstrand et al., 2008; McCalley et al., 2014). As continuous soil moisture and water table level data were not available for the productive season in 2023, we used 10-year (2007-2017) water table depth (WTD) means and standard deviations per thaw stage from Crill et al., (2023) for a rough background estimate in soil moisture conditions.

Table 2: Peat characteristics at CH_4 flux chambers and peat coring plots per permafrost thaw stage (intact, partly and fully thawed). "Core" refers to the plots where peat cores were taken for root and rhizome samples. See peat characteristics at the plot level in Table C1. ± denotes one standard deviation of the mean. Peat temperature was measured at 10 cm depth. WTD = water table depth (cm from peat surface). Note that WTD for chamber plots is the mean annual WTD across the 2007-2017 period per thaw stage (Crill et al., 2023).

Thaw stage	Mean soil temperature (°C)		Mean pH		WTD (cm)		Mean active layer depth (cm)	
	Chamber	Core	Chamber	Core	Chamber	Core	Chamber	Core
Intact	8.6 ± 1.1	8.4 ±1.6	3.01	3.05	-	-	44.3	54
Partly thawed	9.25 ± 0.6	9.6 ± 2.1	3.3	3.5	-9.1 ± 4.6	-20.9	>85	>85
Fully thawed	9.05 ± 0.8	9.6 ± 2.1	4.9	5.5	2.1 ± 4.4	>0	>85	>85

https://doi.org/10.5194/egusphere-2026-467
Preprint. Discussion started: 29 January 2026

2.5 Root and rhizome trait quantification

We cut the frozen peat cores horizontally into minimum 10 cm increments, and then further into four vertical parts (ca. 25%) using a bandsaw. We randomly chose one of the quarters as a subsample for trait measurements. We thawed the subsamples in a refrigerator over 2-3 days and separated the aboveground vascular plants (see species-specific biomass in Table C3). We picked all living roots (light in color and elastic) and rhizomes (stiff, firm bark) from the subsample using tweezers and jeweler's glasses (2.5x magnification). Due to the very high amount of shrub roots, we took a further subsample (ca. 15 g fresh weight) from which we picked all shrub roots. We cleaned the roots and rhizomes with deionized water and grouped them into herbaceous and shrub PFTs based on a combination of branching patterns, color, and thickness (e.g., shrub roots were generally thinner and had higher branching density than herbaceous roots). The forb *Rubus chamaemorus* was grouped into shrub PFT (e.g., Blume-Werry et al., 2019; Chapin et al., 1988), due to root identification challenges. We did not separate coarse and fine roots but instead focused on the average root system properties. The picked roots were stored in 70% ethanol in a refrigerator (4 °C, max. 4 months).

We put the cleaned roots and rhizomes on a transparent tray filled with deionized water and scanned them with an Epson Perfection V700 Photo scanner (Epson, Japan), and analyzed them for root length, surface area and volume using WinRhizo Pro software (v. 2003b, Regent Instruments Inc., Québec, Canada). We used 1400 dpi for shrub roots with very fine roots (<1 mm), 600 dpi for herbaceous roots, and 100-300 dpi for rhizomes. When rhizome length and diameter were not accurately calculated by WinRhizo, we measured them manually using ImageJ.JS. Then, all roots and herbaceous rhizomes were dried in 70 °C and woody shrub rhizomes in 102 °C for 4 days and weighed at 0.00001 g precision to obtain root and rhizome dry weight. To obtain a proxy of belowground gas transport potential (i.e., porosity), we calculated root and rhizome tissue density (TD, g cm^{-3}) by dividing their dry weight by fresh volume. For shrub rhizomes, the TD represents all the different rhizome tissues (e.g., bark, wood and pith). While this is not a direct measurement of the gas transport ability of a woody rhizome, low tissue density could indicate increased rhizome aeration (e.g., pith cavities) and possibly gas transport (Covey & Megonigal, 2019; Vroom et al., 2022). Specific root length (SRL, m g^{-1}) was calculated by dividing total root length by its dry weight.

Since peat core depths varied between plots, we standardized root total length (m m^{-2}), biomass (g m^{-2}) and surface area (SA, m^2 m^{-2}) to 30 cm depth by taking into account core volume and peat bulk density. We also standardized the traits to 10 cm depth for depth-specific analyses. In addition, shrub root and rhizome biomass, length and SA were scaled from the sub-subsample to the increment level and to 30 cm standardized depth. We calculated root and rhizome volumes by summing diameter-class-specific volumes from WinRhizo (Rose, 2017). All traits were calculated per PFT but also summed (biomass, length, and SA) or biomass-weighted (TD, SRL, diameter) to get an across-PFTs trait estimate. We used the rest of the peat

https://doi.org/10.5194/egusphere-2026-467
Preprint. Discussion started: 29 January 2026

core sample (remaining ca. 75%) to determine peat bulk density and gravimetric water content (GWC). We thawed the sample in a refrigerator over 2-3 days, removed the aboveground vascular plants, took a 5 ± 0.2 g subsample, and took its fresh and dry weight to obtain bulk density and GWC.

2.6 CH_4 flux measurements

CH_4 flux data were obtained from automated chambers (see data in Table C4). Briefly, CH_4 flux was measured at each permafrost thaw stage with automated chambers. The details of the chamber measurement system in general are presented in Bäckstrand et al. (2008). In 2012, the chambers were replaced to similar design as in Bubier et al. (2003). In each thaw stage (intact, partly and fully thawed), three transparent automated gas flux chambers (basal area: 0.2 m^2, height: 15-75 cm) measured CH_4 and CO_2 every three hours with 5-8 min enclosure time and 5 min air flushing before and after closure (Bäckstrand et al. 2008; Holmes et al. 2022). The CH_4 concentrations were measured with a Los Gatos Research Fast Greenhouse Gas Analyzer (Los Gatos Research Inc, Los Gatos, CA, USA) and the timing control and data acquisition was done with Campbell CR10x data logger (Campbell Scientific, Logan, UT, USA), which was located inside a temperature-controlled cabin. The CH_4 flux data were fit using linear regression, and data where $R^2 \leq 0.85$ were filtered out.

We aggregated the higher frequency CH_4 flux data to daily scale by taking the daily CH_4 flux median. Median was chosen to estimate the central tendency of CH_4 fluxes due to skewed and non-normal flux data distributions, and to avoid the disproportionate influence of short-lived high CH_4 flux events that may not be related to belowground plant-mediated CH_4 cycling processes that were the main perspective of this study. Then, we subset the daily-aggregated chamber CH_4 flux data to contain the dates of the productive season in 2023. We defined the productive season as the period between the first and last passing of daily median net ecosystem CO_2 exchange (NEE) past zero, as this can be considered as the plant active season relevant for plant-mediated CH_4 fluxes (Körner et al., 2023). For NEE, we utilized the half-hourly gap-filled NEE (NEE_VUT: estimated across 40 friction velocity threshold realizations for each year according to FLUXNET data processing protocols; quality flags=3 filtered out) from the ICOS Abisko-Stordalen Palsa Bog (SE-Sto) eddy covariance data processed with FLUXNET standards (Lundin et al., 2025; Pastorello et al., 2020). The resulting productive season used for CH_4 flux data subsetting was 2023-05-19 to 2023-08-30 (Fig. B1). As a background proxy for potential plant carbon substrate provision, we also utilized the half-hourly gap-filled gross primary production (GPP; GPP_NT_VUT: nighttime partitioning with variable friction velocity thresholds implemented as an ensemble of 40 friction velocity thresholds by the FLUXNET team; see Lundin et al., 2025 and Pastorello et al., 2020 for details) data from Lundin et al. (2025). However, it is important to note that the EC tower footprint covers only intact and partly thawed stages and does not estimate the NEE and GPP for the fully thawed stage (Łakomiec et al., 2021).

To explore the variation in the trait-CH_4 flux relationships during the productive season, we calculated CH_4 flux period values (early, middle and peak CH_4 flux) by fitting Gaussian generalized additive models (GAM) with identity link function

https://doi.org/10.5194/egusphere-2026-467
Preprint. Discussion started: 29 January 2026

for CH_4 flux data per chamber with function gam from package mgcv (Wood, 2011, 2017). In the models, CH_4 flux (response variable) was transformed to approximate normality using inverse hyperbolic sine and date was included as an explanatory variable in a thin plate regression spline. Following an approach similar to TIMESAT (Eklundh & Jönsson, 2015; Jönsson & Eklundh, 2002) and Delwiche et al. (2021), CH_4 flux period values were calculated as follows: 1. peak CH_4 flux: the highest predicted CH_4 flux value during the productive season, 2. early CH_4 flux: the point where the predicted daily CH_4 flux reached 10% of the peak CH_4 flux for the first time, and 3. middle CH_4 flux: the point where the predicted daily CH_4 flux reached 50% of the peak CH_4 flux for the first time. We also calculated the whole season median to represent the whole productive season CH_4 flux estimate per chamber. Since one chamber at intact permafrost thaw stage had GAM $R^2<0.1$, we used a moving 7-day median to estimate the early, middle and peak CH_4 season values. See details of GAM fit in Table C5.

2.7 Porewater CH_4 concentration and isotopic measurements

Data of porewater CH_4 and CO_2 concentrations, $\delta^{13}CH_4$ and $\delta^{13}CO_2$ were obtained from Wilson et al. (2026). The porewater samples were collected from the field near the automated flux chambers using stainless steel sippers on 25th and 26th of July 2023. The bottom of the sippers is perforated, and a syringe is attached to the top of the sipper via a stopcock. The sipper was inserted in the peat to the desired depth (0-4, 10-14, 20-24, 30-34, 40-44, 50-54, 60-64, 70-74, and 80-84 cm below peat surface) and the syringe was used to carefully draw up 30 mL of porewater. The porewater was then injected into pre-evacuated sealed glass serum vials. Phosphoric acid (1 mL, 10%) was added to each vial to preserve the samples and ensure that all dissolved inorganic carbon was in the form of dissolved CO_2 in equilibrium with gaseous CO_2. Porewater CO_2 and CH_4 concentrations and isotopes were analyzed simultaneously via headspace analysis, corrected for solubility using Henry's Law, on a Finnigan Mat Delta V Isotope Ratio Mass Spectrometer coupled to a gas chromatograph (Merritt et al., 1995). The analytical uncertainty based on repeated measurements of a standard was <0.15‰ for $\delta^{13}CO_2$ and $\delta^{13}CH_4$ and <5% for CO_2 and CH_4 concentrations. To obtain a robust estimate of the isotopic fractionation between CO_2 and CH_4, we calculated the isotope fractionation factor (α_C) (e.g., Hodgkins et al., 2014; McCalley et al., 2014) with the following formula:

$$\alpha_C = \frac{\delta^{13}CO_2+1000}{\delta^{13}CH_4+1000} \quad (1)$$

2.8 Statistical analysis

To confirm the similarity of the peat core (n=9) and CH_4 flux plots (n=9), we used principal component analyses (function PCA from package FactoMineR; Lê et al., 2008), PERMANOVA (function adonis2 from package vegan; Oksanen et al., 2025), and Euclidean distances between plots within thaw stages, using normalized plot herbaceous and shrub plant cover and GA, mean soil temperature and pH (see Fig. B2).

https://doi.org/10.5194/egusphere-2026-467
Preprint. Discussion started: 29 January 2026

For assessing general differences in daily median CH_4 flux between thaw stages across the productive season, we built linear mixed effects models where CH_4 flux was the response variable and thaw stage (factor) was the explanatory variable, and chamber (n=3 per thaw stage) was the random effect. To account for the normality of residuals and chamber-dependent temporal autocorrelation, we applied inverse hyperbolic sine transformation to CH_4 fluxes, and modeled temporal autocorrelation with autoregressive autocorrelation structure of order 1 (corAR1). We built three different models, where each had either intact, partly or fully thawed permafrost stage as the reference level, and fit the model with restricted maximum likelihood and obtained p-values (α=0.05) from Wald t-test. Linear mixed effects models were built with function lme from package nlme (Pinheiro & Bates, 2000; Pinheiro J, Bates D, R Core Team, 2023).

Due to the small sample size (n=3 per thaw stage), we were unable to test for statistical differences in belowground traits between thaw stages and sampling depths (traits, porewater CH_4 concentration and isotopic data) and relied on descriptive methods. However, to explore the general direction and strength of the relationships between root and rhizome traits and CH_4 fluxes (early, middle, peak, and season median) across the thaw stages, we used linear regressions with centered and scaled trait and CH_4 flux values. Only models which did not violate assumptions of homoscedasticity, linearity and normality of residuals were included in the analyses. In cases with little trait variation within each thaw stage, pseudoreplication was considered too severe for reliable model estimates, and these model results were not reported. We focused on model R^2, slopes, and model p-values. In cases where linear regressions were unreliable or violated the model assumptions, we explored the relationship strength with Kendall τ correlation coefficients. We acknowledge that the model and correlation estimates can be unstable with small sample size and thus use them as descriptive exploratory tools for estimating the changes in the general directions of the trait-CH_4 flux relationships across thaw stages during the productive season. All data processing and statistical analyses were conducted in R v4.5.1 (R Core Team, 2025).

3 Results

3.1 Shift from shrub to herbaceous roots and rhizomes with decreasing tissue density along permafrost thaw

Belowground traits varied between thaw stages, and the biomass-weighted traits followed shifts from shrub- to herbaceous-dominated plant communities (Fig. 2, Table C1). Notably, herbaceous root and rhizome tissue density (TD) were 1.5x and 2.4x lower in fully thawed than in intact permafrost, respectively (mean ± standard deviation root 0.004 ± 0.0008 g cm^{-3} to 0.003 ± 0.0002 g cm^{-3}; rhizome 0.2 g cm^{-3} ± 0 to 0.08 ± 0.01 g cm^{-3}), and these decreases were reflected in the biomass-weighted values (root: 1.5x, rhizome: 7.4x lower). While specific root length (SRL) was highest at partly thawed stage (mean shrub 193.6 ± 32 m g^{-1}, 1.4x higher than at intact; mean herbaceous 71.6 ± 35 m g^{-1}, 2.3x and 1.2x higher than at intact and fully thawed, respectively), the biomass-weighted means showed a 2.2-fold decrease from intact to fully thawed stage. Summed root biomass and surface area (SA) were 22.2x and 17x lower, respectively, at the fully thawed than intact stage, but herbaceous root biomass (mean: 238.3 ± 172 g m^{-2}) and SA (mean: 19.9 ± 13 m^2 m^{-2}) were highest at partly

https://doi.org/10.5194/egusphere-2026-467
Preprint. Discussion started: 29 January 2026

thawed stage. While shrub rhizome biomass and SA decreased from intact to partly thawed stage, herbaceous rhizomes showed an opposite trend (e.g., mean SA 0.13 ± 0 m^2 m^{-2} to 3.41 ± 0.08 m^2 m^{-2}, 26-fold increase).

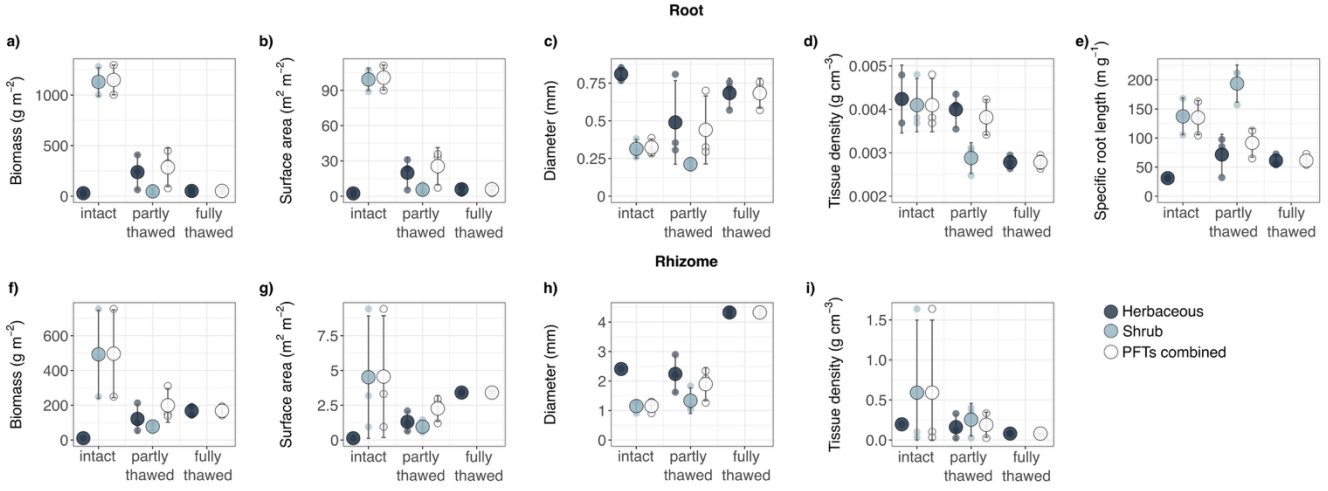

Figure 2: Belowground traits varied between thaw stages. Root traits (a-e) are shown in the top row and rhizome traits (f-i) in the bottom row. Large points represent group means, small points plot-scale measurements, and error bars ± 1 standard deviation of the mean. The colors represent plant functional types (PFT; dark grey: herbaceous, light grey: shrub, white: PFTs combined). Trait values for combined PFTs were summed herbaceous and shrub values (a, b, f, and g) or biomass-weighted means between herbaceous and shrub PFTs (c-e, h and i).

Most of the root biomass was found in the top 10 cm for shrub (CV and mean intact: 69%, 766.0 ± 155 g m^{-2}; partly thawed: 67%, 65.1 ± 28 g m^{-2}) and herbaceous PFTs (CV and mean intact: 56%, 17.5 ± 9 g m^{-2}, partly thawed: 45%, 86.4 ± 89 g m^{-2}, fully thawed: 73%, 27.7 ± 20 g m^{-2}) (Fig. B3). Shrub roots reached the maximum total length of 167.3 km m^{-2} at top 10 cm at the intact stage (Fig. B4). SRL and root TD varied less with depth across thaw stages (max CV SRL: 51%, TD: 31%; partly thawed herbaceous). All herbaceous rhizomes were present in the top 10 cm (mean biomass intact: 11.5 ± 0 g m^{-2}, partly thawed: 101.9 ± 109 g m^{-2}, fully thawed: 107.8 ± 12 g m^{-2}, Fig. B5). Most of the shrub rhizomes were located in the top 10 cm (CV and mean biomass intact: 78.5%, 392.4 ± 227 g m^{-2}; partly thawed: 66.7%, 93.9 ± 15 g m^{-2}), but they were also found in 10-20 cm depth (mean intact: 109.4 ± 154 g m^{-2}, partly thawed: 28.9 ± 0 g m^{-2}).

3.2 Root tissue density, specific root length and diameter correlated best with CH_4 fluxes

The relationships between root traits and CH_4 fluxes (CH_4 flux difference between intact, partly and fully thawed $p<0.05$, fully and partly thawed $p>0.05$, Text A2) differed between PFTs but with little temporal variation. Increasing root TD was associated with decreasing CH_4 flux for herbaceous (min β=-0.86 R^2=0.73 at peak CH_4, max β=-0.91 R^2=0.82 at CH_4 season median) and shrub PFTs (min β=-0.56 R^2=0.31 at CH_4 season median, max β=-0.75 R^2=0.56 at middle CH_4) (Fig. 3, B6). Shrub root diameter had negative (min β=-0.74 R^2=0.55 at CH_4 season median, max β=-0.87 R^2=0.76 at middle CH_4) and

https://doi.org/10.5194/egusphere-2026-467
Preprint. Discussion started: 29 January 2026

SRL positive (min β=0.67 R^2=0.45 at early CH_4, max β=-0.74 R^2=0.54 at middle and peak CH_4) associations with CH_4 fluxes. In general, the direction and strength of the relationships between root traits and CH_4 fluxes did not vary strongly across CH_4 flux season values (Fig. 5, B5).

PFTs combined, all root traits except diameter showed negative trends, where the strongest relationships were for root TD (min β=-0.82 R^2=0.67-0.68 at early, peak and season median CH_4, max β=-0.85 R^2=0.73 at middle CH_4) (Fig. 3, B7). In addition, summed root biomass and SA showed relatively strong negative relationships, with biomass showing slightly stronger negative relationships than SA (biomass: min β=0.68 R^2=0.46 at CH_4 season median, max β=-0.81 R^2=0.66 at early CH_4; SA: min β=-0.63 R^2=0.4 at CH_4 season median, max β=-0.8 R^2=0.64 at early CH_4) (Fig. B7).

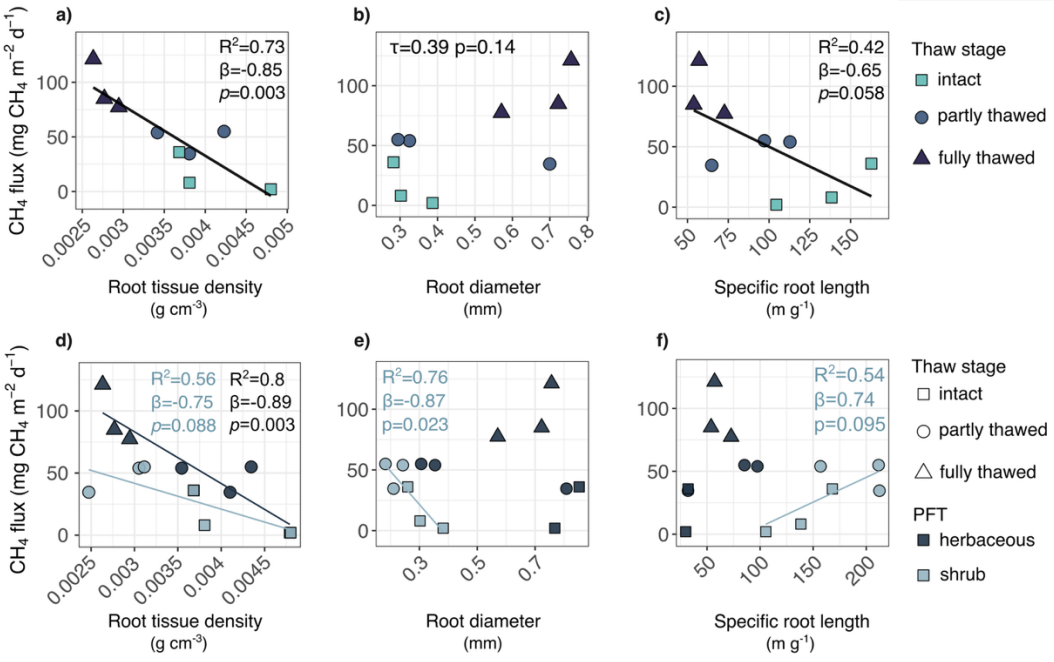

Figure 3: Root tissue density, diameter, and specific length showed strongest relationships with mid-season CH_4 fluxes. a-c) Relationships between root biomass-weighted means and CH_4 fluxes at middle flux period (light blue rectangle: intact, light grey circle: partly thawed, dark purple triangle: fully thawed stage). d-f) PFT-specific (dark gray: herbaceous, light gray: shrub) trait-CH_4 flux relationships at mid-season CH_4 flux. In all plots (a-f), lines represent linear regression for visualization, while R^2 and effect size/slope (β) are based on linear regressions with centered and scaled trait and CH_4 flux values (lines, R^2 and β are only shown when R^2>0.2, model p<0.1, and the linear regression model assumptions were met). Kendall's τ is shown for relationships where linear regression model assumptions were not met, τ≥0.4 and p<0.1. The shown trait-CH_4 flux relationships were selected based on R^2 or τ. See relationships between all CH_4 flux season values and all root traits in Fig. B6 and B7.

https://doi.org/10.5194/egusphere-2026-467
Preprint. Discussion started: 29 January 2026

Herbaceous and shrub rhizome traits showed contrasting relationships with CH_4 fluxes (Fig. 4, B8). Herbaceous rhizome biomass and SA showed positive relationships with CH_4 fluxes, with stronger trends for SA (SA: min β=0.9 R^2=0.8 at peak CH_4, max β=0.97 R^2=0.94-0.95 at early CH_4 and season median; biomass: min β=0.52 R^2=0.52 at early CH_4 and season median, max β=0.75 R^2=0.57 at middle and peak CH_4). Increases in herbaceous rhizome diameter were also associated with slightly higher CH_4 fluxes (min τ=0.33 p=0.348 at peak CH_4, max τ=0.6 p=0.091 at CH_4 season median). In contrast, shrubs had negative trends between rhizome biomass and CH_4 fluxes (min τ=-0.07 p=0.851 at CH_4 season median, max τ=-0.6 p=0.091 at early CH_4). Higher summed rhizome biomass was associated with lower CH_4 fluxes (min β=-0.63 R^2=0.4 at early CH_4, max β=-0.8 R^2=0.63 at CH_4 peak), while the relationship between rhizome diameter and CH_4 flux was positive (min τ=0.43 p=0.138 at CH_4 peak and season median, max τ=0.64 p=0.026 at early CH_4) (Fig. B9).

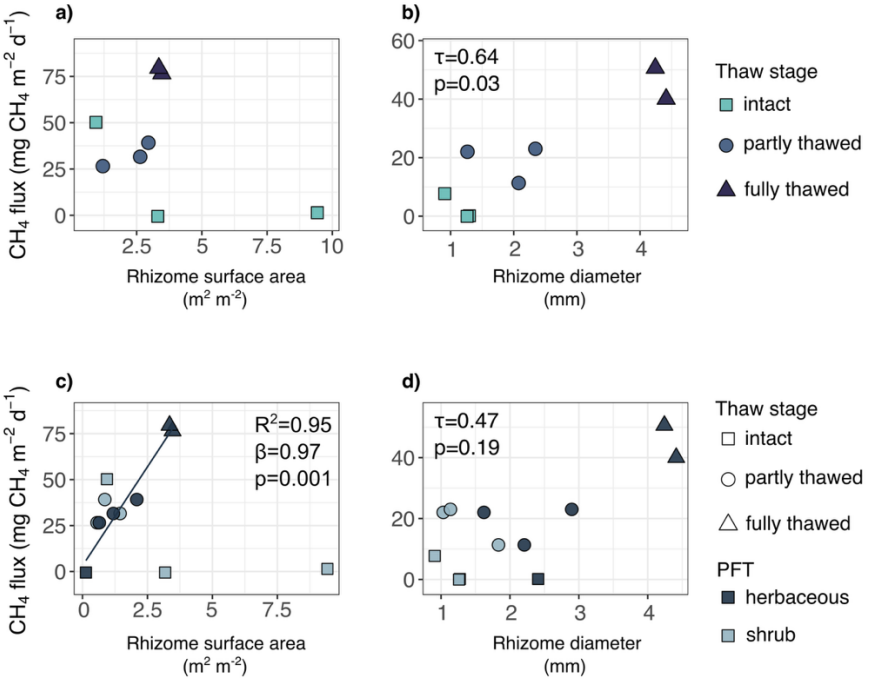

Figure 4: Relationships between rhizome traits and CH_4 fluxes were strongest for surface area and diameter. a-b) Relationships between summed rhizome surface area and CH_4 season median (a) and biomass-weighted rhizome diameter means and early-season CH_4 (b) (light blue rectangles: intact, dark blue circles: partly thawed, and dark purple triangles: fully thawed stage). c-d) Relationships between rhizome surface area and CH_4 season median (c) and rhizome diameter and early-season CH_4 (b) per PFT (dark gray: herbaceous, light gray: shrub). Lines represent linear regressions for visualization, while R^2 and effect size (β) are based on linear regressions with centered and scaled trait and CH_4 flux values (lines, R^2 and β are only shown when R^2>0.2, model p<0.1, and the linear regression model assumptions were met). Kendall's τ is shown for relationships where linear regression model assumptions were not met, τ>0.4 and p<0.1. The shown trait-CH_4 flux relationships were selected based on R^2 or τ. See relationships between all CH_4 flux values and all rhizome traits in Fig. B8 and B9.

https://doi.org/10.5194/egusphere-2026-467
Preprint. Discussion started: 29 January 2026

In comparison with belowground trait relationships, CH_4 fluxes were weakly and positively correlated with plant green area (GA) and soil temperature (Fig. B10). GA, which did not show clear trends with permafrost thaw (Fig. B11), showed no clear relationships with CH_4 fluxes (max τ=-0.62 p=0.05 for shrub at CH_4 season median). Soil temperature did not show clear relationships with CH_4 fluxes (except τ=0.44 p=0.095 at peak CH_4).

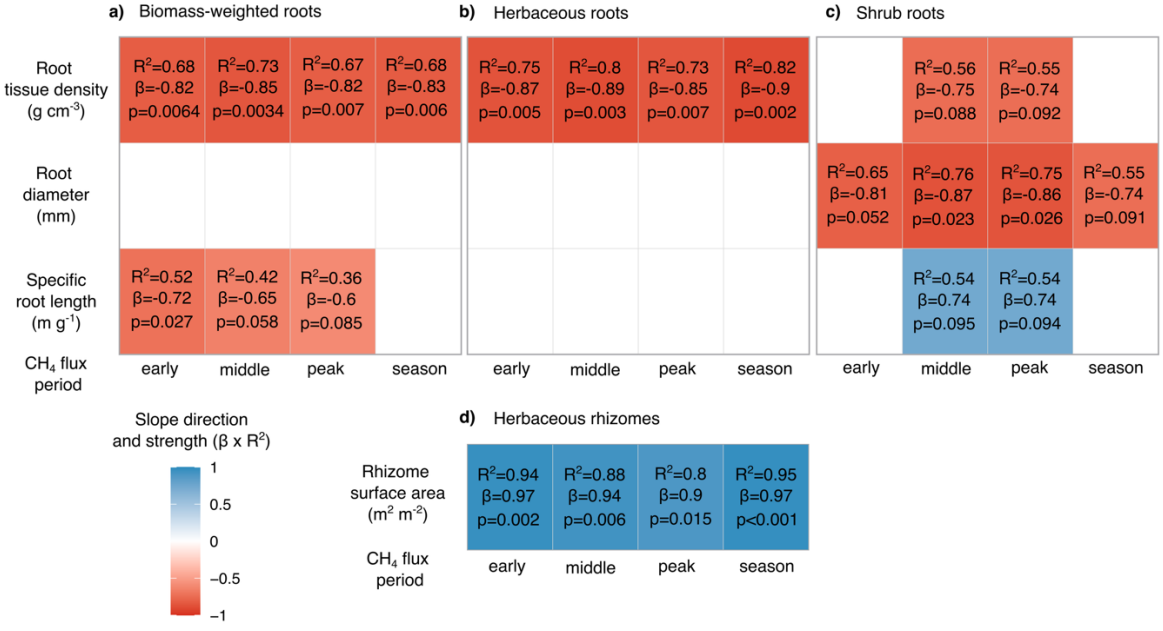

Figure 5: The strength of the relationship between belowground traits and CH_4 fluxes varied only slightly during the productive season. The strength and direction of the relationship is described as the combination of linear regression slope (β; red = negative, blue = positive) and model R^2 (darker colors indicate higher R^2 and vice versa). Model p-values are shown for reference. White cells without labels indicate models where p>0.1, R^2<0.2 or model assumptions were violated. a-c) Strength and direction of the linear regression between CH_4 fluxes and biomass-weighted (a), herbaceous (b) and shrub root traits (c) and herbaceous rhizome surface area (d). Note that only CH_4 fluxes were sampled temporally but root and rhizome traits were sampled once during the productive season. See relationships between all root and rhizome traits and CH_4 flux values in Fig. B6-B9.

4 Discussion

Permafrost thaw in subarctic peatlands can lead to substantial alterations in peatland hydrology, vegetation composition and carbon cycling, and higher CH_4 emissions with higher water table level and more anoxic conditions belowground (Johnston et al., 2014; Knoblauch et al., 2018; Turetsky et al., 2014; Varner et al., 2022). These trends were visible in the Stordalen Mire where CH_4 fluxes increased significantly from intact to fully thawed permafrost stage with maximum CH_4 fluxes in August (Text A2 and Fig. B12), and porewater CH_4 concentrations increased with depth and CH_4 production slightly shifted

https://doi.org/10.5194/egusphere-2026-467
Preprint. Discussion started: 29 January 2026

from hydrogenotrophic to acetoclastic methanogenesis (Fig. B13), as has been observed previously at Stordalen (Hodgkins et al., 2014; Holmes et al., 2022; McCalley et al., 2014; Perryman et al., 2020; Varner et al., 2022).

The increased CH_4 fluxes with permafrost thaw in Stordalen are driven by a complex network consisting of drivers such as higher water table level and increased anoxia (Holmes et al., 2022; Malhotra & Roulet, 2015), increased labile carbon availability (Hodgkins et al., 2014; Holmes et al., 2022; Hough et al., 2022), shifts in microbial communities from hydrogenotrophic to acetoclastic methanogens (McCalley et al., 2014), and increasing dominance and productivity of graminoid vegetation (Christensen et al., 2004; Johansson et al., 2006; Malhotra & Roulet, 2015; Öquist & Svensson, 2002; Varner et al., 2022). For the first time in Stordalen and, to our knowledge, in other thawing permafrost peatlands, we studied the permafrost thaw-driven CH_4 flux variation with a plant trait-based approach with a focus on belowground traits. In general, root and rhizome traits reflected plant community transitions and were consistent with an increase in plant-mediated transport of acetoclastically-produced CH_4.

4.1 Root and rhizome traits reflect plant community shifts along permafrost thaw gradient

The vegetation composition in Stordalen follows the changing hydrology and soil nutrient availability. The vegetation shifts from shrub-dominated (intact stage; e.g., *R. chamaemorus*, *B. nana*, and *E. nigrum*) palsas to increasingly more graminoid- and *Sphagnum*-dominated semi-wet bogs (partly thawed; e.g., *V. oxycoccos*, *C. rotundata*, and *S. capillifolium*) and wet fens (fully thawed; *E. angustifolium*, *E. fluviatile*, and *S. riparium*; Table C1 and C2) (Hough et al., 2022; Johansson et al., 2006; Malhotra & Roulet, 2015; Malmer et al., 2005; Varner et al., 2022). Following these vegetation transitions, plant traits reflect plant adaptation to the changing environmental conditions (Díaz et al., 2016; Dong et al., 2020; Moor et al., 2017; Pan et al., 2019; Reich et al., 1997). While studying plant trait variation and its influence on ecosystem functioning often requires species-specificity to capture changes in diversity (Freschet et al., 2017; Kichenin et al., 2013; Vahsen et al., 2023; Violle et al., 2014) and separation into fine and coarse root fractions (Freschet et al., 2021b; McCormack et al., 2015), CH_4 flux models often utilize PFTs which have been found to adequately represent the collective trait effects on CH_4 fluxes in peatlands (Gray et al., 2013; Laine et al., 2022). Thus, we here focused on root and rhizome traits at the PFT (herbaceous and shrub) level. This approach provides empirical constraints on plant-mediated carbon substrate provision and CH_4 transport that can inform parameterization and sensitivity analyses in process-based wetland CH_4 models, such as LPJ-GUESS (Smith et al., 2001, 2014), and HIMMELI (Raivonen et al., 2017).

Following vegetation community shifts, most belowground shrub biomass was found in the intact stage while herbaceous biomass increased from intact to fully thawed stage. The shrub root biomass values were lower than previous estimates for *R. chamaemorus*, *E. nigrum* and *A. polifolia* (total >2000 g m^{-2}) in Stordalen (Wallén, 1986), but are much higher than recent belowground biomass estimates (~280 g m^{-2}; Hough et al., 2022). In addition, Hough et al. (2022) reported higher total root biomass at the fully thawed (~218 g m^{-2}) than partly thawed stage (~146 g m^{-2}), whereas this study showed the opposite (Fig.

https://doi.org/10.5194/egusphere-2026-467
Preprint. Discussion started: 29 January 2026

2). These differences could arise from different root biomass standardization and sampling methods, a problem highlighted in root ecology (Freschet et al., 2021a): Wallén (1986) calculated fine root biomass based on ^{14}C activity which can lead to overestimations (Wallén, 1986), while Hough et al. (2022) sampled a larger area (625 cm^2) than in our study (~79 cm^2), leading to differences particularly at the fully thawed stage, where graminoids root more vertically than laterally. Nonetheless, root biomass decreased by depth, as is common particularly for shrubs (Iversen et al., 2015; Wallén, 1986). As we observed *R. chamaemorus* roots up to 30 cm depth, similar to Wallén (1986) and Keuper et al. (2017) in Stordalen and by Metsävainio (1931) in Finnish peatlands, and as *E. angustifolium* and *E. fluviatile* roots have been found at 40 cm depth (Iversen et al., 2015; Metsävainio, 1931; Shaver & Billings, 1975), the maximum rooting may occur deeper than our sampling depth (ca. 30 cm).

Variation in tissue density (TD) and specific root length (SRL) (Fig. 2) with thaw suggest changes in plant gas transport and resource acquisition. Increasing soil moisture (via higher water table level; Table 2) and subsequent aerenchyma formation (e.g., Jackson & Armstrong, 1999) may have decreased TD. The increase in herbaceous rhizome SA may reflect greater aerenchyma proportion, confirming rhizome SA as a proxy for plant gas transport capacity. SRL was highest and root diameter lowest at the partly thawed stage, possibly reflecting increased resource acquisition particularly for shrubs with high SRL and low root TD (Bergmann et al., 2020). As the peat C/N ratio is highest in the partly thawed stage (Hodgkins et al., 2014), the high SRL may reflect low N availability, shifts in species and species-specific resource acquisition (Hewitt et al., 2019; Keuper et al., 2017). However, as fine root SRL is more meaningful for resource acquisition (Bergmann et al., 2020; McCormack et al., 2015), our results based on the whole root system provide only a rough estimate. Nonetheless, 99% of total shrub root length was <2 mm in diameter (vs. 31%, 75%, and 63% in intact to fully thawed stages, respectively, for herbaceous), and thus within the traditional fine root definition (McCormack et al., 2015).

4.2 Belowground traits reflect increasing plant-mediated CH_4 transport

While the main CH_4 flux drivers in Stordalen are likely related to soil moisture and water table height (Holmes et al., 2022; Öquist & Svensson, 2002), the plant belowground traits indicated 1) maintained carbon substrate provision and 2) increasing plant-mediated CH_4 transport across the permafrost thaw gradient. In Stordalen, permafrost thaw has led to increasing plant-derived labile carbon availability and acetoclastic methanogenesis (Hodgkins et al., 2014; Holmes et al., 2022; McCalley et al., 2014; Ström & Christensen, 2007), but plant-mediated CH_4 transport has so far been mostly assumed based on literature and plant aboveground characteristics and activity, such as number of shoots and gross photosynthetic rates (Öquist & Svensson, 2002).

Shrub roots suggested increasing carbon substrate provision. The higher CH_4 fluxes with increasing shrub SRL (and smaller diameter; Bergmann et al., 2020) may be related to increased root exudation (Guyonnet et al., 2018; Wen et al., 2022). The negative root TD-CH_4 flux relationships support this, as higher root TD may be associated with lower root exudation (Wen

https://doi.org/10.5194/egusphere-2026-467
Preprint. Discussion started: 29 January 2026

et al., 2022). In contrast, herbaceous SRL was weakly associated with CH_4 fluxes, possibly due to decoupling of root exudation and SRL in some Cyperaceae species in nutrient-limited environments (Wen et al., 2022), and the SRL also including coarse roots (Picon-Cochard et al., 2012). However, based on the ^{13}C-depleted $\delta^{13}CH_4$ and high α_C, hydrogenotrophic methanogenesis, driven by methanogens such as *Methanobacterium* and Candidatus *Methanoflorens stordalenmirensis*, may have dominated in the topmost peat, and most of the dissolved, less bioavailable organic carbon possibly originated from *Sphagnum* in the partly thawed stage (Hodgkins et al., 2014; McCalley et al., 2014; Mondav et al., 2014; Wilson et al., 2022). Nonetheless, the lower α_C, more enriched $\delta^{13}CH_4$, and higher CH_4 concentrations below the root sampling depth (30-44 cm) indicated acetoclastic methanogenesis (Fig. B13) (e.g., by *Methanosarcina*; McCalley et al., 2014), possibly fueled by root exudates (Saarnio et al., 2004; Ström et al., 2003; Ström & Christensen, 2007). Indeed, based on photosynthetic rates, the partly thawed stage has been estimated to have more labile carbon for methanogenesis (Öquist & Svensson, 2002), and *E. angustifolium* and *E. vaginatum* have high potential root exudation rates in Stordalen (Ström & Christensen, 2007). Thus, roots may have exuded labile carbon, but with shrubs having a lesser effect on the net CH_4 flux.

Herbaceous plant coverage increased with thaw, which was reflected in traits indicating plant-mediated CH_4 transport (Fig. 2, Table C1). Higher herbaceous rhizome SA was positively associated with greater CH_4 fluxes, which, together with the positive diameter-CH_4 flux trends, could indicate enhanced CH_4 transport via larger and more porous rhizomes (Määttä & Malhotra, 2024). Rhizome-mediated CH_4 transport could be particularly relevant for plants with pressurized gas transport, such as *Equisetum* spp., where pressure gradients between the atmosphere, leaves, and rhizomes can drive CH_4 emission via old leaves and broken stems (Vroom et al., 2022). As shrub rhizomes were not associated with CH_4 fluxes (Fig. 4, B8), they may not drive plant–mediated CH_4 cycling in Stordalen, though standardized measurements of, e.g., rhizome length and biomass are needed to confirm this (e.g., Freschet et al., 2021a).

Plant-mediated CH_4 transport may have been pronounced in the fully thawed stage with high herbaceous plant coverage and low porewater CH_4 concentrations (Table C1 and Fig. B13), indicating plant CH_4 uptake. As low root and rhizome TD indicates higher porosity (Ye & Ryser, 2022), the negative relationships between root TD and CH_4 flux suggest increased plant-mediated CH_4 transport. The isotopic evidence (heavier $\delta^{13}CH_4$ and lower α_C) may further suggest plant-mediated transport of acetoclastically-produced CH_4 at the fully thawed stage (Chanton, 2005). This supports previous findings of higher herbaceous shoot numbers increasing CH_4 flux in the fully thawed stage (Öquist & Svensson, 2002). In Stordalen, most of the plant-mediated CH_4 transport likely occurs via diffusion, typical for *Carex* spp., *E. angustifolium*, and *E. vaginatum* (e.g., Ge et al., 2025; Noyce et al., 2014; Bhullar et al., 2013). CH_4 diffusion may be more efficient through *E. angustifolium* with low root branching in the fully thawed than at partly thawed stage with more densely rooted *Carex* species (Schimel 1995; Shaver & Billings, 1975; Table C1). However, pressurized CH_4 transport via *Equisetum fluviatile* (in fully thawed stage) could be negligible and requires further investigation as we did not separate the belowground material into species (Hyvönen et al., 1998; Kankaala & Bergström, 2004). As graminoid (e.g., *E. angustifolium*) roots have low

https://doi.org/10.5194/egusphere-2026-467
Preprint. Discussion started: 29 January 2026

bioavailability in the fully thawed stage (Hough et al., 2022), and root porosity and decomposability may be decoupled (Pan et al., 2019; Ye & Ryser, 2022), the low root and rhizome TD were unlikely to lead to increased decomposition and carbon substrate provision.

Simultaneously to plant-mediated CH_4 transport, herbaceous roots may have enhanced rhizospheric CH_4 oxidation. Methanotrophic CH_4 consumption increases with thaw in Stordalen with changes in methanotroph communities from e.g., *Methylocystaceae* in the partly thawed stage to *Methylococcaceae* in the fully thawed stage, which may result from greater plant-mediated rhizospheric oxidation and acetoclastic methanogenesis (Perryman et al., 2020; Singleton et al., 2018). In addition, *Sphagnum* spp. can host methanotrophic CH_4-consuming bacteria (e.g., Larmola et al., 2010; Putkinen et al., 2014; Raghoebarsing et al., 2005). Thus, the heavier $\delta^{13}CH_4$ in the fully and partly thawed stages could also indicate increased CH_4 oxidation close to O_2-rich air at the topmost peat or in the oxidized rhizosphere at ca. 20-44 cm depth (Perryman et al., 2020; Singleton et al., 2018). However, rhizospheric $\delta^{13}CH_4$ enrichment can also result from faster plant $\delta^{12}CH_4$ uptake and increased plant-mediated CH_4 transport (Chanton, 2005). Thus, based on the lower α_C (i.e., maintained acetoclastic methanogenesis) at 20-44 cm depth, and the strongly negative relationships between root TD and CH_4 fluxes it seems that the CH_4-oxidizing effect of herbaceous plants particularly in the fully thawed stage is overcome by provision of carbon for methanogenesis and, shown here with belowground traits for the first time, enhanced plant-mediated CH_4 transport.

4.3 Belowground trait relationships with CH_4 fluxes did not vary within the productive season

The relationships between the static belowground traits and early, middle, peak, and season median CH_4 fluxes differed only slightly in strength. This may result from the lack of temporal root and rhizome sampling within the productive season. However, as an exploratory analysis, our results may indicate higher herbaceous plant-mediated CH_4 transport at the middle CH_4 flux period (Fig. 5). In contrast to our hypotheses, shrub root traits were more strongly associated with middle and peak CH_4 fluxes whereas herbaceous root (TD) and rhizome (SA) traits were strongly associated with CH_4 fluxes throughout the season. This could result from *E. angustifolium* and *E. vaginatum* root porosities not responding strongly to changes in waterlogging (Smirnoff & Crawford, 1983), possibly keeping plant-mediated CH_4 transport constant. In addition, coarse root diameter does not vary strongly temporally (Picon-Cochard et al., 2012), possibly contributing to the lack of temporal trends between root diameter and CH_4 fluxes. Thus, the root TD-CH_4 flux relationships may have reflected higher CH_4-transporting herbaceous root biomass at the middle and peak CH_4 flux period (July-September; Shaver & Billings, 1977) instead of temporal TD and diameter variation. Indeed, diffusive plant-mediated CH_4 transport via *Carex* spp. could be high during the mid- and peak-growing season, as for example *Carex rostrata* (present at the partly and fully thawed stages but not captured by our aboveground measurements; see Table C1 and e.g., Hough et al., 2022) has been found to transport most CH_4 at high summer and early autumn (Ge et al., 2025; Noyce et al., 2014). As *Carex*, *Eriophorum* and *Equisetum* rhizomes are perennial (Husby, 2013; Shaver, 1976), the pre-existing rhizomes may have contributed to CH_4 transport particularly in the

https://doi.org/10.5194/egusphere-2026-467
Preprint. Discussion started: 29 January 2026

beginning of the productive season with active root growth (esp. *E. angustifolium*; Shaver & Billings, 1975), resulting in strong rhizome-CH_4 flux relationships (Fig. 5).

Our exploratory analyses suggested stronger shrub carbon substrate provision (SRL and diameter) at middle and peak CH_4 flux periods (Fig. 5). While uncertain due to the static trait values, these results could be supported by the greater gross primary production (GPP) at the intact and partly thawed stages (Łakomiec et al., 2021) in July and August (max monthly medians: 3.87 and 2.79 μmol CO_2 m^{-2} s^{-1}, respectively; Fig. B1), as GPP can be a proxy for root exudation and correlates with increased wetland CH_4 emissions (Knox et al., 2021; Whiting & Chanton, 1993). However, the biomass-weighted SRL trends were negative, which could result from species-specific SRL variation and the heterogeneous herbaceous root system (Gao et al., 2024; Picon-Cochard et al., 2011). The stronger negative trends in the beginning of the productive season may arise from increased plant carbon investment into herbaceous root growth in comparison with shrubs (Billings et al., 1978; Kummerow & Russell, 1980; Wang et al., 2016). However, within the intact and partly thawed stages and in a mixture of herbaceous and shrub plants, the SRL-CH_4 flux trends could in fact be positive (Fig. 3, B6), but inferential statistics with larger sample sizes per thaw stage are required to investigate this further. As temporal variation in SRL and its relationship with root exudation can be negligible throughout growing season (Gao et al., 2024) and studies in (sub)arctic peatlands are lacking (Iversen et al., 2015), the negative trends between biomass-weighted SRL and CH_4 fluxes across the thaw gradient remain uncertain.

Taken together, the temporal variation in root and rhizome traits may have contributed to CH_4 fluxes but belowground trait sampling throughout the productive season is needed to investigate these relationships further. Given the uncertain herbaceous SRL and root diameter relationships, future studies could benefit from separating the roots into coarse and fine fractions, measuring the associated root exudation rates, and utilizing minirhizotrons (Iversen et al., 2012; Phillips et al., 2008) to disentangle the temporal variation in root carbon substrate provision and CH_4 transport across the permafrost thaw gradient.

5 Conclusions

Permafrost thaw alters peatland methane (CH_4) fluxes through changes in soil anoxia, nutrient and labile carbon availability, and vegetation composition. Here, we focused on the influence of vegetation shift from shrub to herbaceous-dominated communities by exploring the relationships between community-level (herbaceous and shrub) plant belowground (root and rhizome) traits and CH_4 fluxes along a permafrost thaw gradient in a subarctic peatland. The belowground traits reflected the vegetation community shifts, with decreasing shrub belowground biomass and root tissue density along the thaw gradient. Root tissue density was strongly and negatively correlated with CH_4 fluxes, and increasing herbaceous rhizome surface area was associated with higher CH_4 fluxes. These relationships indicated increasing plant-mediated CH_4 transport with thaw,

https://doi.org/10.5194/egusphere-2026-467
Preprint. Discussion started: 29 January 2026

which was supported by lower pore water CH_4 concentrations in the fully thawed stage. Simultaneously, shrub specific root length (SRL) was positively, and root diameter negatively related with CH_4 fluxes, suggesting increased labile carbon substrate provision for acetoclastic methanogenesis. The relationships did not vary strongly during the productive season, but this was likely a result of the static belowground trait values, warranting further temporal trait sampling.

We encourage further observational and experimental research particularly into the relationships between root and rhizome tissue density, SRL and CH_4 fluxes. The observed relationships could be further investigated with larger sample sizes and by combining temporal root trait sampling, root separation into fine and coarse fractions, and root exudation measurements to especially quantify the relationship between SRL and root exudation. Nonetheless, as root and rhizome trait data are scarce particularly from permafrost peatlands, and as the contribution of roots and rhizomes on plant-mediated CH_4 fluxes is understudied, this study provided valuable belowground proxies for plant-mediated CH_4 transport and fluxes. These proxies can inform future observational and experimental studies, as well as process-based wetland models by improving parameterization particularly related to plant-mediated CH_4 transport and helping fill gaps in our understanding of plant-mediated CH_4 cycling.

6 Appendices

Appendix A: Texts

Text A1: Vegetation surveys

To evaluate the similarity between the CH_4 flux chamber plots and peat core plots, we conducted vegetation surveys using the point-intercept method on July 19th-23rd 2023. We used a 1.01 m^2 survey grid divided into 36 subquadrats (16.8 cm x 16.8 cm = 0.03 m^2) and 25 intercept points. We lowered a dowel (60 cm long, 0.5 cm diameter) at each intercept point and noted the presence (i.e., "hit") of each vascular plant and moss species that the dowel touched. At the peat core plots, the grid was always positioned towards northeast from the measurer and with the core in the middle of the grid. At the chamber plots, the grid was positioned so that the chamber collar was approximately in the middle of the northeast edge of the grid (due to the chamber structure, we were unable to set the collar perfectly in the middle of the grid). The ground cover (e.g., litter and water), plant and moss species were surveyed separately. For ground cover data, if the measuring dowel hit multiple classes, only the class that touched the dowel first was recorded. Species and ground cover percentages were obtained by dividing the sum of hits for a species, vegetation (herbaceous, shrub and moss) or ground cover class by the total number of intercepts (n=25), multiplied by 100.

Text A2: Chamber CH_4 flux analyses

The fully thawed permafrost stage had the highest CH_4 flux (median=76.1, IQR=62 mg CH_4 m^{-2} d^{-1}), followed by partly thawed stage (median=31.8, IQR=32.3 mg CH_4 m^{-2} d^{-1}) but CH_4 fluxes at partly and fully thawed stages did not differ

https://doi.org/10.5194/egusphere-2026-467
Preprint. Discussion started: 29 January 2026

significantly ($p>0.05$). Intact stage had the lowest CH_4 fluxes (overall median=2.17, IQR=29 mg CH_4 m^{-2} d^{-1}, $p<0.05$). At all thaw stages, CH_4 flux increased from the beginning to the end of the productive season: the maximum monthly median CH_4 fluxes were observed in August (max CH_4 flux: fully thawed 375.88, partly thawed 160.84, intact 127.15 mg CH_4 m^{-2} d^{-1}), while minima were reached in July at intact (-5.6 mg CH_4 m^{-2} d^{-1}) and June at partly thawed (1.54 mg CH_4 m^{-2} d^{-1}) and fully thawed (11.59 mg CH_4 m^{-2} d^{-1}) stages. In general, variation in CH_4 flux (coefficient of variation, CV) was larger between thaw stages (81%; May: 105%, August: 69%) than within them but the intact stage had large within-stage CH_4 flux variation (106%) which increased from May (58%) to August (133%), while the other stages had relatively low variation (partly thawed: 34%, fully thawed: 27%).

Appendix B: Figures

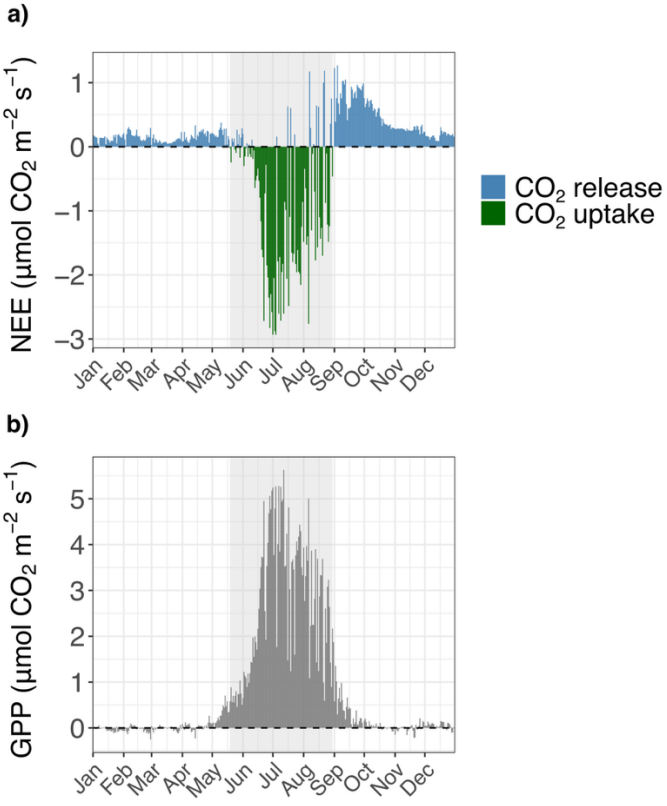

Figure B1: Net ecosystem CO_2 exchange (NEE; µmol CO_2 m^{-2} s^{-1}) (a) and gross primary production (GPP; µmol CO_2 m^{-2} s^{-1}) (b) during the productive season in 2023. a) The productive season was defined as the period between the first and last passing of daily median NEE past zero (highlighted in gray; 19th of May 2023 to 30th of August 2023) (Körner et al., 2023). b) Daily median GPP is shown for reference as a proxy for plant-mediated carbon substrate provision at the ecosystem scale (Knox et al., 2021). NEE and GPP data: Lundin et al., 2025. Note that the NEE and GPP data likely mostly originate from intact and partly thawed permafrost stages and do not cover the fully thawed stage (Łakomiec et al., 2021).

https://doi.org/10.5194/egusphere-2026-467
Preprint. Discussion started: 29 January 2026

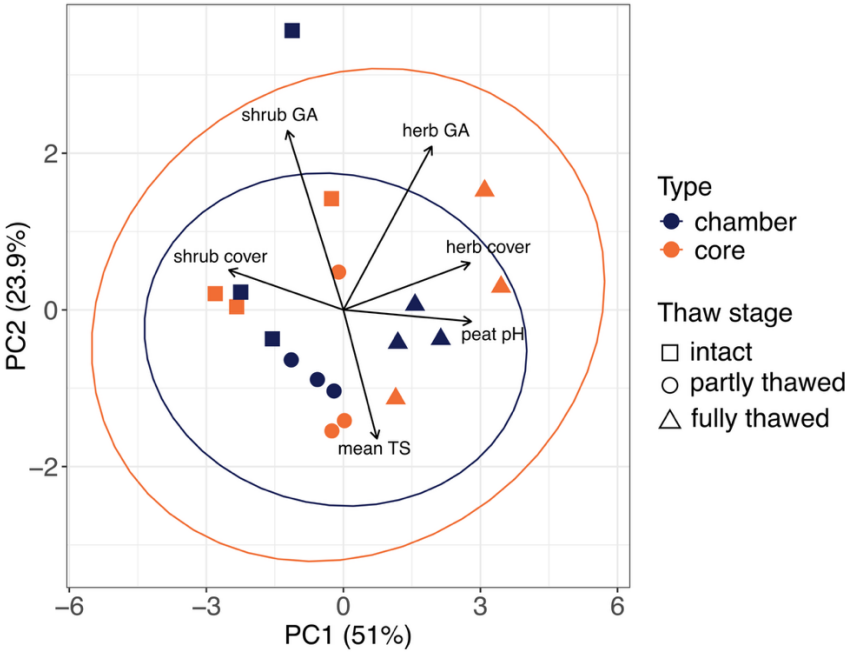

595

Figure B2: The similarity of peat core (n=9) and automated chamber CH_4 flux measurement (n=9) plots based on principal component analysis (PCA). In the figure, chamber and core plots are represented by dark purple and orange points, respectively, while thaw stages are shown in different shapes (rectangle = intact permafrost, circle = partly thawed permafrost, triangle = fully thawed permafrost). The ellipses represent 95% data ellipses for the chamber and core plots within the multivariate space defined 600 **by the first two principal components (chamber = dark purple, orange = core). The PCA was based on normalized plot herbaceous and shrub plant cover and green area (GA), mean soil temperature (mean TS) and peat or porewater pH (here, referred to as peat pH), using function PCA from package FactoMineR (Lê et al., 2008) (results shown in the figure). In addition, we used PERMANOVA with function adonis2 from package vegan (Oksanen et al., 2025) and Euclidean distances between plots within thaw stages to estimate the similarity between core and chamber plots based on the same environmental variables. Based on these** 605 **assessments, the peat core plots had a larger spread in multivariate space than CH_4 flux plots mostly due to slightly higher shrub or herbaceous plant cover in one plot within each thaw stage, but the differences were not significant with the sample size n=9 (p=0.94). Thus, the root and rhizome measurements could be used to roughly represent belowground traits in the CH_4 flux measurement plots. However, we acknowledge that the measured root and rhizome traits do not exactly correspond to those within the CH_4 flux plots and took this into account in the result interpretation.**

https://doi.org/10.5194/egusphere-2026-467
Preprint. Discussion started: 29 January 2026

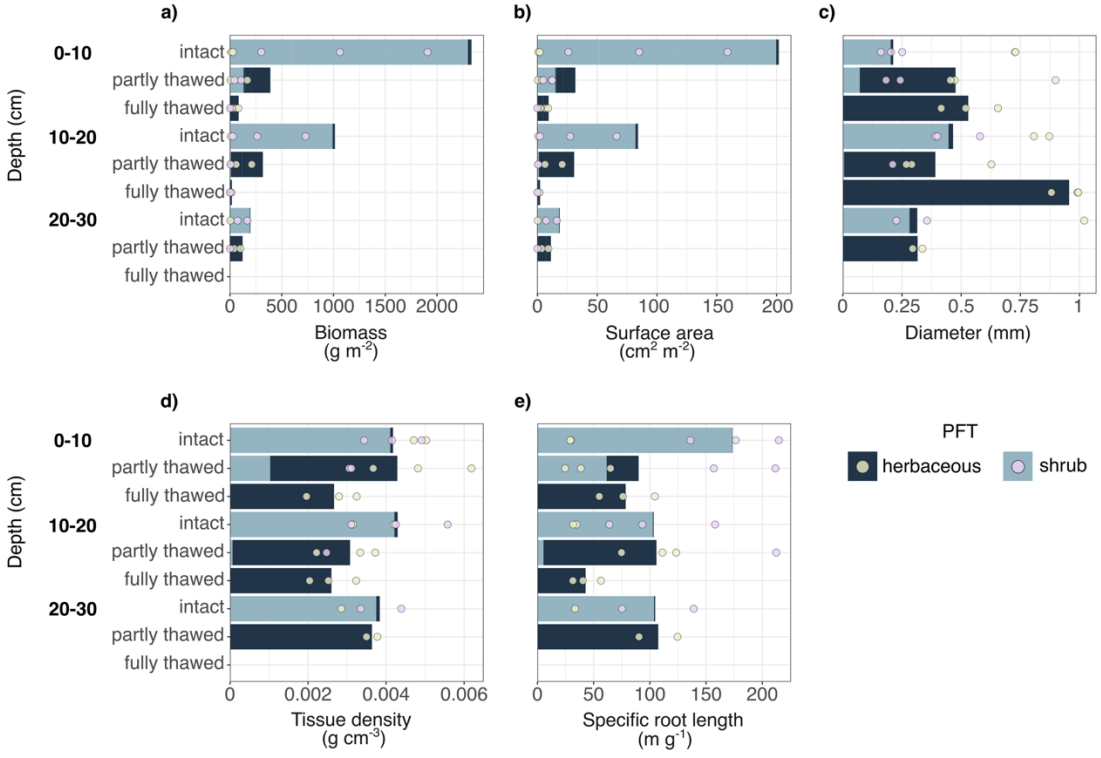

Figure B3: Root traits across the depth profile (0-10, 10-20, 20-30 cm) per thaw stage and plant functional type (PFT). The stacked bar colors (dark blue: herbaceous, light blue: shrub) represent the proportion of the PFT on the total biomass (a) or surface area (b), or the contribution of each PFT on the biomass-weighted trait mean (c-e). The points (light green: herbaceous, light purple: shrub) represent depth-per-plot measurements. a-b) and e) Root biomass, surface area and length were standardized to 10 cm depth increments. c)-e) Biomass-weighted trait means.

https://doi.org/10.5194/egusphere-2026-467
Preprint. Discussion started: 29 January 2026

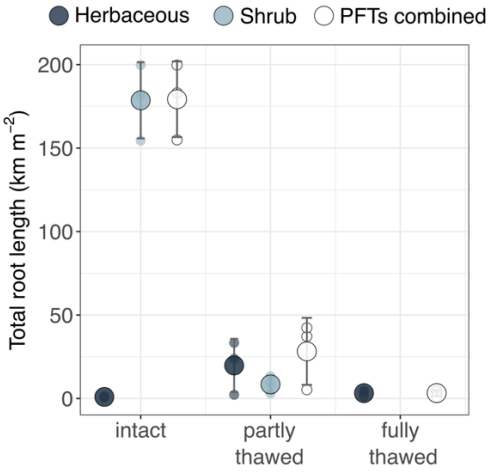

Figure B4: Root total length (km m^{-2}) across thaw stages per and across plant functional types (PFT). Large points indicate thaw stage mean and small points plot-scale measurements. Colors indicate PFTs (dark grey: herbaceous, light grey: shrub, white: PFTs summed). Error bars represent 1 standard deviation of the mean. Root total length was standardized to 30 cm depth in all plots.

https://doi.org/10.5194/egusphere-2026-467
Preprint. Discussion started: 29 January 2026

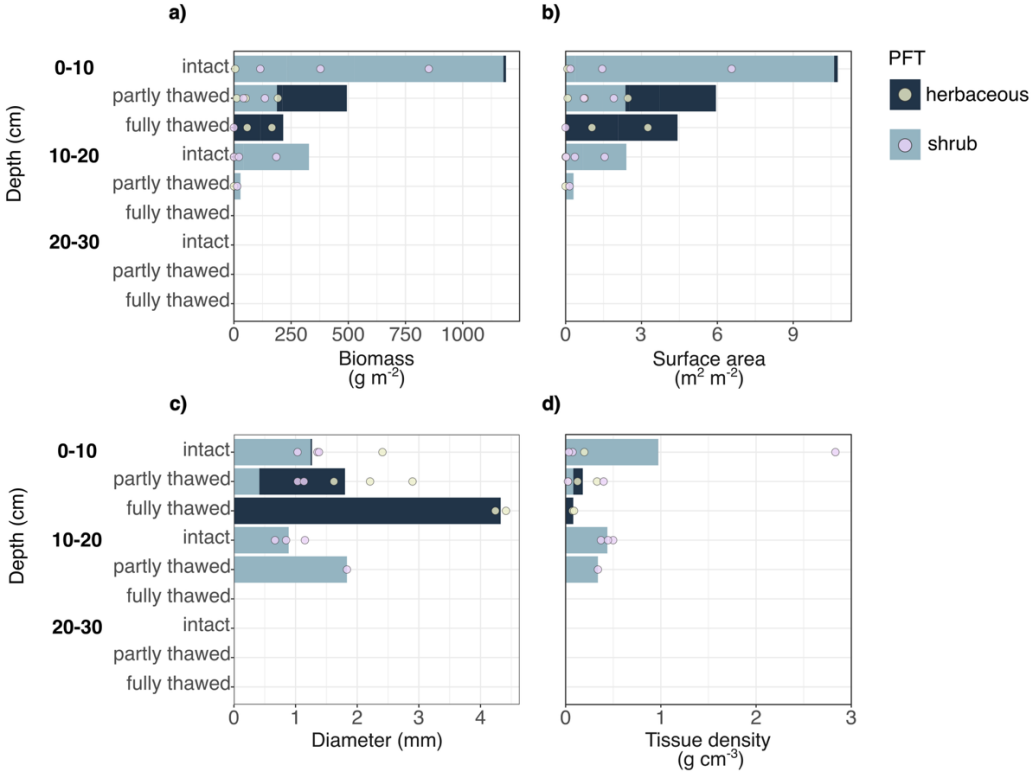

Figure B5: Rhizome traits across the depth profile (0-10, 10-20, 20-30 cm) per thaw stage and plant functional type (PFT). The stacked bar colors (dark blue: herbaceous, light blue: shrub) represent the proportion of the PFT on the total biomass (a) or surface area (b), or the contribution of each PFT on the biomass-weighted trait mean (c-d). The points (light green: herbaceous, light purple: shrub) represent depth-per-plot measurements. a-b) and e) Root biomass, surface area and length were standardized to 10 cm depth increments. c-d) Biomass-weighted trait means.

https://doi.org/10.5194/egusphere-2026-467
Preprint. Discussion started: 29 January 2026

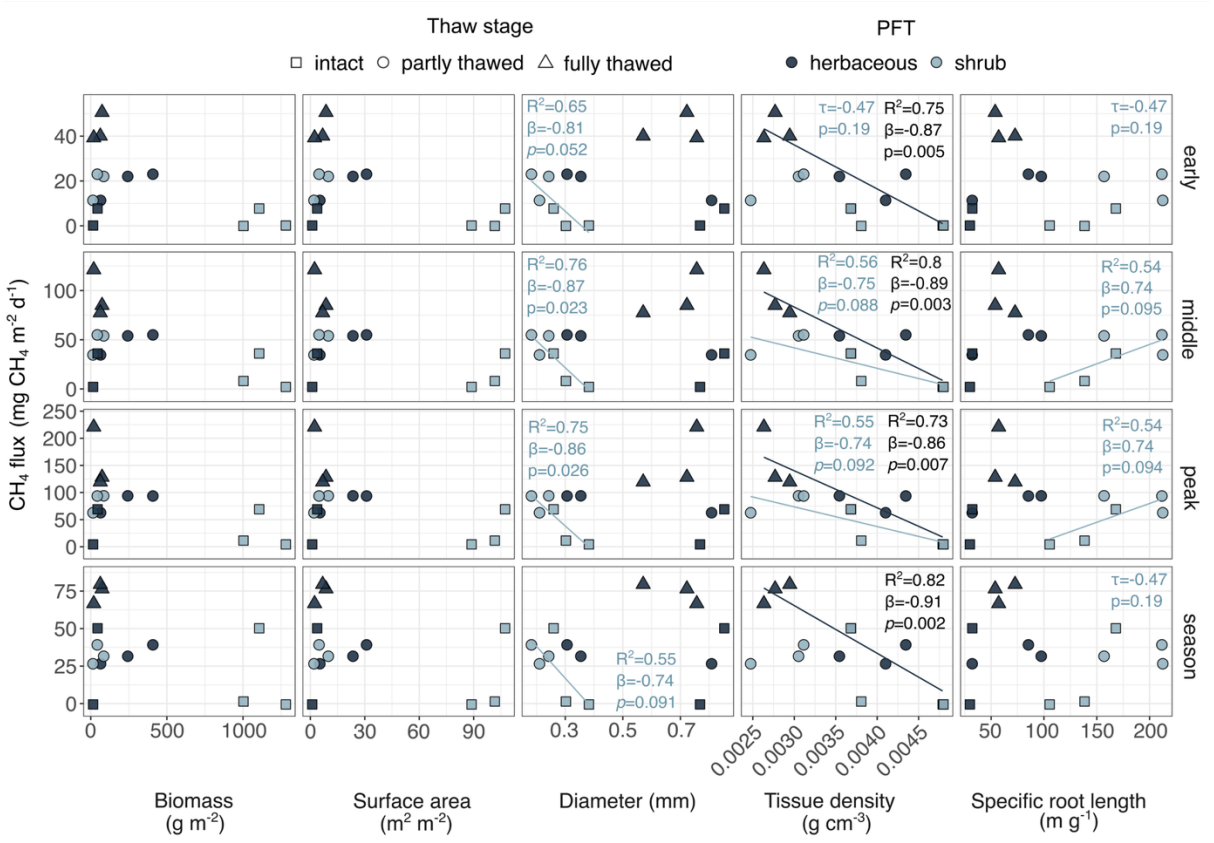

Figure B6: Relationship between root traits (columns) and all CH_4 flux season values (rows). The different point shapes represent thaw stages (rectangle = intact permafrost, circle = partly thawed permafrost, and triangle = fully thawed permafrost), while colors represent plant functional types (PFT) (dark blue = herbaceous, light blue = shrub). Lines represent linear regression fit for visualization, while R^2 and effect size (β) are based on linear regressions with centered and scaled trait and CH_4 flux values (lines, R^2 and β are only shown when $R^2>0.2$, model $p<0.1$, and the linear regression model assumptions were met). Kendall's τ is shown for relationships where linear regression model assumptions were not met and $\tau>0.2$ (note that due to sample n=9, the correlation p-values should be interpreted with caution).

https://doi.org/10.5194/egusphere-2026-467
Preprint. Discussion started: 29 January 2026

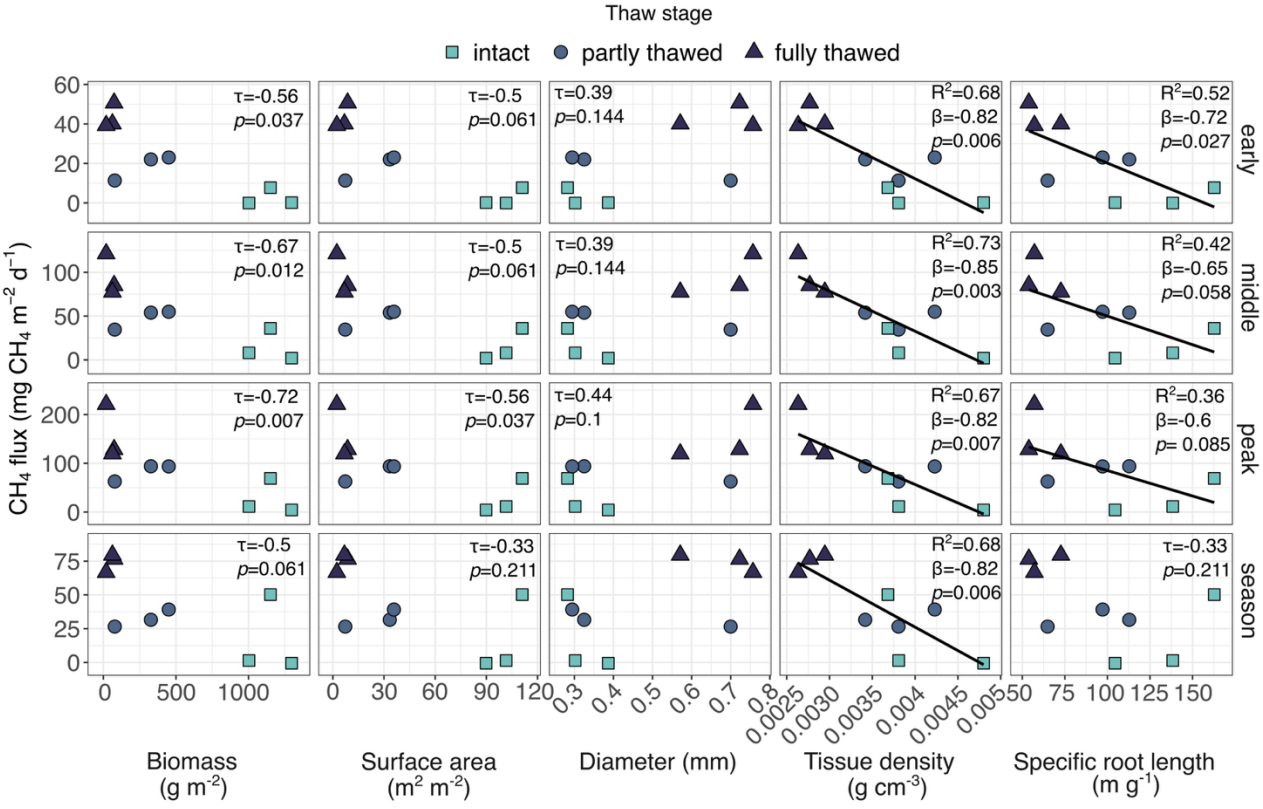

Figure B7: Relationship between root traits (columns) and CH_4 flux season values (rows) with plant functional types (PFT) averaged (root diameter, tissue density, and specific length; weighted mean using root biomass) and summed (root biomass and surface area). The lines represent linear regression fit used for visualization, while R^2 and effect size (β) are reported for linear regressions with centered and scaled CH_4 flux and trait values. Point shapes and colors represent different thaw stages (light blue rectangle = intact permafrost, dark blue circle = partly thawed permafrost, purple triangle = fully thawed permafrost). Kendall's τ is shown for relationships where linear regression model assumptions were not met and τ>0.2 (note that due to sample n=9, the correlation p-values should be interpreted with caution).

https://doi.org/10.5194/egusphere-2026-467
Preprint. Discussion started: 29 January 2026

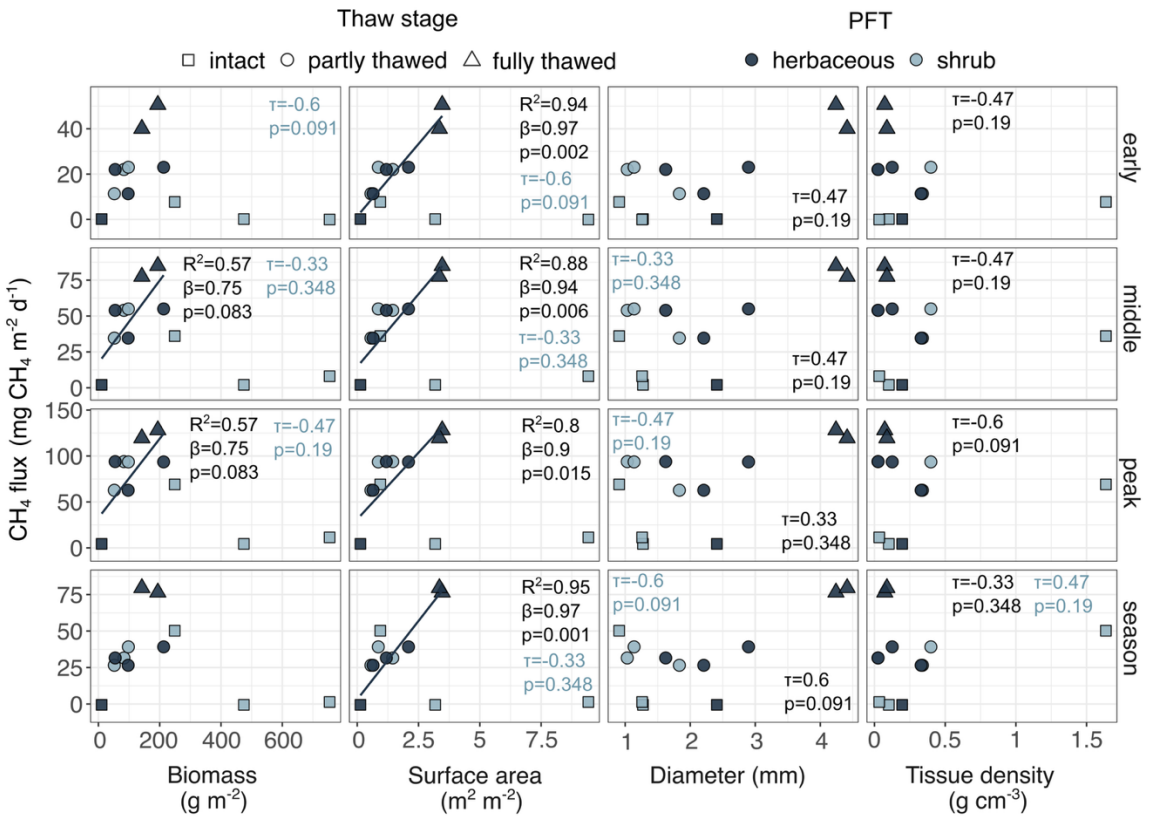

Figure B8: Relationship between rhizome traits (columns) and all CH_4 flux season values (rows). The different point shapes represent thaw stages (rectangle = intact permafrost, circle = partly thawed permafrost, and triangle = fully thawed permafrost), while colors represent plant functional types (PFT; dark blue = herbaceous, light blue = shrub). Lines represent linear regression fit for visualization, while R^2 and effect size (β) are based on linear regressions with centered and scaled trait and CH_4 flux values (lines, R^2 and β are only shown when R^2>0.2, model p<0.1, and the linear regression model assumptions were met). Kendall's τ is shown for relationships where linear regression model assumptions were not met and τ>0.2 (note that due to sample n=9, the correlation p-values should be interpreted with caution).

https://doi.org/10.5194/egusphere-2026-467
Preprint. Discussion started: 29 January 2026

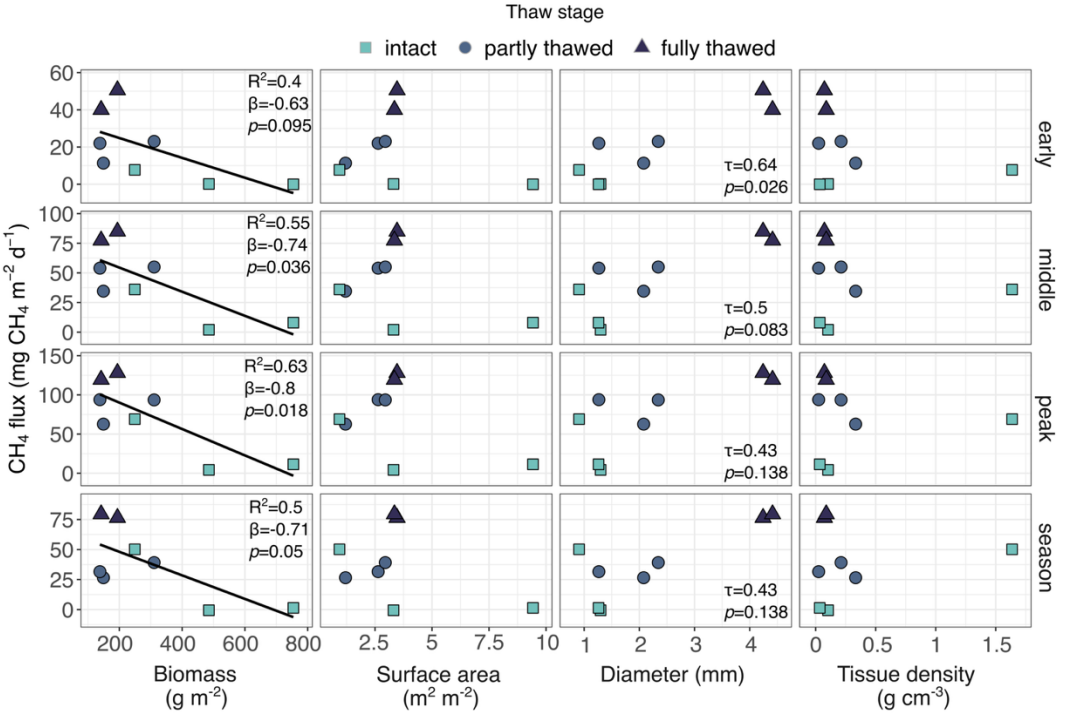

Figure B9: Relationship between rhizome traits (columns) and CH_4 flux season values (rows) with plant functional types (PFTs) averaged (rhizome diameter and tissue density; weighted mean using rhizome biomass) and summed (rhizome biomass and surface area). The lines represent linear regression fit used for visualization, while R^2 and effect size (β) are reported for linear regressions with centered and scaled CH_4 flux and trait values (when R^2>0.2, model p<0.1, and linear regression model assumptions were met). Point shapes and colors represent different thaw stages (light blue rectangle = intact permafrost, dark blue circle = partly thawed permafrost, purple triangle = fully thawed permafrost). Kendall's τ is shown for relationships where linear regression model assumptions were not met and τ>0.2 (note that due to sample n=9, the correlation p-values should be interpreted with caution).

https://doi.org/10.5194/egusphere-2026-467
Preprint. Discussion started: 29 January 2026

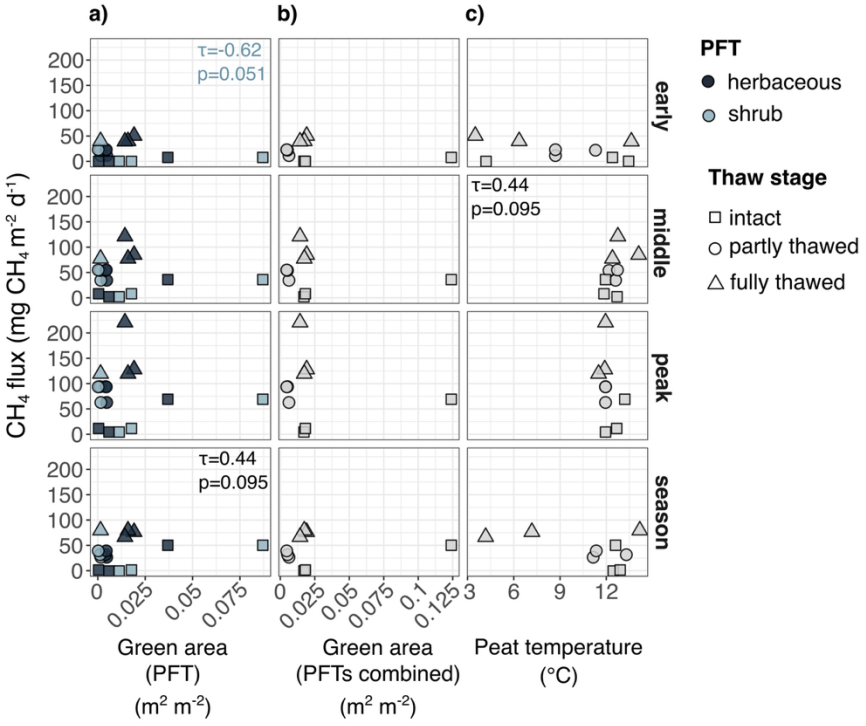

Figure B10: Relationship between plant functional type (PFT)-specific plant green area (column a), plant green area summed across PFTs (column b), soil temperature (column c), and CH_4 flux season values (rows). Kendall τ correlation coefficient (τ) is reported for the relationship when p≤0.1 and τ>0.2 (note that due to sample n=9, the correlation p-values should be interpreted with caution). The different point shapes represent thaw stages (rectangle = intact permafrost, circle = partly thawed permafrost, and triangle = fully thawed permafrost). a) Colors represent different PFTs (dark blue = herbaceous, light blue = shrub).

https://doi.org/10.5194/egusphere-2026-467
Preprint. Discussion started: 29 January 2026

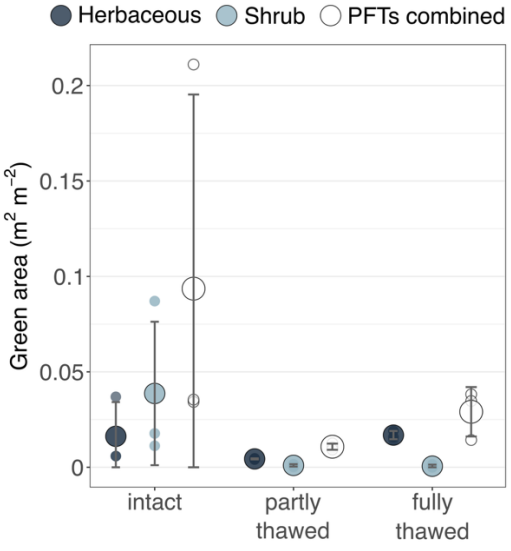

Figure B11: The plant green area (GA; m^2 m^{-2}) varied slightly between thaw stages. Large points represent group means, small points plot-scale measurements, and error bars ±1 standard deviation. The colors represent plant functional type (PFT) groups: dark grey is herbaceous, light grey is shrub, and white is the sum of PFT GAs. Herbaceous GA coefficient of variation (CV) was highest within intact permafrost (137%), while shrub GA varied most within intact permafrost (109%). Note that shrubs (*Betula nana*) were only found in one plot and were only 3% of the total GA in the fully thawed permafrost stage.

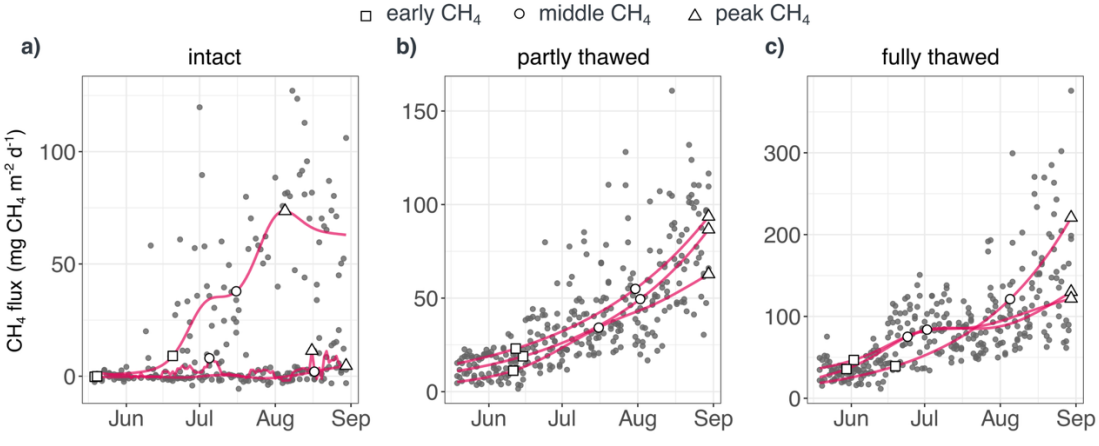

Figure B12: Daily median CH_4 flux with CH_4 flux period values over the productive season at intact (a), partly thawed (b) and fully thawed (c) stages. a-c) Red lines represent chamber-specific GAM fit ($R^2 \geq 0.2$), except for one chamber in a) where GAM $R^2 < 0.1$, and the line represents the moving 7-day median CH_4 flux. Squares represent early, circles middle and triangles peak CH_4 flux season. See chamber GAM R^2 in Table C5.

https://doi.org/10.5194/egusphere-2026-467
Preprint. Discussion started: 29 January 2026

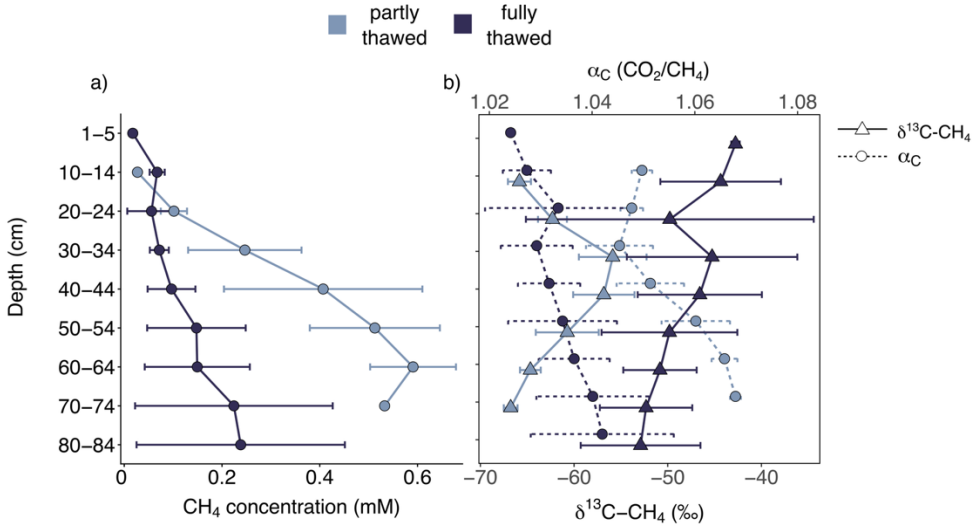

680 **Figure B13: Porewater CH_4 concentration (mM) (a), $\delta^{13}C$-CH_4 (‰) and carbon isotope fractionation factor (α_C CO_2/CH_4) (b) from peat surface to 84 cm depth at partly and fully thawed permafrost stages. Line and point colors represent thaw stages. a) Porewater CH_4 concentration. b) Top x axis: α_C (dashed lines with triangles), where higher values indicate larger fractionation (i.e., more hydrogenotrophy) and vice versa (i.e., more acetoclasty), bottom x axis: $\delta^{13}C$-CH_4 (solid lines with circles). α_C and $\delta^{13}C$-CH_4 lines have been slightly shifted vertically for visualization. Briefly, mean CH_4 concentrations increased from 0.027 ± 0.004**
685 **(standard deviation) mM to 0.533 ± 0.0007 mM at 70-74 cm depth at the partly thawed stage and from 0.017 ± 0.007 mM to 0.238 ± 0.213 mM at 80-84 cm depth at the fully thawed stage. $\delta^{13}C$-CH_4 values became enriched at ca. 30-44 cm (partly thawed ca. -56.4 ‰, fully thawed ca. -46 ‰), and this enrichment was associated with a decrease in α_C (ca. 1.048 partly thawed, ca. 1.03 fully thawed).**

690

https://doi.org/10.5194/egusphere-2026-467
Preprint. Discussion started: 29 January 2026

Appendix C: Tables

Table C1: Plant cover (%) by species and herbaceous and shrub vegetation classes, litter and water surface cover (%), and peat characteristics in each chamber and peat coring ("core") plot (as peat cores were selected to represent each individual chamber, the core and chamber plots have the same ID number). Note that the intact 1 chamber plot was on a collapsing palsa. Chamber plot WTD is the mean annual WTD across the 2007-2017 period per thaw stage (Crill et al., 2023). Values after "±" are one standard deviation of the mean. WTD = water table depth (cm; from the peat surface).

Plot	Species	Plant cover (%)		Litter and water cover (%)		Mean soil temp (°C)		pH		WTD (cm)		Active layer depth (cm)	
		Chamber	Core	Chamber	Core	Chamber	Core	Chamber	Core	Chamber	Core	Chamber	Core
Intact 1	*Eriophorum vaginatum*	48	28	Litter: 20	Litter: 16	9.52 ± 0.88	9.34 ± 1.49	3.1	3.0	-	-	47	37.5
	Vaccinium uliginosum	48	28										
	Andromeda polifolia	32	24	Water: 0	Water: 0								
	Empetrum nigrum	24	56										
	Rubus chamaemorus	0	8										
	Vaccinium vitis-idaea	0	4										
	Dicranum sp.	8	52										
	Polytrichum sp.	4	0										
	Shrub	104	120										
	Herbaceous	48	28										
Intact 3	*A. polifolia*	52	48	Litter: 28	Litter: 16	7.7 ± 0.6	7.7 ± 1.1	3.1	3.0	-	-	41.5	39
	E. nigrum	16	16										
	R. chamaemorus	4	32										
	V. uliginosum	4	0	Water: 0	Water: 0								
	Carex rotundata	4	0										
	Betula nana	0	28										
	V. vitis-idaea	0	4										
	E. vaginatum	0	4										
	Ptilidium ciliare	48	20										
	Dicranum sp.	8	20										
	Shrub	76	128										
	Herbaceous	4	4										
Intact 5	*E. vaginatum*	84	92	Litter: 0	Litter: 4	8.7 ± 0.8	8.3 ± 1.9	2.8	3.2	-	-	-	85
	V. uliginosum	24	20										
	R. chamaemorus	16	4										
	E. nigrum	12	20	Water: 12	Water: 0								
	A. polifolia	8	8										
	B. nana	8	12										
	Sphagnum	32	0										

https://doi.org/10.5194/egusphere-2026-467
Preprint. Discussion started: 29 January 2026

	balticum *Dicranum* sp. Herbaceous Shrub	0 84 68	8 92 64										
Partly thawed 2	*C. rotundata* *E. vaginatum* *S. capillifolium* Herbaceous Shrub	52 0 100 52 0	0 80 100 80 0	Litter: 0 Water: 0	Litter: 0 Water: 0	9.5 ± 0.6	7.0 ± 1.2	3.3	3.2	-9.1 ± 4.6	-14.67	>85	>85
Partly thawed 4	*C. rotundata* *V. oxycoccos* *A. polifolia* *E. angustifolium* *E. vaginatum* *Drosera rotundifolia* *S. capillifolium* *P. ciliare* Herbaceous Shrub	52 48 28 0 0 0 100 0 52 76	60 20 24 8 4 4 72 16 76 44	Litter: 16 Water: 0	Litter: 20 Water: 0	9.1 ± 0.5	10.9 ± 1.03	3.2	3.8	-9.1 ± 4.6	-21	>85	>85
Partly thawed 6	*V. oxycoccos* *C. rotundata* *E. angustifolium* *S. capillifolium* Herbaceous Shrub	16 40 0 88 40 40	36 36 24 96 60 36	Litter: 44 Water: 0	Litter: 8 Water: 0	9.1 ± 0.6	10.9 ± 0.7	3.3	3.4	-9.1 ± 4.6	-27	>85	>85
Fully thawed 7	*E. angustifolium* *Equisetum fluviatile* Herbaceous Shrub	96 40 136 0	100 20 120 0	Litter: 0 Water: 12	Litter: 4 Water: 0	9.7 ± 0.3	8.7 ± 0.4	5.1	5.7	2.1 ± 4.4	0	>85	>85
Fully thawed 8	*E. angustifolium* *E. fluviatile* *Comarum palustre* *S. riparium* Herbaceous Shrub	88 24 4 12 116 0	100 68 12 0 180 0	Litter: 0 Water: 0	Litter: 0 Water: 0	8.4 ± 1.0	9.6 ± 0.3	5.0	6.0	2.1 ± 4.4	0	>85	>85
Fully thawed 9	*E. angustifolium* *S. riparium* Herbaceous Shrub	92 40 92 0	84 96 84 0	Litter: 0 Water: 0	Litter: 24 Water: 0	9.1 ± 0.3	10.1 ± 0.4	4.7	4.8	2.1 ± 4.4	0	>85	>85

700

https://doi.org/10.5194/egusphere-2026-467
Preprint. Discussion started: 29 January 2026

Table C2: Species included in the vegetation green area (GA) measurements per thaw stage. Mean GA (with standard deviation) is reported for each species across the three plots per thaw stage, and comprises the sum of stem and leaf green area (m^2 m^{-2}).

Thaw stage	Species	Mean GA (m^2 m^{-2})
Intact	*Andromeda polifolia*	0.1083 ± 0.06
	Betula nana	0.0243 ± 0.02
	Carex rotundata	0.0088 ± 0
	Empetrum nigrum	0.0833 ± 0.07
	Eriophorum vaginatum	0.4792 ± 0.54
	Rubus chamaemorus	0.1599 ± 22.34
	Vaccinium uliginosum	0.1899 ± 0.25
	Vaccinium vitis-idaea	0.005 ± 0.004
Partly thawed	*Andromeda polifolia*	0.0349 ± 0.04
	Betula nana	0.0162 ± 0.02
	Carex rotundata	0.1629 ± 0.07
	Drosera rotundifolia	0.0011 ± 0
	Empetrum nigrum	0.0293 ± 0
	Eriophorum angustifolium	0.0537 ± 0
	Eriophorum vaginatum	0.3159 ± 0.16
	Rubus chamaemorus	0.0263 ± 0
	Vaccinium oxycoccos	0.0113 ± 0.01
	Vaccinium uliginosum	0.0009 ± 0
Fully thawed	*Betula nana*	0.0104 ± 0
	Carex canescens	0.0029 ± 0
	Comarum palustre	0.0861 ± 0.06
	Equisetum fluviatile	0.8958 ± 0.63
	Eriophorum angustifolium	0.6507 ± 0.64
	Galium palustre	0.0124 ± 0

https://doi.org/10.5194/egusphere-2026-467
Preprint. Discussion started: 29 January 2026

Table C3: Vascular plant species growing directly on the peat cores and their leaf, stem, and flower biomass. As peat cores were selected to represent each individual chamber, the core and chamber plots have the same ID number. Note that the biomass estimates are likely underestimations due to some plant material being lost in the field. We show this table primarily for the species list.

		Biomass (g)			
Plot	**Species**	**Leaf**	**Stem**	**Flower**	**Total**
Intact 1	*E. vaginatum*	0.06741	0.00309	0	0.0705
	V. uliginosum	0.13576	0.55449	0	0.69025
	E. nigrum	0.02116	0.02316	0	0.04432
	A. polifolia	0.07106	0.04793	0	0.11899
	R. chamaemorus	0.03169	0.00783	0	0.03952
Intact 3	*V. uliginosum*	0.01615	0.09076	0	0.10691
	E. nigrum	0.09819	0.152203	0	0.250393
	A. polifolia	0.24815	0.33348	0	0.58163
	E. vaginatum	0.00862	0	0	0.00862
Intact 5	*E. vaginatum*	0.5163	0.04528	0	0.56158
	A. polifolia	0.09981	0.03223	0	0.13204
	E. nigrum	0.41146	0.53396	0	0.94542
	V. uliginosum	0.09566	0.3616	0	0.45726
	V. oxycoccos	0.01806	0.03149	0	0.04955
Partly thawed 2	*E. vaginatum*	1.19198	0.45312	0.02525	1.67035
Partly thawed 4	*E. angustifolium*	0.00545	0.1116	0	0.11705
	V. oxycoccos	0.00636	0.0093	0	0.01566
	A. polifolia	0.0471	0.03144	0.00791	0.08645
	C. rotundata	0.0683	0.07754	0	0.14584
Partly thawed 6	*V. oxycoccos*	0.04531	0.04715	0	0.09246
	C. rotundata	0.50924	0.1	0.03343	0.64267
	E. angustifolium	0.11302	0.05956	0	0.17258
Fully thawed 7	*E. angustifolium*	0.00481	0.00434	0	0.00915
Fully thawed 8	NA (only dead vegetation)	0	0	0	0
Fully thawed 9	*E. angustifolium*	0.01042	0	0	0.01042

https://doi.org/10.5194/egusphere-2026-467
Preprint. Discussion started: 29 January 2026

720

Table C4: Automated chamber CH_4 flux (mg CH_4 m^{-2} d^{-1}) data aggregated to daily scale with medians. Each thaw stage (intact, partly thawed and fully thawed permafrost) has three chambers, resulting in 9 chambers in total across the gradient. Date is reported as YYYY-MM-DD. Peat temperature was measured at each chamber in °C.

date	chamber_id	ch4_flux_mgch4m2d1	peat_temp	thaw_stage
2023-05-19	1	-1.5742155	3.7	intact
2023-05-21	1	0.11011842	7.7	intact
2023-05-22	1	-2.0749876	11.6	intact
2023-05-23	1	2.73592456	9.8	intact
2023-05-24	1	0.6504314	6.5	intact
2023-05-25	1	-0.2753291	5.9	intact
2023-05-27	1	-1.4930673	3.5	intact
2023-05-28	1	0.53437161	7.25	intact
2023-05-29	1	-0.8084409	NA	intact
2023-05-30	1	-0.8862095	6	intact
2023-05-31	1	-1.0112265	5.9	intact
2023-06-01	1	-0.5574734	3.6	intact
2023-06-02	1	-0.998409	4.7	intact
2023-06-03	1	-0.376127	5.4	intact
2023-06-04	1	-0.9622294	6	intact
2023-06-10	1	-0.6405388	11.25	intact
2023-06-11	1	58.2029094	10.5	intact
2023-06-12	1	-1.0596144	9.8	intact
2023-06-13	1	0.30756114	7.9	intact
2023-06-14	1	-0.4510569	10.3	intact
2023-06-16	1	-1.4557005	11.8	intact
2023-06-17	1	-0.9726219	14.8	intact
2023-06-18	1	-1.6011772	15.3	intact
2023-06-19	1	-1.5296095	15.6	intact
2023-06-20	1	-0.9589859	15.55	intact
2023-06-21	1	0.33550547	15.1	intact
2023-06-22	1	-0.653831	15.5	intact
2023-06-23	1	-0.7277735	15.4	intact
2023-06-24	1	-0.8945707	12.6	intact
2023-06-25	1	-1.2535992	12.15	intact
2023-06-26	1	-0.5782371	12.5	intact
2023-06-27	1	-0.9384954	15.85	intact
2023-06-28	1	-0.5582339	13.55	intact

https://doi.org/10.5194/egusphere-2026-467
Preprint. Discussion started: 29 January 2026

2023-06-29	1	6.13238862	16.3	intact
2023-07-02	1	-1.7506662	11.45	intact
2023-07-03	1	-0.4727376	10.2	intact
2023-07-04	1	0.12544433	14.2	intact
2023-07-05	1	4.68531914	11.7	intact
2023-07-06	1	-1.5189094	12.2	intact
2023-07-08	1	0.85818027	14.8	intact
2023-07-09	1	-1.1912977	13.6	intact
2023-07-10	1	-1.7284981	18.1	intact
2023-07-11	1	24.6812614	17.3	intact
2023-07-14	1	-0.5412949	NA	intact
2023-07-15	1	0.135732	13	intact
2023-07-16	1	19.4200096	10.2	intact
2023-07-17	1	0.28613647	11.6	intact
2023-07-18	1	0.29784641	12.7	intact
2023-07-19	1	-2.4859508	11.9	intact
2023-07-20	1	-1.9277671	10.8	intact
2023-07-21	1	-2.1024176	12.4	intact
2023-07-23	1	1.34978199	10.6	intact
2023-07-24	1	-1.4619621	12.8	intact
2023-07-26	1	-1.0331124	NA	intact
2023-07-27	1	-1.8103016	17.45	intact
2023-07-29	1	-2.4061967	15.35	intact
2023-07-30	1	-2.8735807	13.75	intact
2023-08-01	1	0.81351311	13.75	intact
2023-08-02	1	0.96200058	13.8	intact
2023-08-03	1	-0.6077703	15.3	intact
2023-08-04	1	-1.471697	14.5	intact
2023-08-05	1	-0.1108434	12.75	intact
2023-08-06	1	-2.2913776	12	intact
2023-08-07	1	1.36918011	NA	intact
2023-08-08	1	-1.4553593	12.2	intact
2023-08-09	1	0.86322717	15.5	intact
2023-08-10	1	2.81393942	14.4	intact
2023-08-11	1	-1.3108983	13.2	intact
2023-08-12	1	1.56942242	14.4	intact
2023-08-13	1	112.869073	11.5	intact
2023-08-14	1	-1.3360591	14.2	intact
2023-08-15	1	2.17306634	14.05	intact

https://doi.org/10.5194/egusphere-2026-467
Preprint. Discussion started: 29 January 2026

2023-08-16	1	1.08742737	12.7	intact
2023-08-17	1	-1.4419661	14.3	intact
2023-08-18	1	40.8011232	NA	intact
2023-08-19	1	10.2510742	10.05	intact
2023-08-20	1	0.99956116	11.6	intact
2023-08-22	1	3.08381065	12.8	intact
2023-08-23	1	4.17373264	13.8	intact
2023-08-24	1	-3.1773699	11.9	intact
2023-08-25	1	7.96674475	11.95	intact
2023-08-26	1	15.2623273	NA	intact
2023-08-27	1	20.5337876	NA	intact
2023-08-28	1	2.50175877	NA	intact
2023-08-29	1	3.97112172	NA	intact
2023-08-30	1	2.83833648	NA	intact
2023-05-19	2	4.54583509	3.3	partly_thawed
2023-05-20	2	7.69370639	4.2	partly_thawed
2023-05-21	2	5.64355684	4.7	partly_thawed
2023-05-22	2	9.71601188	4.8	partly_thawed
2023-05-23	2	9.48145508	5.65	partly_thawed
2023-05-24	2	11.003204	4.8	partly_thawed
2023-05-25	2	5.37497615	4.4	partly_thawed
2023-05-26	2	7.53370138	2.9	partly_thawed
2023-05-27	2	3.58609512	3.3	partly_thawed
2023-05-28	2	4.74635682	4.05	partly_thawed
2023-05-29	2	4.02995337	5.55	partly_thawed
2023-05-30	2	7.52663379	4.8	partly_thawed
2023-05-31	2	19.5718206	4.25	partly_thawed
2023-06-01	2	6.15147443	3.25	partly_thawed
2023-06-02	2	5.0943476	3.7	partly_thawed
2023-06-03	2	12.548897	5.85	partly_thawed
2023-06-04	2	9.62860469	7	partly_thawed
2023-06-06	2	3.89185836	5.9	partly_thawed
2023-06-07	2	9.58988704	6.35	partly_thawed
2023-06-08	2	7.33867681	5.7	partly_thawed
2023-06-09	2	4.58170903	6.6	partly_thawed
2023-06-10	2	15.5404233	6.8	partly_thawed
2023-06-11	2	10.7936538	8.1	partly_thawed
2023-06-12	2	15.3763969	8.7	partly_thawed
2023-06-13	2	1.53925322	8.5	partly_thawed

https://doi.org/10.5194/egusphere-2026-467
Preprint. Discussion started: 29 January 2026

2023-06-14	2	3.40438595	8.3	partly_thawed
2023-06-15	2	6.48323423	7.4	partly_thawed
2023-06-16	2	14.5803252	8.1	partly_thawed
2023-06-17	2	15.6389211	9.5	partly_thawed
2023-06-18	2	31.8205059	11.25	partly_thawed
2023-06-19	2	44.1913954	11.75	partly_thawed
2023-06-20	2	13.9612921	12.15	partly_thawed
2023-06-21	2	17.662008	13.3	partly_thawed
2023-06-22	2	9.89155847	12.9	partly_thawed
2023-06-23	2	40.8826325	12.5	partly_thawed
2023-06-24	2	79.8489491	10.55	partly_thawed
2023-06-25	2	35.8147969	9.8	partly_thawed
2023-06-26	2	11.7850491	10.4	partly_thawed
2023-06-27	2	13.2740956	10.6	partly_thawed
2023-06-28	2	26.8731422	12.2	partly_thawed
2023-06-29	2	41.6668303	12.75	partly_thawed
2023-06-30	2	14.373135	13.7	partly_thawed
2023-07-01	2	16.4751695	12.8	partly_thawed
2023-07-02	2	22.8080135	12.3	partly_thawed
2023-07-03	2	11.721194	10.7	partly_thawed
2023-07-04	2	57.5855112	9.3	partly_thawed
2023-07-05	2	61.3964171	11.95	partly_thawed
2023-07-06	2	41.2109233	10.7	partly_thawed
2023-07-07	2	19.3064479	11.55	partly_thawed
2023-07-08	2	49.6842127	13.5	partly_thawed
2023-07-09	2	25.3841544	11.9	partly_thawed
2023-07-10	2	80.350965	11.95	partly_thawed
2023-07-11	2	32.5066099	13.5	partly_thawed
2023-07-12	2	19.6550007	13	partly_thawed
2023-07-13	2	23.3160879	12.7	partly_thawed
2023-07-14	2	20.6782469	13	partly_thawed
2023-07-15	2	28.6238958	12.95	partly_thawed
2023-07-16	2	31.3170475	11.1	partly_thawed
2023-07-17	2	69.0423737	10.4	partly_thawed
2023-07-18	2	31.1485143	12.3	partly_thawed
2023-07-19	2	78.4602003	11.05	partly_thawed
2023-07-20	2	110.588726	10.2	partly_thawed
2023-07-21	2	33.5477807	11.2	partly_thawed
2023-07-22	2	21.0885265	10.6	partly_thawed

https://doi.org/10.5194/egusphere-2026-467
Preprint. Discussion started: 29 January 2026

2023-07-23	2	22.028071	10.4	partly_thawed
2023-07-24	2	35.5289275	10.8	partly_thawed
2023-07-25	2	23.7492942	11.15	partly_thawed
2023-07-26	2	65.9468251	12.3	partly_thawed
2023-07-27	2	128.110722	12.8	partly_thawed
2023-07-28	2	79.8050552	12.5	partly_thawed
2023-07-29	2	56.8759984	13.6	partly_thawed
2023-07-30	2	63.2536861	13.5	partly_thawed
2023-07-31	2	25.0430848	13.2	partly_thawed
2023-08-01	2	26.9955982	13.15	partly_thawed
2023-08-02	2	19.9212208	11.9	partly_thawed
2023-08-03	2	26.5437726	12.3	partly_thawed
2023-08-04	2	34.0101748	12.95	partly_thawed
2023-08-05	2	16.7294357	12.2	partly_thawed
2023-08-06	2	75.4574909	10.4	partly_thawed
2023-08-07	2	31.5647914	10.7	partly_thawed
2023-08-08	2	29.7783092	11.4	partly_thawed
2023-08-09	2	21.8526552	13.2	partly_thawed
2023-08-10	2	68.1945167	13.6	partly_thawed
2023-08-11	2	24.4209532	12.5	partly_thawed
2023-08-12	2	43.2268626	11.85	partly_thawed
2023-08-13	2	53.5576399	11.9	partly_thawed
2023-08-14	2	45.2274227	12.35	partly_thawed
2023-08-15	2	160.839658	13.15	partly_thawed
2023-08-16	2	70.8737833	12.4	partly_thawed
2023-08-17	2	46.837311	12	partly_thawed
2023-08-18	2	57.8732317	11.05	partly_thawed
2023-08-19	2	47.9671115	10.55	partly_thawed
2023-08-20	2	49.4545866	11	partly_thawed
2023-08-21	2	42.9428792	11.9	partly_thawed
2023-08-22	2	131.905466	13	partly_thawed
2023-08-23	2	123.85888	12.95	partly_thawed
2023-08-24	2	41.2154506	12	partly_thawed
2023-08-25	2	68.6044776	11.9	partly_thawed
2023-08-26	2	95.0039126	11	partly_thawed
2023-08-27	2	50.7697585	9.5	partly_thawed
2023-08-28	2	30.4250286	10.8	partly_thawed
2023-08-29	2	47.3675987	11.85	partly_thawed
2023-08-30	2	65.9836321	11.85	partly_thawed

https://doi.org/10.5194/egusphere-2026-467
Preprint. Discussion started: 29 January 2026

2023-05-19	3	-2.5803204	6.8	intact
2023-05-20	3	1.15638671	7.3	intact
2023-05-22	3	-1.255402	6.7	intact
2023-05-23	3	2.81969798	8.6	intact
2023-05-25	3	1.16149635	NA	intact
2023-05-27	3	0.86285343	6.9	intact
2023-05-28	3	-0.7032227	NA	intact
2023-05-29	3	0.4901487	7.1	intact
2023-05-30	3	0.49772473	6.25	intact
2023-05-31	3	-2.4676236	5.9	intact
2023-06-02	3	0.95680016	7.5	intact
2023-06-07	3	-0.7658941	8.6	intact
2023-06-10	3	3.43841411	12.4	intact
2023-06-11	3	-0.2294732	10.1	intact
2023-06-12	3	-0.6377087	9.3	intact
2023-06-17	3	2.07956174	12	intact
2023-06-18	3	-0.6556424	13.55	intact
2023-06-19	3	8.85655461	15.5	intact
2023-06-22	3	-1.0366715	14.6	intact
2023-06-23	3	2.08647798	14.45	intact
2023-06-25	3	4.67578604	NA	intact
2023-06-26	3	11.3090816	13.3	intact
2023-06-27	3	17.8449859	16.1	intact
2023-06-28	3	-4.1519838	14.6	intact
2023-06-29	3	1.75473305	14.5	intact
2023-07-01	3	-0.6927129	13.7	intact
2023-07-02	3	1.7895277	11.7	intact
2023-07-04	3	9.72225636	10	intact
2023-07-05	3	6.35966235	13.9	intact
2023-07-08	3	10.5210357	13.95	intact
2023-07-09	3	-1.9971268	13.4	intact
2023-07-10	3	6.57636546	13	intact
2023-07-11	3	1.14897533	13.2	intact
2023-07-13	3	0.73874793	NA	intact
2023-07-14	3	0.51801415	13.2	intact
2023-07-16	3	24.1586777	9.9	intact
2023-07-17	3	-5.6006408	10.7	intact
2023-07-18	3	-1.4566826	13	intact
2023-07-20	3	9.4840076	11.1	intact

https://doi.org/10.5194/egusphere-2026-467
Preprint. Discussion started: 29 January 2026

2023-07-21	3	-0.0788323	11.8	intact
2023-07-25	3	2.78941254	NA	intact
2023-07-27	3	1.47809052	15.45	intact
2023-07-28	3	3.36932495	12.8	intact
2023-07-29	3	-3.8347945	16.9	intact
2023-07-30	3	3.91550813	13.45	intact
2023-08-02	3	1.05771355	13.85	intact
2023-08-04	3	-3.0436606	16.1	intact
2023-08-05	3	-1.9844905	15	intact
2023-08-06	3	1.33543291	12.5	intact
2023-08-07	3	-2.0934105	NA	intact
2023-08-08	3	-1.7480627	NA	intact
2023-08-09	3	4.22978638	15	intact
2023-08-10	3	3.99420254	14.7	intact
2023-08-11	3	2.7661995	13	intact
2023-08-12	3	2.3091427	14.2	intact
2023-08-13	3	43.9516494	11.2	intact
2023-08-14	3	2.99366857	12.5	intact
2023-08-16	3	11.3838865	NA	intact
2023-08-17	3	-1.2168881	11.6	intact
2023-08-19	3	17.0250587	9.9	intact
2023-08-20	3	-2.0284502	13.4	intact
2023-08-21	3	-1.1364975	12.5	intact
2023-08-22	3	8.52438518	13.2	intact
2023-08-24	3	13.7368039	12.9	intact
2023-08-25	3	14.7329223	10	intact
2023-08-26	3	3.78757965	NA	intact
2023-08-27	3	5.75274085	NA	intact
2023-08-28	3	1.54015746	NA	intact
2023-08-29	3	12.2598751	NA	intact
2023-08-30	3	-3.0880699	NA	intact
2023-05-19	4	15.3260797	6.35	partly_thawed
2023-05-20	4	16.3046112	6	partly_thawed
2023-05-21	4	15.2011339	7.2	partly_thawed
2023-05-22	4	18.8625876	5.6	partly_thawed
2023-05-23	4	18.642289	NA	partly_thawed
2023-05-24	4	21.6231619	NA	partly_thawed
2023-05-25	4	19.0604258	4.4	partly_thawed
2023-05-26	4	8.61206747	4.8	partly_thawed

https://doi.org/10.5194/egusphere-2026-467
Preprint. Discussion started: 29 January 2026

2023-05-27	4	18.7376978	4.95	partly_thawed
2023-05-28	4	18.0772622	5.6	partly_thawed
2023-05-29	4	9.3410204	7.7	partly_thawed
2023-05-30	4	19.9154388	5.3	partly_thawed
2023-05-31	4	20.2870883	4.8	partly_thawed
2023-06-01	4	9.6420955	3.6	partly_thawed
2023-06-02	4	19.5970952	8	partly_thawed
2023-06-03	4	13.967649	6.4	partly_thawed
2023-06-04	4	11.4367081	7.9	partly_thawed
2023-06-05	4	5.52809115	6.1	partly_thawed
2023-06-06	4	7.39703184	8.6	partly_thawed
2023-06-07	4	22.8335209	7.5	partly_thawed
2023-06-08	4	12.5212654	6.95	partly_thawed
2023-06-09	4	8.69966321	11.8	partly_thawed
2023-06-10	4	16.8196508	11.3	partly_thawed
2023-06-11	4	21.3494983	10.9	partly_thawed
2023-06-12	4	19.6490378	11	partly_thawed
2023-06-13	4	3.75432939	12.55	partly_thawed
2023-06-14	4	11.4690303	10.2	partly_thawed
2023-06-15	4	9.8235872	10.9	partly_thawed
2023-06-16	4	19.1560774	13.4	partly_thawed
2023-06-17	4	23.2823381	14.5	partly_thawed
2023-06-18	4	27.1226898	15.5	partly_thawed
2023-06-19	4	23.6041287	16.5	partly_thawed
2023-06-20	4	21.2917605	14	partly_thawed
2023-06-21	4	30.6550238	15.7	partly_thawed
2023-06-22	4	14.1761334	14.7	partly_thawed
2023-06-23	4	29.6107856	15.25	partly_thawed
2023-06-24	4	26.1851638	12.7	partly_thawed
2023-06-25	4	19.1723247	13.35	partly_thawed
2023-06-26	4	22.4637231	12.4	partly_thawed
2023-06-27	4	23.2891672	14.95	partly_thawed
2023-06-28	4	27.026658	14.8	partly_thawed
2023-06-29	4	34.9020762	16.45	partly_thawed
2023-06-30	4	13.4209663	14.4	partly_thawed
2023-07-01	4	22.8990118	13.05	partly_thawed
2023-07-02	4	30.5293099	11.25	partly_thawed
2023-07-03	4	22.4349558	10.2	partly_thawed
2023-07-04	4	38.6929169	13.1	partly_thawed

https://doi.org/10.5194/egusphere-2026-467
Preprint. Discussion started: 29 January 2026

2023-07-05	4	28.215731	12.1	partly_thawed
2023-07-06	4	35.5901705	13.75	partly_thawed
2023-07-07	4	26.4246888	13.2	partly_thawed
2023-07-08	4	20.2482046	14.7	partly_thawed
2023-07-09	4	35.9015093	15.65	partly_thawed
2023-07-10	4	41.3976089	15.85	partly_thawed
2023-07-11	4	41.5938532	15	partly_thawed
2023-07-12	4	26.1006239	13.5	partly_thawed
2023-07-13	4	31.041448	13.7	partly_thawed
2023-07-14	4	40.3052808	13.3	partly_thawed
2023-07-15	4	32.1065483	14.1	partly_thawed
2023-07-16	4	28.8956505	11.45	partly_thawed
2023-07-17	4	48.3482861	13.3	partly_thawed
2023-07-18	4	41.0063463	13.45	partly_thawed
2023-07-19	4	43.5113186	12	partly_thawed
2023-07-20	4	58.1198302	12.35	partly_thawed
2023-07-21	4	44.4942575	12.75	partly_thawed
2023-07-22	4	37.1977352	12	partly_thawed
2023-07-23	4	36.2617427	12.15	partly_thawed
2023-07-24	4	36.6393035	12.75	partly_thawed
2023-07-25	4	35.4331152	13.75	partly_thawed
2023-07-26	4	41.8456117	15	partly_thawed
2023-07-27	4	49.2020487	15.85	partly_thawed
2023-07-28	4	55.169586	16	partly_thawed
2023-07-29	4	46.2299463	15.05	partly_thawed
2023-07-30	4	51.4052057	13.95	partly_thawed
2023-07-31	4	38.8404046	13.85	partly_thawed
2023-08-01	4	43.0606422	14.4	partly_thawed
2023-08-02	4	44.7060991	13.95	partly_thawed
2023-08-03	4	34.382709	14.6	partly_thawed
2023-08-04	4	43.6758417	14.65	partly_thawed
2023-08-05	4	30.6957938	13.8	partly_thawed
2023-08-06	4	59.0955896	13.55	partly_thawed
2023-08-07	4	48.3871803	12.3	partly_thawed
2023-08-08	4	51.7724684	15	partly_thawed
2023-08-09	4	38.4434676	15.55	partly_thawed
2023-08-10	4	74.9909469	14.35	partly_thawed
2023-08-11	4	55.5844904	13.9	partly_thawed
2023-08-12	4	66.6026489	13.9	partly_thawed

https://doi.org/10.5194/egusphere-2026-467
Preprint. Discussion started: 29 January 2026

2023-08-13	4	58.589253	13.6	partly_thawed
2023-08-14	4	83.0673361	13.95	partly_thawed
2023-08-15	4	89.1140624	15.35	partly_thawed
2023-08-16	4	87.0601228	13.3	partly_thawed
2023-08-17	4	67.5630045	13.55	partly_thawed
2023-08-18	4	80.3882045	12.3	partly_thawed
2023-08-19	4	72.6660605	12.8	partly_thawed
2023-08-20	4	47.6804448	13.5	partly_thawed
2023-08-21	4	69.7409064	14.35	partly_thawed
2023-08-22	4	103.851364	14.75	partly_thawed
2023-08-23	4	100.810651	14.55	partly_thawed
2023-08-24	4	98.2969009	13.95	partly_thawed
2023-08-25	4	77.4292843	13	partly_thawed
2023-08-26	4	71.6129038	13.05	partly_thawed
2023-08-27	4	87.5944317	13.3	partly_thawed
2023-08-28	4	61.3708353	11.8	partly_thawed
2023-08-29	4	96.4069224	13	partly_thawed
2023-08-30	4	109.6439	13.7	partly_thawed
2023-05-25	5	1.46122778	4.85	intact
2023-05-26	5	0.6737177	2.5	intact
2023-05-29	5	0.54930674	4.4	intact
2023-05-30	5	2.60528065	5.2	intact
2023-05-31	5	-1.4114502	3	intact
2023-06-01	5	4.15535495	2.3	intact
2023-06-09	5	20.0151705	5.35	intact
2023-06-10	5	8.1201162	3.8	intact
2023-06-11	5	-0.4248935	10.1	intact
2023-06-12	5	3.14745001	6.8	intact
2023-06-13	5	0.593267	7.4	intact
2023-06-20	5	-2.0807684	13.9	intact
2023-06-21	5	27.2457403	14.9	intact
2023-06-22	5	32.2566005	15.3	intact
2023-06-23	5	60.9184426	14.8	intact
2023-06-24	5	11.4244715	11.95	intact
2023-06-26	5	33.3394485	11.3	intact
2023-06-27	5	24.0565414	13.3	intact
2023-06-29	5	57.0662104	12.8	intact
2023-06-30	5	35.8270265	14.7	intact
2023-07-01	5	119.791475	14.85	intact

https://doi.org/10.5194/egusphere-2026-467
Preprint. Discussion started: 29 January 2026

2023-07-02	5	89.6080711	13.25	intact
2023-07-03	5	57.8293841	12	intact
2023-07-04	5	40.1150495	12.4	intact
2023-07-05	5	35.7539116	11.85	intact
2023-07-06	5	22.465272	13.15	intact
2023-07-07	5	30.4546503	15.9	intact
2023-07-08	5	10.4237423	13.1	intact
2023-07-09	5	5.68477271	11.5	intact
2023-07-10	5	60.0125744	11.35	intact
2023-07-11	5	39.538247	15.9	intact
2023-07-12	5	14.1616398	13.7	intact
2023-07-13	5	49.5157043	14.05	intact
2023-07-14	5	37.5150978	15.4	intact
2023-07-15	5	25.6094225	11.7	intact
2023-07-16	5	33.9046124	9.6	intact
2023-07-17	5	29.4406576	13	intact
2023-07-20	5	79.9097731	12.3	intact
2023-07-21	5	56.6512727	12.2	intact
2023-07-22	5	70.3010276	12.6	intact
2023-07-24	5	61.2907393	12.7	intact
2023-07-25	5	58.2712421	12.6	intact
2023-07-26	5	56.4967571	12.35	intact
2023-07-27	5	50.2199107	13.3	intact
2023-07-28	5	62.2479228	13.55	intact
2023-07-29	5	52.9781105	14.1	intact
2023-08-01	5	88.4730115	14.1	intact
2023-08-02	5	39.9236586	12.9	intact
2023-08-04	5	75.8082139	14.5	intact
2023-08-05	5	81.302771	11.4	intact
2023-08-06	5	81.8067879	9.9	intact
2023-08-07	5	80.1733121	12.5	intact
2023-08-08	5	127.154145	16	intact
2023-08-09	5	47.2237119	15.5	intact
2023-08-10	5	123.58489	13.9	intact
2023-08-11	5	89.7526167	13.2	intact
2023-08-12	5	91.5041605	14.9	intact
2023-08-13	5	80.9764569	11.5	intact
2023-08-14	5	95.7200264	14.55	intact
2023-08-15	5	70.2118506	13.35	intact

https://doi.org/10.5194/egusphere-2026-467
Preprint. Discussion started: 29 January 2026

2023-08-16	5	81.7665149	11.6	intact
2023-08-17	5	11.3585358	11.8	intact
2023-08-18	5	33.9012364	11.85	intact
2023-08-19	5	59.6545486	11.5	intact
2023-08-20	5	70.2551536	10.9	intact
2023-08-21	5	66.8491835	13.65	intact
2023-08-22	5	65.2073029	13.7	intact
2023-08-23	5	86.9935888	14.1	intact
2023-08-24	5	73.8134836	12.9	intact
2023-08-25	5	80.2930753	10.6	intact
2023-08-26	5	71.1902386	11.6	intact
2023-08-27	5	44.9537462	12.4	intact
2023-08-28	5	50.1999253	11.5	intact
2023-08-29	5	52.3861745	12.7	intact
2023-08-30	5	106.122498	11.9	intact
2023-05-19	6	8.3630998	3.1	partly_thawed
2023-05-20	6	11.6693504	3.1	partly_thawed
2023-05-21	6	18.0408983	3.95	partly_thawed
2023-05-22	6	22.6504773	4.2	partly_thawed
2023-05-23	6	19.8541094	4.4	partly_thawed
2023-05-24	6	14.2022763	3.7	partly_thawed
2023-05-25	6	18.2098957	3.6	partly_thawed
2023-05-26	6	14.6898552	3.05	partly_thawed
2023-05-27	6	13.337191	3.2	partly_thawed
2023-05-28	6	17.0115001	4.4	partly_thawed
2023-05-29	6	17.7840109	4.15	partly_thawed
2023-05-30	6	20.0638626	3.9	partly_thawed
2023-05-31	6	22.4345768	3.9	partly_thawed
2023-06-01	6	20.6394943	3.1	partly_thawed
2023-06-02	6	21.4132642	4.45	partly_thawed
2023-06-03	6	23.4969754	5.4	partly_thawed
2023-06-04	6	18.4901259	5	partly_thawed
2023-06-05	6	12.4229704	4.85	partly_thawed
2023-06-06	6	16.9432259	5.6	partly_thawed
2023-06-07	6	23.442394	6.2	partly_thawed
2023-06-08	6	19.689198	5.65	partly_thawed
2023-06-09	6	30.7806593	6.75	partly_thawed
2023-06-10	6	29.6977711	6.65	partly_thawed
2023-06-11	6	19.6793493	7.05	partly_thawed

https://doi.org/10.5194/egusphere-2026-467
Preprint. Discussion started: 29 January 2026

2023-06-12	6	16.8144302	7.8	partly_thawed
2023-06-13	6	12.5208428	7.4	partly_thawed
2023-06-14	6	20.2614767	7.7	partly_thawed
2023-06-15	6	22.5828409	7.3	partly_thawed
2023-06-16	6	38.2572792	7.7	partly_thawed
2023-06-17	6	39.1763921	8.7	partly_thawed
2023-06-18	6	39.1541315	10.2	partly_thawed
2023-06-19	6	40.0347046	11.1	partly_thawed
2023-06-20	6	25.1664938	11.05	partly_thawed
2023-06-21	6	39.1694686	12.5	partly_thawed
2023-06-22	6	13.3026781	11.45	partly_thawed
2023-06-23	6	43.5449617	13.45	partly_thawed
2023-06-24	6	40.9599485	11.45	partly_thawed
2023-06-25	6	33.7630086	11.3	partly_thawed
2023-06-26	6	14.108924	10.3	partly_thawed
2023-06-27	6	29.1704193	11.3	partly_thawed
2023-06-28	6	34.0001316	11.7	partly_thawed
2023-06-29	6	57.9189061	12.3	partly_thawed
2023-06-30	6	21.4170225	12	partly_thawed
2023-07-01	6	19.7927166	11.55	partly_thawed
2023-07-02	6	33.649174	11.2	partly_thawed
2023-07-03	6	22.3059869	9.8	partly_thawed
2023-07-04	6	77.5904311	9.4	partly_thawed
2023-07-05	6	42.6626879	10.55	partly_thawed
2023-07-06	6	43.1515249	10.15	partly_thawed
2023-07-07	6	48.6732313	10.8	partly_thawed
2023-07-08	6	39.6743724	12.35	partly_thawed
2023-07-09	6	48.1502657	11.45	partly_thawed
2023-07-10	6	85.2151002	11.6	partly_thawed
2023-07-11	6	73.426825	12.6	partly_thawed
2023-07-12	6	28.3342259	11.7	partly_thawed
2023-07-13	6	24.0755872	11.7	partly_thawed
2023-07-14	6	19.4538447	12	partly_thawed
2023-07-15	6	48.9913041	12.25	partly_thawed
2023-07-16	6	20.5889678	10.3	partly_thawed
2023-07-17	6	68.5586901	10.7	partly_thawed
2023-07-18	6	50.322429	11.95	partly_thawed
2023-07-19	6	49.8566426	10.9	partly_thawed
2023-07-20	6	58.7793876	10.3	partly_thawed

https://doi.org/10.5194/egusphere-2026-467
Preprint. Discussion started: 29 January 2026

2023-07-21	6	35.0609548	11.3	partly_thawed
2023-07-22	6	26.8719461	11	partly_thawed
2023-07-23	6	29.127419	10.55	partly_thawed
2023-07-24	6	32.3729623	10.9	partly_thawed
2023-07-25	6	32.8231256	11.3	partly_thawed
2023-07-26	6	50.4473485	11.95	partly_thawed
2023-07-27	6	110.332247	12.55	partly_thawed
2023-07-28	6	92.7295683	12.75	partly_thawed
2023-07-29	6	60.3420529	13.45	partly_thawed
2023-07-30	6	53.361103	12.7	partly_thawed
2023-07-31	6	29.3270414	12.25	partly_thawed
2023-08-01	6	36.8111944	11.9	partly_thawed
2023-08-02	6	48.9128661	12.75	partly_thawed
2023-08-03	6	24.4034451	12.9	partly_thawed
2023-08-04	6	50.6965068	14.1	partly_thawed
2023-08-05	6	59.7348555	13.05	partly_thawed
2023-08-06	6	101.669452	11.3	partly_thawed
2023-08-07	6	46.415161	12	partly_thawed
2023-08-08	6	50.7337198	12.15	partly_thawed
2023-08-09	6	50.8757148	14.2	partly_thawed
2023-08-10	6	107.105636	14.2	partly_thawed
2023-08-11	6	57.6274551	13.3	partly_thawed
2023-08-12	6	68.3311498	12.55	partly_thawed
2023-08-13	6	50.7633661	12.6	partly_thawed
2023-08-14	6	105.827707	13.2	partly_thawed
2023-08-15	6	104.659029	13.9	partly_thawed
2023-08-16	6	90.186093	13.2	partly_thawed
2023-08-17	6	47.7516914	13.1	partly_thawed
2023-08-18	6	68.4988103	12.25	partly_thawed
2023-08-19	6	83.7797336	11.95	partly_thawed
2023-08-20	6	65.4200639	11.7	partly_thawed
2023-08-21	6	86.6755397	12.9	partly_thawed
2023-08-22	6	101.218752	13.6	partly_thawed
2023-08-23	6	105.18271	13.7	partly_thawed
2023-08-24	6	110.510497	12.8	partly_thawed
2023-08-25	6	101.360275	12.25	partly_thawed
2023-08-26	6	110.248594	11.4	partly_thawed
2023-08-27	6	74.1478638	11.9	partly_thawed
2023-08-28	6	63.0693781	11.9	partly_thawed

https://doi.org/10.5194/egusphere-2026-467
Preprint. Discussion started: 29 January 2026

2023-08-29	6	97.0584329	12.35	partly_thawed
2023-08-30	6	116.592803	13	partly_thawed
2023-05-19	7	49.334863	2.05	fully_thawed
2023-05-20	7	46.9200393	2.05	fully_thawed
2023-05-21	7	52.0751732	2.3	fully_thawed
2023-05-22	7	75.3469779	2.35	fully_thawed
2023-05-23	7	44.6685192	3	fully_thawed
2023-05-24	7	33.8936121	2.9	fully_thawed
2023-05-25	7	37.6489882	2.65	fully_thawed
2023-05-26	7	34.7523409	2.6	fully_thawed
2023-05-27	7	39.9671258	2.6	fully_thawed
2023-05-28	7	39.3415505	3.65	fully_thawed
2023-05-29	7	34.1545325	3.25	fully_thawed
2023-05-30	7	36.1480781	3.15	fully_thawed
2023-05-31	7	31.5812416	3.25	fully_thawed
2023-06-01	7	34.2491326	2.75	fully_thawed
2023-06-02	7	36.3974991	3.65	fully_thawed
2023-06-03	7	36.4606779	4	fully_thawed
2023-06-04	7	33.4537363	4.05	fully_thawed
2023-06-05	7	30.5260161	4	fully_thawed
2023-06-06	7	39.7875148	4.35	fully_thawed
2023-06-07	7	44.0400964	4.4	fully_thawed
2023-06-08	7	39.0480798	4.3	fully_thawed
2023-06-09	7	50.2600447	4.5	fully_thawed
2023-06-10	7	72.8707437	4.4	fully_thawed
2023-06-11	7	54.8621741	5.3	fully_thawed
2023-06-12	7	46.3315212	5.85	fully_thawed
2023-06-13	7	46.4795599	5.7	fully_thawed
2023-06-14	7	49.2634297	5.75	fully_thawed
2023-06-15	7	52.4206463	5.8	fully_thawed
2023-06-16	7	74.340552	5.15	fully_thawed
2023-06-17	7	80.1579366	4.9	fully_thawed
2023-06-18	7	92.6844436	5.8	fully_thawed
2023-06-19	7	112.902023	6.45	fully_thawed
2023-06-20	7	76.8289006	7.1	fully_thawed
2023-06-21	7	103.716188	9.15	fully_thawed
2023-06-22	7	64.6615473	7.75	fully_thawed
2023-06-23	7	104.424053	8.5	fully_thawed
2023-06-24	7	91.6352675	7.5	fully_thawed

https://doi.org/10.5194/egusphere-2026-467
Preprint. Discussion started: 29 January 2026

2023-06-25	7	108.874606	7.15	fully_thawed
2023-06-26	7	78.4405403	6.4	fully_thawed
2023-06-27	7	97.4924365	7.45	fully_thawed
2023-06-28	7	138.313482	7.35	fully_thawed
2023-06-29	7	150.786801	6.75	fully_thawed
2023-06-30	7	82.7247754	7.15	fully_thawed
2023-07-01	7	93.5174097	6.65	fully_thawed
2023-07-02	7	84.1199896	6.65	fully_thawed
2023-07-03	7	68.8906932	5.35	fully_thawed
2023-07-04	7	125.311515	4.65	fully_thawed
2023-07-05	7	82.7811367	6.6	fully_thawed
2023-07-06	7	115.519992	5.8	fully_thawed
2023-07-07	7	83.6127463	6.15	fully_thawed
2023-07-08	7	117.799471	7.45	fully_thawed
2023-07-09	7	127.258105	7.15	fully_thawed
2023-07-10	7	134.356642	5.05	fully_thawed
2023-07-11	7	119.822284	6.3	fully_thawed
2023-07-12	7	63.2641997	6.6	fully_thawed
2023-07-13	7	73.3970921	6.95	fully_thawed
2023-07-14	7	64.4319988	7.35	fully_thawed
2023-07-15	7	87.7517355	8.2	fully_thawed
2023-07-16	7	60.0648654	6.65	fully_thawed
2023-07-17	7	86.8304636	6.3	fully_thawed
2023-07-18	7	89.9447192	7.4	fully_thawed
2023-07-19	7	104.248884	7.1	fully_thawed
2023-07-20	7	96.1184814	7.2	fully_thawed
2023-07-21	7	72.9758352	8.2	fully_thawed
2023-07-22	7	50.8879982	8.25	fully_thawed
2023-07-23	7	47.890464	7.85	fully_thawed
2023-07-24	7	67.628543	8.05	fully_thawed
2023-07-25	7	66.104418	8.3	fully_thawed
2023-07-26	7	59.0960214	8.85	fully_thawed
2023-07-27	7	107.272419	8.55	fully_thawed
2023-07-28	7	125.58199	9.45	fully_thawed
2023-07-29	7	105.040756	10.35	fully_thawed
2023-07-30	7	71.9771293	9.4	fully_thawed
2023-07-31	7	49.8456284	10	fully_thawed
2023-08-01	7	67.1301054	10.3	fully_thawed
2023-08-02	7	68.0543255	9.55	fully_thawed

https://doi.org/10.5194/egusphere-2026-467
Preprint. Discussion started: 29 January 2026

2023-08-03	7	53.418273	10.25	fully_thawed
2023-08-04	7	87.755188	12	fully_thawed
2023-08-05	7	107.694219	11.25	fully_thawed
2023-08-06	7	142.426043	9.6	fully_thawed
2023-08-07	7	59.0778337	10.3	fully_thawed
2023-08-08	7	70.8195516	11.5	fully_thawed
2023-08-09	7	61.1767954	13.2	fully_thawed
2023-08-10	7	122.236264	13.4	fully_thawed
2023-08-11	7	76.1331003	12.6	fully_thawed
2023-08-12	7	86.5827151	12.55	fully_thawed
2023-08-13	7	87.0160802	11.85	fully_thawed
2023-08-14	7	134.443476	12.7	fully_thawed
2023-08-15	7	177.273142	13.35	fully_thawed
2023-08-16	7	123.484146	12.3	fully_thawed
2023-08-17	7	131.386761	12.1	fully_thawed
2023-08-18	7	171.532134	11.05	fully_thawed
2023-08-19	7	103.586558	10.75	fully_thawed
2023-08-20	7	76.0763399	11.15	fully_thawed
2023-08-21	7	89.1069265	12.2	fully_thawed
2023-08-22	7	147.526551	12.65	fully_thawed
2023-08-23	7	182.018833	12.9	fully_thawed
2023-08-24	7	242.91605	11.9	fully_thawed
2023-08-25	7	112.696976	11	fully_thawed
2023-08-26	7	204.616261	10.2	fully_thawed
2023-08-27	7	88.5555957	10.1	fully_thawed
2023-08-28	7	69.6624609	10.95	fully_thawed
2023-08-29	7	83.0563735	11.75	fully_thawed
2023-08-30	7	198.675869	11.95	fully_thawed
2023-05-19	8	34.7006239	9.4	fully_thawed
2023-05-20	8	20.7060914	11.2	fully_thawed
2023-05-21	8	39.7632249	10.7	fully_thawed
2023-05-22	8	51.4766506	12.9	fully_thawed
2023-05-23	8	39.2495605	9.95	fully_thawed
2023-05-24	8	33.4763883	8.9	fully_thawed
2023-05-25	8	21.6617507	7.9	fully_thawed
2023-05-26	8	31.3390259	4.5	fully_thawed
2023-05-27	8	32.3995898	6.85	fully_thawed
2023-05-28	8	19.3751497	7.65	fully_thawed
2023-05-29	8	20.5861088	7.35	fully_thawed

https://doi.org/10.5194/egusphere-2026-467
Preprint. Discussion started: 29 January 2026

2023-05-30	8	37.5520532	6.75	fully_thawed
2023-05-31	8	23.703279	4.75	fully_thawed
2023-06-01	8	24.8348066	6	fully_thawed
2023-06-02	8	36.1691973	7.35	fully_thawed
2023-06-03	8	35.2229112	7.9	fully_thawed
2023-06-04	8	34.5912683	8.05	fully_thawed
2023-06-05	8	23.7471868	7.1	fully_thawed
2023-06-06	8	34.8645607	9	fully_thawed
2023-06-07	8	51.7544084	10.15	fully_thawed
2023-06-08	8	30.2154105	9	fully_thawed
2023-06-09	8	55.8270964	9.85	fully_thawed
2023-06-10	8	58.3342632	12.4	fully_thawed
2023-06-11	8	63.8823588	13.5	fully_thawed
2023-06-12	8	58.3933537	13.25	fully_thawed
2023-06-13	8	42.5780141	11.7	fully_thawed
2023-06-14	8	38.3218216	11.3	fully_thawed
2023-06-15	8	42.1898655	12.3	fully_thawed
2023-06-16	8	91.4366961	16	fully_thawed
2023-06-17	8	97.7764602	15.85	fully_thawed
2023-06-18	8	115.451319	18.45	fully_thawed
2023-06-19	8	104.867502	18.55	fully_thawed
2023-06-20	8	93.700883	17.95	fully_thawed
2023-06-21	8	86.0736841	18.05	fully_thawed
2023-06-22	8	64.7044161	17.9	fully_thawed
2023-06-23	8	121.630873	15.35	fully_thawed
2023-06-24	8	123.917059	11.9	fully_thawed
2023-06-25	8	114.339939	15.8	fully_thawed
2023-06-26	8	82.7727499	15.2	fully_thawed
2023-06-27	8	100.223707	16.65	fully_thawed
2023-06-28	8	111.760012	18.2	fully_thawed
2023-06-29	8	125.297228	20.15	fully_thawed
2023-06-30	8	85.4755693	16.45	fully_thawed
2023-07-01	8	74.3489467	14.85	fully_thawed
2023-07-02	8	103.054436	8.95	fully_thawed
2023-07-03	8	83.7350237	10.5	fully_thawed
2023-07-04	8	124.946855	17.05	fully_thawed
2023-07-05	8	89.2157471	12.4	fully_thawed
2023-07-06	8	101.540381	16.95	fully_thawed
2023-07-07	8	90.7057301	18.65	fully_thawed

https://doi.org/10.5194/egusphere-2026-467
Preprint. Discussion started: 29 January 2026

2023-07-08	8	82.0840488	14.55	fully_thawed
2023-07-09	8	99.1335258	17	fully_thawed
2023-07-10	8	103.139045	19.3	fully_thawed
2023-07-11	8	91.7801651	22.8	fully_thawed
2023-07-12	8	43.576118	15.9	fully_thawed
2023-07-13	8	60.9340832	14.95	fully_thawed
2023-07-14	8	60.0526603	13.7	fully_thawed
2023-07-15	8	76.4054909	15	fully_thawed
2023-07-16	8	45.7691207	13.25	fully_thawed
2023-07-17	8	88.0293306	15.75	fully_thawed
2023-07-18	8	79.4695261	14.5	fully_thawed
2023-07-19	8	72.7707008	11.7	fully_thawed
2023-07-20	8	100.605945	13.7	fully_thawed
2023-07-21	8	54.6632769	13.2	fully_thawed
2023-07-22	8	49.1530095	12.85	fully_thawed
2023-07-23	8	52.0787468	12.45	fully_thawed
2023-07-24	8	55.5108827	13.2	fully_thawed
2023-07-25	8	55.0531341	14.75	fully_thawed
2023-07-26	8	80.6270529	14.8	fully_thawed
2023-07-27	8	179.422789	17	fully_thawed
2023-07-28	8	135.095657	18.4	fully_thawed
2023-07-29	8	121.325816	16.25	fully_thawed
2023-07-30	8	112.376703	15.35	fully_thawed
2023-07-31	8	65.010212	16.8	fully_thawed
2023-08-01	8	98.6857163	15.35	fully_thawed
2023-08-02	8	98.081123	15.55	fully_thawed
2023-08-03	8	55.3702881	15.25	fully_thawed
2023-08-04	8	118.522215	16.7	fully_thawed
2023-08-05	8	138.729082	12.55	fully_thawed
2023-08-06	8	190.065485	15.6	fully_thawed
2023-08-07	8	64.4686313	14.7	fully_thawed
2023-08-08	8	72.2752781	17.45	fully_thawed
2023-08-09	8	78.5584928	17.3	fully_thawed
2023-08-10	8	158.331138	14.8	fully_thawed
2023-08-11	8	79.5334828	14.4	fully_thawed
2023-08-12	8	96.4098046	13.55	fully_thawed
2023-08-13	8	74.9828709	13.95	fully_thawed
2023-08-14	8	140.817714	14.8	fully_thawed
2023-08-15	8	249.731429	16.1	fully_thawed

https://doi.org/10.5194/egusphere-2026-467
Preprint. Discussion started: 29 January 2026

2023-08-16	8	151.419455	12.8	fully_thawed
2023-08-17	8	151.557401	12.35	fully_thawed
2023-08-18	8	163.595921	14	fully_thawed
2023-08-19	8	80.9519732	12.15	fully_thawed
2023-08-20	8	62.6858435	13.65	fully_thawed
2023-08-21	8	71.1987865	14.6	fully_thawed
2023-08-22	8	197.024031	14.7	fully_thawed
2023-08-23	8	225.034049	14.75	fully_thawed
2023-08-24	8	154.545038	15.05	fully_thawed
2023-08-25	8	100.121819	13.5	fully_thawed
2023-08-26	8	142.596869	15.45	fully_thawed
2023-08-27	8	68.0651359	12.9	fully_thawed
2023-08-28	8	61.5780643	13.3	fully_thawed
2023-08-29	8	89.8932177	12.75	fully_thawed
2023-08-30	8	194.667128	14.35	fully_thawed
2023-05-19	9	21.8601571	1.3	fully_thawed
2023-05-20	9	15.2725512	1.35	fully_thawed
2023-05-21	9	23.3541124	1.3	fully_thawed
2023-05-22	9	46.1883437	1.2	fully_thawed
2023-05-23	9	28.4648803	1.6	fully_thawed
2023-05-24	9	20.6993939	1.65	fully_thawed
2023-05-25	9	23.3251575	1.6	fully_thawed
2023-05-26	9	25.8304637	1.7	fully_thawed
2023-05-27	9	29.0562812	1.7	fully_thawed
2023-05-28	9	28.4121618	1.8	fully_thawed
2023-05-29	9	21.9174638	1.7	fully_thawed
2023-05-30	9	30.1660976	2	fully_thawed
2023-05-31	9	18.2088374	1.85	fully_thawed
2023-06-01	9	28.7907459	1.95	fully_thawed
2023-06-02	9	31.9483831	2.2	fully_thawed
2023-06-03	9	15.9631516	2.9	fully_thawed
2023-06-04	9	17.8134991	3.2	fully_thawed
2023-06-05	9	17.2227231	2.7	fully_thawed
2023-06-06	9	27.7192954	3.3	fully_thawed
2023-06-07	9	30.9188492	3.4	fully_thawed
2023-06-08	9	16.9136484	3.1	fully_thawed
2023-06-09	9	32.4575906	3.6	fully_thawed
2023-06-10	9	30.0779752	3.1	fully_thawed
2023-06-11	9	43.2075311	3.1	fully_thawed

https://doi.org/10.5194/egusphere-2026-467
Preprint. Discussion started: 29 January 2026

2023-06-12	9	18.1121587	3.4	fully_thawed
2023-06-13	9	11.5920986	3.3	fully_thawed
2023-06-14	9	20.0512105	3.1	fully_thawed
2023-06-15	9	28.7655978	2.8	fully_thawed
2023-06-16	9	42.6659009	1.6	fully_thawed
2023-06-17	9	43.4093611	0.9	fully_thawed
2023-06-18	9	34.4648482	1.1	fully_thawed
2023-06-19	9	53.9728336	1.2	fully_thawed
2023-06-20	9	35.0823231	1.1	fully_thawed
2023-06-21	9	44.3443703	3.45	fully_thawed
2023-06-22	9	40.5118492	1.15	fully_thawed
2023-06-23	9	66.3432432	4.15	fully_thawed
2023-06-24	9	71.9940645	3.95	fully_thawed
2023-06-25	9	66.9624634	4.3	fully_thawed
2023-06-26	9	37.829216	2.7	fully_thawed
2023-06-27	9	43.2616535	3.3	fully_thawed
2023-06-28	9	35.4868038	3.15	fully_thawed
2023-06-29	9	56.0230485	2.5	fully_thawed
2023-06-30	9	36.3826788	3.1	fully_thawed
2023-07-01	9	36.7027491	2.6	fully_thawed
2023-07-02	9	62.9398655	4.05	fully_thawed
2023-07-03	9	34.0261777	3.7	fully_thawed
2023-07-04	9	106.305431	2.1	fully_thawed
2023-07-05	9	69.6056053	4.6	fully_thawed
2023-07-06	9	55.6372893	3.6	fully_thawed
2023-07-07	9	54.1536993	2.05	fully_thawed
2023-07-08	9	56.7964652	4.7	fully_thawed
2023-07-09	9	84.4408589	3.75	fully_thawed
2023-07-10	9	138.094439	2.6	fully_thawed
2023-07-11	9	90.4711308	3.1	fully_thawed
2023-07-12	9	49.3281588	3.7	fully_thawed
2023-07-13	9	67.5695327	4.2	fully_thawed
2023-07-14	9	64.166318	5.5	fully_thawed
2023-07-15	9	92.4036704	6.8	fully_thawed
2023-07-16	9	61.672136	6.2	fully_thawed
2023-07-17	9	118.601218	5.9	fully_thawed
2023-07-18	9	86.5749823	7.9	fully_thawed
2023-07-19	9	110.341088	8	fully_thawed
2023-07-20	9	94.3315022	7.7	fully_thawed

https://doi.org/10.5194/egusphere-2026-467
Preprint. Discussion started: 29 January 2026

2023-07-21	9	77.8990507	8.75	fully_thawed
2023-07-22	9	76.7521751	8.85	fully_thawed
2023-07-23	9	65.2453703	8.6	fully_thawed
2023-07-24	9	80.0353096	9.3	fully_thawed
2023-07-25	9	62.3878736	9.7	fully_thawed
2023-07-26	9	97.3968974	9.15	fully_thawed
2023-07-27	9	191.698098	9.7	fully_thawed
2023-07-28	9	193.206865	10.7	fully_thawed
2023-07-29	9	92.986422	11.3	fully_thawed
2023-07-30	9	117.88812	11.5	fully_thawed
2023-07-31	9	83.9161709	10.45	fully_thawed
2023-08-01	9	82.0950356	11.6	fully_thawed
2023-08-02	9	136.809756	11.6	fully_thawed
2023-08-03	9	96.5049759	11.7	fully_thawed
2023-08-04	9	113.08585	13.1	fully_thawed
2023-08-05	9	102.427354	12.75	fully_thawed
2023-08-06	9	299.392644	12.3	fully_thawed
2023-08-07	9	94.2441887	12.15	fully_thawed
2023-08-08	9	88.0675217	10.9	fully_thawed
2023-08-09	9	104.1454	13.1	fully_thawed
2023-08-10	9	202.513157	13.4	fully_thawed
2023-08-11	9	109.054042	13.1	fully_thawed
2023-08-12	9	100.641251	12.7	fully_thawed
2023-08-13	9	90.3502941	12.9	fully_thawed
2023-08-14	9	113.301802	12.65	fully_thawed
2023-08-15	9	270.537667	12.6	fully_thawed
2023-08-16	9	233.716298	12.65	fully_thawed
2023-08-17	9	153.002257	12.3	fully_thawed
2023-08-18	9	165.807156	12.1	fully_thawed
2023-08-19	9	269.796425	11.5	fully_thawed
2023-08-20	9	115.506318	11.55	fully_thawed
2023-08-21	9	200.724416	11.9	fully_thawed
2023-08-22	9	285.042443	12.5	fully_thawed
2023-08-23	9	263.455436	12.65	fully_thawed
2023-08-24	9	146.866361	12	fully_thawed
2023-08-25	9	135.188755	10.9	fully_thawed
2023-08-26	9	302.047003	11.45	fully_thawed
2023-08-27	9	160.286048	11	fully_thawed
2023-08-28	9	95.1710018	11.15	fully_thawed

https://doi.org/10.5194/egusphere-2026-467
Preprint. Discussion started: 29 January 2026

2023-08-29	9	164.601244	11.2	fully_thawed
2023-08-30	9	375.879582	11.7	fully_thawed

Table C5: Results of generalized additive models (GAM) used for determining CH_4 flux season values. Note: Intact 3 plot GAM R^2_{adj}<0.1, and the CH_4 flux periods are based on moving 7-day medians. CI = 95% confidence interval.

Chamber	R^2_{adj}	p-value	CH_4 flux period	CH_4 flux period value (mg CH_4 m^{-2} d^{-1})	95% CI	CH_4 flux period date (YYYY-MM-DD)
Intact 1	0.19	<0.001	Early	0.135	-0.43 - 0.74	2023-08-01
			Middle	2.029	0.91 - 4	2023-08-21
			Peak	4.297	1.45 - 11.78	2023-08-30
Intact 2	-	-	Early	-0.05	-	2023-05-20
			Middle	8.041	-	2023-07-05
			Peak	11.384	-	2023-08-16
Intact 3	0.63	<0.001	Early	7.717	4.89 - 12.14	2023-06-18
			Middle	36.032	24.8 - 52.35	2023-07-10
			Peak	69.088	47.49 - 100.5	2023-08-11
Partly thawed 1	0.62	<0.001	Early	11.335	9.18 - 13	2023-06-12
			Middle	34.584	28.18 - 42.44	2023-07-15
			Peak	62.697	42.24 - 93.05	2023-08-30
Partly thawed 2	0.8	<0.001	Early	22.021	19.24 - 25.21	2023-06-25
			Middle	53.96	47.02 - 61.93	2023-08-08
			Peak	93.89	72.48 - 121.63	2023-08-30
Partly thawed 3	0.67	<0.001	Early	23.018	20.89 - 25.36	2023-06-12
			Middle	54.945	50.33 - 59.98	2023-07-31
			Peak	93.581	81.22 - 107.82	2023-08-30
Fully thawed 1	0.66	<0.001	Early	50.609	38.82 - 65.97	2023-05-19
			Middle	84.967	73.8 - 97.82	2023-06-21
			Peak	128.204	110.11 - 149.27	2023-08-25
Fully thawed 2	0.66	<0.001	Early	40.038	33.88 - 47.31	2023-06-07
			Middle	77.439	65.64 - 91.37	2023-06-18
			Peak	119.496	100.37 - 142.27	2023-08-19
Fully thawed 3	0.8	<0.001	Early	39.268	36.12 - 42.7	2023-06-19
			Middle	121.25	110.57 - 132.96	2023-08-05
			Peak	220.851	192.54 - 253.33	2023-08-30

Data availability

The belowground trait and vegetation survey data together with edaphic variables (Määttä and Malhotra, 2026) can be openly accessed at https://doi.org/10.5281/zenodo.18269229. The porewater CH_4 and $\delta^{13}C$ data (Wilson et al., 2026) is available with open access at https://doi.org/10.5281/zenodo.18363867. The daily-aggregated automated chamber CH_4 flux data from the productive season is shown in the Appendices (Table C4). The full dataset will be published in the EMERGE-DB database (Bolduc et al., 2020) by May 2026 (https://emerge-db.asc.ohio-state.edu/).

https://doi.org/10.5194/egusphere-2026-467
Preprint. Discussion started: 29 January 2026

Author contributions

TM and AM conceptualized the study and prepared the original manuscript draft. Data curation and provision of resources was done by TM, RV, PC, SH, RW, SB, and JC. TM conducted the formal analysis, investigation, and visualization, and collected and processed the belowground trait data. Chamber CH_4 flux data was collected and provided by RV and PC, and porewater gas data by SH, SB, RW and JC. AM and TM acquired funding for the study and coordinated the project. AM supervised the project. All authors contributed to the review and editing of the manuscript.

Competing interests

The authors declare that they have no conflict of interest.

Acknowledgements

We thank Melina Bucher and Charmaine Bassfeld for their assistance in the field and laboratory work. We are grateful to Yves Brügger and Thomas Keller for their help in the laboratory at the University of Zurich, and also to Martina Peter, Felix Zimmermann, and Mara Wieser for providing access to, and support in, the laboratory at the Swiss Federal Research Institute WSL. We also thank Christina Biasi and Maija Marushchak, and Apryl Perry, Carmody McCalley and Cheristy Jones for automated chamber CH_4 flux data, and Nitin Chaudhary for valuable insights. We acknowledge funding from the Swiss Polar Institute Polar Access Grant (PAF-2023-001) awarded to TM, Universität Zürich Stiftung für Wissenschaftliche Forschung (STWF-22-028) and the Swiss National Science Foundation (project 200021_215214) awarded to AM. AM was also supported by an Early Career Award from the U.S. Department of Energy, Office of Science, Biological and Environmental Research. We thank Alisa Heuchel, the Swedish Polar Research Secretariat and SITES for the support of the work done at the Abisko Scientific Research Station. SITES is supported by the Swedish Research Council. Porewater and automated chamber flux data were collected and analyzed using funding from the EMERGE Biology Integration Institute, funded by the National Science Foundation, Biology Integration Institutes Program, Award #2022070 awarded to Virginia Rich and RV. RV was also funded by the US Department of Energy's Genomic Sciences Program grant (DE-SC0023456).

https://doi.org/10.5194/egusphere-2026-467
Preprint. Discussion started: 29 January 2026

References

Armstrong, W., Justin, S. H. F. W., Beckett, P. M., and Lythe, S.: Root adaptation to soil waterlogging, Aquat. Bot., 39, 57–73, https://doi.org/10.1016/0304-3770(91)90022-w, 1991.

Bäckstrand, K., Crill, P. M., Mastepanov, M., Christensen, T. R., and Bastviken, D.: Non-methane volatile organic compound flux from a subarctic mire in Northern Sweden, Tellus B Chem. Phys. Meteorol., 60, 226, https://doi.org/10.1111/j.1600-0889.2007.00331.x, 2008.

Bergmann, J., Weigelt, A., van der Plas, F., Laughlin, D. C., Kuyper, T. W., Guerrero-Ramirez, N., Valverde-Barrantes, O. J., Bruelheide, H., Freschet, G. T., Iversen, C. M., Kattge, J., McCormack, M. L., Meier, I. C., Rillig, M. C., Roumet, C., Semchenko, M., Sweeney, C. J., van Ruijven, J., York, L. M., and Mommer, L.: The fungal collaboration gradient dominates the root economics space in plants, Sci. Adv., 6, https://doi.org/10.1126/sciadv.aba3756, 2020.

van den Berg, M., van den Elzen, E., Ingwersen, J., Kosten, S., Lamers, L. P. M., and Streck, T.: Contribution of plant-induced pressurized flow to CH4 emission from a Phragmites fen, Sci. Rep., 10, 12304, https://doi.org/10.1038/s41598-020-69034-7, 2020.

Bhullar, G. S., Edwards, P. J., and Olde Venterink, H.: Variation in the plant-mediated methane transport and its importance for methane emission from intact wetland peat mesocosms, J. Plant Ecol., 6, 298–304, https://doi.org/10.1093/jpe/rts045, 2013.

Billings, W. D., Peterson, K. M., and Shaver, G. R.: Growth, turnover, and respiration rates of roots and tillers in tundra graminoids, in: Ecological Studies, Springer New York, New York, NY, 415–434, https://doi.org/10.1007/978-1-4612-6307-4_18, 1978.

Blume-Werry, G., Wilson, S. D., Kreyling, J., and Milbau, A.: The hidden season: growing season is 50% longer below than above ground along an arctic elevation gradient, New Phytol., 209, 978–986, https://doi.org/10.1111/nph.13655, 2016.

Blume-Werry, G., Milbau, A., Teuber, L. M., Johansson, M., and Dorrepaal, E.: Dwelling in the deep - strongly increased root growth and rooting depth enhance plant interactions with thawing permafrost soil, New Phytol., 223, 1328–1339, https://doi.org/10.1111/nph.15903, 2019.

https://doi.org/10.5194/egusphere-2026-467
Preprint. Discussion started: 29 January 2026

Bolduc, B., Hodgkins, S. B., Varner, R. K., Crill, P. M., McCalley, C. K., Chanton, J. P., Tyson, G. W., Riley, W. J., Palace, M., Duhaime, M. B., Hough, M. A., Saleska, S. R., Sullivan, M. B., Rich, V. I., and IsoGenie Project Coordinators, IsoGenie Project Team, A2A Project Team: The IsoGenie database: an interdisciplinary data management solution for ecosystems biology and environmental research, PeerJ, 8, e9467, https://doi.org/10.7717/peerj.9467, 2020.

Bouchard, V., Frey, S. D., Gilbert, J. M., and Reed, S. E.: Effects of macrophyte functional group richness on emergent freshwater wetland functions, Ecology, 88, 2903–2914, https://doi.org/10.1890/06-1144.1, 2007.

Bubier, J., Crill, P., Mosedale, A., Frolking, S., and Linder, E.: Peatland responses to varying interannual moisture conditions as measured by automatic CO2chambers: PEATLAND RESPONSES TO INTERANNUAL MOISTURE, Global Biogeochem. Cycles, 17, https://doi.org/10.1029/2002gb001946, 2003.

Chanton, J., Whiting, G., Blair, N., Lindau, C., and Bollich, P.: Methane emission from rice: Stable isotopes, diurnal variations, and CO2 exchange, Global Biogeochemical Cycles, 11, 15–27, 1997.

Chanton, J. P.: The effect of gas transport on the isotope signature of methane in wetlands, Org. Geochem., 36, 753–768, https://doi.org/10.1016/j.orggeochem.2004.10.007, 2005.

Chanton, J. P. and Dacey, J. W. H.: Effects of vegetation on methane flux, reservoirs, and carbon isotopic composition, in: Trace Gas Emissions by Plants, Elsevier, 65–92, https://doi.org/10.1016/b978-0-12-639010-0.50008-x, 1991.

Chapin, F. S., III, Fetcher, N., Kielland, K., Everett, K. R., and Linkins, A. E.: Productivity and nutrient cycling of Alaskan tundra: Enhancement by flowing soil water, Ecology, 69, 693–702, https://doi.org/10.2307/1941017, 1988.

Christensen, T. R., Jonasson, S., Callaghan, T. V., and Havström, M.: On the potential CO2 release from tundra soils in a changing climate, Appl. Soil Ecol., 11, 127–134, https://doi.org/10.1016/s0929-1393(98)00146-2, 1999.

Christensen, T. R., Johansson, T., Åkerman, H. J., Mastepanov, M., Malmer, N., Friborg, T., Crill, P., and Svensson, B. H.: Thawing sub-arctic permafrost: Effects on vegetation and methane emissions, Geophys. Res. Lett., 31, https://doi.org/10.1029/2003gl018680, 2004.

Covey, K. R. and Megonigal, J. P.: Methane production and emissions in trees and forests, New Phytol., 222, 35–51, https://doi.org/10.1111/nph.15624, 2019.

https://doi.org/10.5194/egusphere-2026-467
Preprint. Discussion started: 29 January 2026

Crill, P., McCalley, C., and Crew, A. F.: Manual active layer and and water table depth measurements from the autochamber sites at Stordalen Mire, northern Sweden (2003-2017), https://doi.org/10.5281/ZENODO.10420396, 2023.

Delwiche, K. B., Knox, S. H., Malhotra, A., Fluet-Chouinard, E., McNicol, G., Feron, S., Ouyang, Z., Papale, D., Trotta, C., Canfora, E., and Others: FLUXNET-CH4: A global, multi-ecosystem dataset and analysis of methane seasonality from freshwater wetlands, Earth System Science Data Discussions, 2021, 1–111, 2021.

Díaz, S., Kattge, J., Cornelissen, J. H. C., Wright, I. J., Lavorel, S., Dray, S., Reu, B., Kleyer, M., Wirth, C., Colin Prentice, I., Garnier, E., Bönisch, G., Westoby, M., Poorter, H., Reich, P. B., Moles, A. T., Dickie, J., Gillison, A. N., Zanne, A. E., Chave, J., Joseph Wright, S., Sheremet'ev, S. N., Jactel, H., Baraloto, C., Cerabolini, B., Pierce, S., Shipley, B., Kirkup, D., Casanoves, F., Joswig, J. S., Günther, A., Falczuk, V., Rüger, N., Mahecha, M. D., and Gorné, L. D.: The global spectrum of plant form and function, Nature, 529, 167–171, https://doi.org/10.1038/nature16489, 2016.

Dong, N., Prentice, I. C., Wright, I. J., Evans, B. J., Togashi, H. F., Caddy-Retalic, S., McInerney, F. A., Sparrow, B., Leitch, E., and Lowe, A. J.: Components of leaf-trait variation along environmental gradients, New Phytol., 228, 82–94, https://doi.org/10.1111/nph.16558, 2020.

Dullo, B. W., Grootjans, A. P., Roelofs, J. G. M., Senbeta, A. F., Fritz, C., and Lamers, L. P. M.: Radial oxygen loss by the cushion plant Eriocaulon schimperi prevents methane emissions from an East-African mountain mire, Plant Biol. (Stuttg.), 19, 736–741, https://doi.org/10.1111/plb.12586, 2017.

Eissenstat, D. M., Wells, C. E., Yanai, R. D., and Whitbeck, J. L.: Building roots in a changing environment: implications for root longevity, New Phytol., 147, 33–42, https://doi.org/10.1046/j.1469-8137.2000.00686.x, 2000.

Eklundh, L. and Jönsson, P.: TIMESAT: A software package for time-series processing and assessment of vegetation dynamics, in: Remote Sensing Time Series, Springer International Publishing, Cham, 141–158, https://doi.org/10.1007/978-3-319-15967-6_7, 2015.

Freschet, G. T., Valverde-Barrantes, O. J., Tucker, C. M., Craine, J. M., McCormack, M. L., Violle, C., Fort, F., Blackwood, C. B., Urban-Mead, K. R., Iversen, C. M., Bonis, A., Comas, L. H., Cornelissen, J. H. C., Dong, M., Guo, D., Hobbie, S. E., Holdaway, R. J., Kembel, S. W., Makita, N., Onipchenko, V. G., Picon-Cochard, C., Reich, P. B., de la Riva, E. G., Smith, S. W., Soudzilovskaia, N. A., Tjoelker, M. G., Wardle, D. A., and Roumet, C.: Climate, soil and plant functional types as drivers of global fine-root trait variation, J. Ecol., 105, 1182–1196, https://doi.org/10.1111/1365-2745.12769, 2017.

https://doi.org/10.5194/egusphere-2026-467
Preprint. Discussion started: 29 January 2026

Freschet, G. T., Pagès, L., Iversen, C. M., Comas, L. H., Rewald, B., Roumet, C., Klimešová, J., Zadworny, M., Poorter, H., Postma, J. A., Adams, T. S., Bagniewska-Zadworna, A., Bengough, A. G., Blancaflor, E. B., Brunner, I., Cornelissen, J. H. C., Garnier, E., Gessler, A., Hobbie, S. E., Meier, I. C., Mommer, L., Picon-Cochard, C., Rose, L., Ryser, P., Scherer-Lorenzen, M., Soudzilovskaia, N. A., Stokes, A., Sun, T., Valverde-Barrantes, O. J., Weemstra, M., Weigelt, A., Wurzburger, N., York, L. M., Batterman, S. A., Gomes de Moraes, M., Janeček, Š., Lambers, H., Salmon, V., Tharayil, N., and McCormack, M. L.: A starting guide to root ecology: strengthening ecological concepts and standardising root classification, sampling, processing and trait measurements, New Phytol., 232, 973–1122, https://doi.org/10.1111/nph.17572, 2021a.

Freschet, G. T., Roumet, C., Comas, L. H., Weemstra, M., Bengough, A. G., Rewald, B., Bardgett, R. D., De Deyn, G. B., Johnson, D., Klimešová, J., Lukac, M., McCormack, M. L., Meier, I. C., Pagès, L., Poorter, H., Prieto, I., Wurzburger, N., Zadworny, M., Bagniewska-Zadworna, A., Blancaflor, E. B., Brunner, I., Gessler, A., Hobbie, S. E., Iversen, C. M., Mommer, L., Picon-Cochard, C., Postma, J. A., Rose, L., Ryser, P., Scherer-Lorenzen, M., Soudzilovskaia, N. A., Sun, T., Valverde-Barrantes, O. J., Weigelt, A., York, L. M., and Stokes, A.: Root traits as drivers of plant and ecosystem functioning: current understanding, pitfalls and future research needs, New Phytol., 232, 1123–1158, https://doi.org/10.1111/nph.17072, 2021b.

Fritz, C., Pancotto, V. A., Elzenga, J. T. M., Visser, E. J. W., Grootjans, A. P., Pol, A., Iturraspe, R., Roelofs, J. G. M., and Smolders, A. J. P.: Zero methane emission bogs: extreme rhizosphere oxygenation by cushion plants in Patagonia, New Phytol., 190, 398–408, https://doi.org/10.1111/j.1469-8137.2010.03604.x, 2011.

Frolking, S., Roulet, N. T., Tuittila, E., Bubier, J. L., Quillet, A., Talbot, J., and Richard, P. J. H.: A new model of Holocene peatland net primary production, decomposition, water balance, and peat accumulation, Earth Syst. Dyn., 1, 1–21, https://doi.org/10.5194/esd-1-1-2010, 2010.

Ge, M., Korrensalo, A., Putkinen, A., Laiho, R., Kohl, L., Pihlatie, M., Lohila, A., Mäkiranta, P., Siljanen, H., Tuittila, E.-S., Wang, J., and Koskinen, M.: CH4 transport in wetland plants under controlled environmental conditions – separating the impacts of phenology from environmental variables, Plant and Soil, 507, 671–691, https://doi.org/10.1007/s11104-024-06756-x, 2025.

Gerard, G. and Chanton, J.: Quantification of methane oxidation in the rhizosphere of emergent aquatic macrophytes: defining upper limits, Biogeochemistry, 23, 79–97, https://doi.org/10.1007/bf00000444, 1993.

https://doi.org/10.5194/egusphere-2026-467
Preprint. Discussion started: 29 January 2026

Gorham, E.: Northern peatlands: Role in the carbon cycle and probable responses to climatic warming, Ecol. Appl., 1, 182–195, https://doi.org/10.2307/1941811, 1991.

Gray, A., Levy, P. E., Cooper, M. D. A., Jones, T., Gaiawyn, J., Leeson, S. R., Ward, S. E., Dinsmore, K. J., Drewer, J., Sheppard, L. J., Ostle, N. J., Evans, C. D., Burden, A., and Zieliński, P.: Methane indicator values for peatlands: a comparison of species and functional groups, Glob. Chang. Biol., 19, 1141–1150, https://doi.org/10.1111/gcb.12120, 2013.

Greenup, A., Bradford, M., Mcnamara, N., Ineson, P., and Lee, J.: The role of Eriophorum vaginatum in CH4 flux from an ombrotrophic peatland, Plant and Soil, 227, 265–272, 2000.

Guyonnet, J. P., Cantarel, A. A. M., Simon, L., and Haichar, F. E. Z.: Root exudation rate as functional trait involved in plant nutrient-use strategy classification, Ecol. Evol., 8, 8573–8581, https://doi.org/10.1002/ece3.4383, 2018.

Hackney, C. T. and De La Cruz, A. A.: In situ decomposition of roots and rhizomes of two tidal marsh plants, Ecology, 61, 226–231, https://doi.org/10.2307/1935178, 1980.

Henneberg, A., Sorrell, B. K., and Brix, H.: Internal methane transport through Juncus effusus: experimental manipulation of morphological barriers to test above- and below-ground diffusion limitation, New Phytol., 196, 799–806, https://doi.org/10.1111/j.1469-8137.2012.04303.x, 2012.

Henneberg, A., Brix, H., and Sorrell, B. K.: The interactive effect of Juncus effusus and water table position on mesocosm methanogenesis and methane emissions, Plant Soil, 400, 45–54, https://doi.org/10.1007/s11104-015-2707-y, 2016.

Hewitt, R. E., Taylor, D. L., Genet, H., McGuire, A. D., and Mack, M. C.: Below-ground plant traits influence tundra plant acquisition of newly thawed permafrost nitrogen, J. Ecol., 107, 950–962, https://doi.org/10.1111/1365-2745.13062, 2019.

Hodgkins, S. B., Tfaily, M. M., McCalley, C. K., Logan, T. A., Crill, P. M., Saleska, S. R., Rich, V. I., and Chanton, J. P.: Changes in peat chemistry associated with permafrost thaw increase greenhouse gas production, Proc. Natl. Acad. Sci. U. S. A., 111, 5819–5824, https://doi.org/10.1073/pnas.1314641111, 2014.

Hogg, E. H.: Decay potential of hummock and hollow sphagnum peats at different depths in a Swedish raised bog, Oikos, 66, 269, https://doi.org/10.2307/3544814, 1993.

Holmes, M. E., Crill, P. M., Burnett, W. C., McCalley, C. K., Wilson, R. M., Frolking, S., Chang, K.-Y., Riley, W. J., Varner, R. K., Hodgkins, S. B., McNichol, A. P., Saleska, S. R., Rich, V. I., Chanton, J. P., IsoGenie Project Coordinators,

https://doi.org/10.5194/egusphere-2026-467
Preprint. Discussion started: 29 January 2026

and IsoGenie Field Team: Carbon accumulation, flux, and fate in stordalen mire, a permafrost peatland in transition, Global Biogeochem. Cycles, 36, https://doi.org/10.1029/2021gb007113, 2022.

Hough, M., McCabe, S., Vining, S. R., Pickering Pedersen, E., Wilson, R. M., Lawrence, R., Chang, K.-Y., Bohrer, G., IsoGenie Coordinators, Riley, W. J., Crill, P. M., Varner, R. K., Blazewicz, S. J., Dorrepaal, E., Tfaily, M. M., Saleska, S. R., and Rich, V. I.: Coupling plant litter quantity to a novel metric for litter quality explains C storage changes in a thawing permafrost peatland, Glob. Chang. Biol., 28, 950–968, https://doi.org/10.1111/gcb.15970, 2022.

Husby, C.: Biology and functional ecology of Equisetum with emphasis on the giant horsetails, Bot. Rev., 79, 147–177, https://doi.org/10.1007/s12229-012-9113-4, 2013.

Hyvönen, T., Ojala, A., Kankaala, P., and Martikainen, P. J.: Methane release from stands of water horsetail (Equisetum fluviatile) in a boreal lake, Freshw. Biol., 40, 275–284, https://doi.org/10.1046/j.1365-2427.1998.00351.x, 1998.

Iversen, C. M., Murphy, M. T., Allen, M. F., Childs, J., Eissenstat, D. M., Lilleskov, E. A., Sarjala, T. M., Sloan, V. L., and Sullivan, P. F.: Advancing the use of minirhizotrons in wetlands, Plant Soil, 352, 23–39, https://doi.org/10.1007/s11104-011-0953-1, 2012.

Iversen, C. M., Sloan, V. L., Sullivan, P. F., Euskirchen, E. S., McGuire, A. D., Norby, R. J., Walker, A. P., Warren, J. M., and Wullschleger, S. D.: The unseen iceberg: plant roots in arctic tundra, New Phytol., 205, 34–58, https://doi.org/10.1111/nph.13003, 2015.

Jackson, M. and Armstrong, W.: Formation of aerenchyma and the processes of plant ventilation in relation to soil flooding and submergence, Plant Biol. (Stuttg.), 1, 274–287, https://doi.org/10.1055/s-2007-978516, 1999.

Joabsson, A. and Christensen, T. R.: Methane emissions from wetlands and their relationship with vascular plants: an Arctic example: METHANE EMISSION and VASCULAR PLANTS, Glob. Chang. Biol., 7, 919–932, https://doi.org/10.1046/j.1354-1013.2001.00044.x, 2001.

Joabsson, A., Christensen, T. R., and Wallén, B.: Vascular plant controls on methane emissions from northern peatforming wetlands, Trends Ecol. Evol., 14, 385–388, https://doi.org/10.1016/s0169-5347(99)01649-3, 1999.

https://doi.org/10.5194/egusphere-2026-467
Preprint. Discussion started: 29 January 2026

Johansson, T., Malmer, N., Crill, P. M., Friborg, T., Åkerman, J. H., Mastepanov, M., and Christensen, T. R.: Decadal vegetation changes in a northern peatland, greenhouse gas fluxes and net radiative forcing, Glob. Chang. Biol., 12, 2352–2369, https://doi.org/10.1111/j.1365-2486.2006.01267.x, 2006.

Johnston, C. E., Ewing, S. A., Harden, J. W., Varner, R. K., Wickland, K. P., Koch, J. C., Fuller, C. C., Manies, K., and Jorgenson, M. T.: Effect of permafrost thaw on CO 2 and CH 4 exchange in a western Alaska peatland chronosequence, Environ. Res. Lett., 9, 085004, https://doi.org/10.1088/1748-9326/9/8/085004, 2014.

Jönsson, P. and Eklundh, L.: Seasonality extraction by function fitting to time-series of satellite sensor data, IEEE Trans. Geosci. Remote Sens., 40, 1824–1832, https://doi.org/10.1109/tgrs.2002.802519, 2002.

Kankaala, P. and Bergström, I.: Emission and oxidation of methane in Equisetum fluviatile stands growing on organic sediment and sand bottoms, Biogeochemistry, 67, 21–37, https://doi.org/10.1023/b:biog.0000015277.17288.7a, 2004.

Keuper, F., Dorrepaal, E., van Bodegom, P. M., van Logtestijn, R., Venhuizen, G., van Hal, J., and Aerts, R.: Experimentally increased nutrient availability at the permafrost thaw front selectively enhances biomass production of deep-rooting subarctic peatland species, Glob. Chang. Biol., 23, 4257–4266, https://doi.org/10.1111/gcb.13804, 2017.

Kichenin, E., Wardle, D. A., Peltzer, D. A., Morse, C. W., and Freschet, G. T.: Contrasting effects of plant inter- and intraspecific variation on community-level trait measures along an environmental gradient, Funct. Ecol., 27, 1254–1261, https://doi.org/10.1111/1365-2435.12116, 2013.

Knoblauch, C., Beer, C., Liebner, S., Grigoriev, M. N., and Pfeiffer, E.-M.: Methane production as key to the greenhouse gas budget of thawing permafrost, Nat. Clim. Chang., 8, 309–312, https://doi.org/10.1038/s41558-018-0095-z, 2018.

Knox, S. H., Bansal, S., McNicol, G., Schafer, K., Sturtevant, C., Ueyama, M., Valach, A. C., Baldocchi, D., Delwiche, K., Desai, A. R., Euskirchen, E., Liu, J., Lohila, A., Malhotra, A., Melling, L., Riley, W., Runkle, B. R. K., Turner, J., Vargas, R., Zhu, Q., Alto, T., Fluet-Chouinard, E., Goeckede, M., Melton, J. R., Sonnentag, O., Vesala, T., Ward, E., Zhang, Z., Feron, S., Ouyang, Z., Alekseychik, P., Aurela, M., Bohrer, G., Campbell, D. I., Chen, J., Chu, H., Dalmagro, H. J., Goodrich, J. P., Gottschalk, P., Hirano, T., Iwata, H., Jurasinski, G., Kang, M., Koebsch, F., Mammarella, I., Nilsson, M. B., Ono, K., Peichl, M., Peltola, O., Ryu, Y., Sachs, T., Sakabe, A., Sparks, J. P., Tuittila, E.-S., Vourlitis, G. L., Wong, G. X., Windham-Myers, L., Poulter, B., and Jackson, R. B.: Identifying dominant environmental predictors of freshwater wetland methane fluxes across diurnal to seasonal time scales, Glob. Chang. Biol., 27, 3582–3604, https://doi.org/10.1111/gcb.15661, 2021.

https://doi.org/10.5194/egusphere-2026-467
Preprint. Discussion started: 29 January 2026

Koelbener, A., Ström, L., Edwards, P. J., and Olde Venterink, H.: Plant species from mesotrophic wetlands cause relatively high methane emissions from peat soil, Plant Soil, 326, 147–158, https://doi.org/10.1007/s11104-009-9989-x, 2010.

Končalová, H.: Anatomical adaptations to waterlogging in roots of wetland graminoids: limitations and drawbacks, Aquat. Bot., 38, 127–134, https://doi.org/10.1016/0304-3770(90)90102-q, 1990.

Körner, C., Möhl, P., and Hiltbrunner, E.: Four ways to define the growing season, Ecol. Lett., 26, 1277–1292, https://doi.org/10.1111/ele.14260, 2023.

Kummerow, J. and Russell, M.: Seasonal root growth in the arctic tussock tundra, Oecologia, 47, 196–199, https://doi.org/10.1007/BF00346820, 1980.

Laanbroek, H. J.: Methane emission from natural wetlands: interplay between emergent macrophytes and soil microbial processes. A mini-review, Ann. Bot., 105, 141–153, https://doi.org/10.1093/aob/mcp201, 2010.

Laine, A. M., Korrensalo, A., and Tuittila, E.-S.: Plant functional traits play the second fiddle to plant functional types in explaining peatland CO2 and CH4 gas exchange, Sci. Total Environ., 834, 155352, https://doi.org/10.1016/j.scitotenv.2022.155352, 2022.

Łakomiec, P., Holst, J., Friborg, T., Crill, P., Rakos, N., Kljun, N., Olsson, P.-O., Eklundh, L., Persson, A., and Rinne, J.: Field-scale CH4 emission at a subarctic mire with heterogeneous permafrost thaw status, Biogeosciences, 18, 5811–5830, https://doi.org/10.5194/bg-18-5811-2021, 2021.

Larmola, T., Tuittila, E.-S., Tiirola, M., Nykänen, H., Martikainen, P. J., Yrjälä, K., Tuomivirta, T., and Fritze, H.: The role of Sphagnum mosses in the methane cycling of a boreal mire, Ecology, 91, 2356–2365, https://doi.org/10.1890/09-1343.1, 2010.

Lawrence, D. M., Slater, A. G., Romanovsky, V. E., and Nicolsky, D. J.: Sensitivity of a model projection of near-surface permafrost degradation to soil column depth and representation of soil organic matter, J. Geophys. Res., 113, https://doi.org/10.1029/2007jf000883, 2008.

Lê, S., Josse, J., and Husson, F.: FactoMineR: AnRPackage for Multivariate Analysis, J. Stat. Softw., 25, https://doi.org/10.18637/jss.v025.i01, 2008.

Lundin, E., Crill, P., Grudd, H., Holst, J., Kristoffersson, A., Meire, A., Molder, M., and Rakos, N.: ETC L2 Fluxnet (half-hourly) from Abisko-Stordalen Palsa Bog, 2025.

Luoto, M., Heikkinen, R. K., and Carter, T. R.: Loss of palsa mires in Europe and biological consequences, Environ. Conserv., 31, 30–37, https://doi.org/10.1017/s0376892904001018, 2004.

Määttä, T. and Malhotra, A.: The hidden roots of wetland methane emissions, Glob. Chang. Biol., 30, e17127, https://doi.org/10.1111/gcb.17127, 2024.

Määttä, T. and Malhotra, A.: Plant belowground trait and vegetation survey data from the Stordalen mire 2023, https://doi.org/10.5281/ZENODO.18269229, 2026.

Malhotra, A. and Roulet, N. T.: Environmental correlates of peatland carbon fluxes in a thawing landscape: do transitional thaw stages matter?, Biogeosciences, 12, 3119–3130, https://doi.org/10.5194/bg-12-3119-2015, 2015.

Malmer, N., Johansson, T., Olsrud, M., and Christensen, T. R.: Vegetation, climatic changes and net carbon sequestration in a North-Scandinavian subarctic mire over 30 years, Glob. Chang. Biol., 0, 051006062331004–???, https://doi.org/10.1111/j.1365-2486.2005.01042.x, 2005.

McCalley, C. K., Woodcroft, B. J., Hodgkins, S. B., Wehr, R. A., Kim, E.-H., Mondav, R., Crill, P. M., Chanton, J. P., Rich, V. I., Tyson, G. W., and Saleska, S. R.: Methane dynamics regulated by microbial community response to permafrost thaw, Nature, 514, 478–481, https://doi.org/10.1038/nature13798, 2014.

McCormack, M. L., Dickie, I. A., Eissenstat, D. M., Fahey, T. J., Fernandez, C. W., Guo, D., Helmisaari, H.-S., Hobbie, E. A., Iversen, C. M., Jackson, R. B., Leppälammi-Kujansuu, J., Norby, R. J., Phillips, R. P., Pregitzer, K. S., Pritchard, S. G., Rewald, B., and Zadworny, M.: Redefining fine roots improves understanding of below-ground contributions to terrestrial biosphere processes, New Phytol., 207, 505–518, https://doi.org/10.1111/nph.13363, 2015.

McGuire, A. D., Anderson, L. G., Christensen, T. R., Dallimore, S., Guo, L., Hayes, D. J., Heimann, M., Lorenson, T. D., Macdonald, R. W., and Roulet, N.: Sensitivity of the carbon cycle in the Arctic to climate change, Ecol. Monogr., 79, 523–555, https://doi.org/10.1890/08-2025.1, 2009.

https://doi.org/10.5194/egusphere-2026-467
Preprint. Discussion started: 29 January 2026

Merritt, D. A., Hayes, J. M., and Des Marais, D. J.: Carbon isotopic analysis of atmospheric methane by isotope-ratio-monitoring gas chromatography-mass spectrometry, J. Geophys. Res., 100, 1317–1326, https://doi.org/10.1029/94jd02689, 1995.

Metsävainio, K.: Untersuchungen über das Wurzelsystem der Moorpflanzen, Annales botanici Societatis zoologicae-botanicae Fennicae Vanamo, 1, 1–422, 1931.

Mondav, R., Woodcroft, B. J., Kim, E.-H., McCalley, C. K., Hodgkins, S. B., Crill, P. M., Chanton, J., Hurst, G. B., VerBerkmoes, N. C., Saleska, S. R., Hugenholtz, P., Rich, V. I., and Tyson, G. W.: Discovery of a novel methanogen prevalent in thawing permafrost, Nat. Commun., 5, 3212, https://doi.org/10.1038/ncomms4212, 2014.

Moor, H., Rydin, H., Hylander, K., Nilsson, M. B., Lindborg, R., and Norberg, J.: Towards a trait-based ecology of wetland vegetation, J. Ecol., 105, 1623–1635, https://doi.org/10.1111/1365-2745.12734, 2017.

Noyce, G. L., Varner, R. K., Bubier, J. L., and Frolking, S.: Effect ofCarex rostrataon seasonal and interannual variability in peatland methane emissions, J. Geophys. Res. Biogeosci., 119, 24–34, https://doi.org/10.1002/2013jg002474, 2014.

Noyce, G. L., Smith, A. J., Kirwan, M. L., Rich, R. L., and Megonigal, J. P.: Oxygen priming induced by elevated CO2 reduces carbon accumulation and methane emissions in coastal wetlands, Nat. Geosci., 16, 63–68, https://doi.org/10.1038/s41561-022-01070-6, 2023.

Oksanen, J., Simpson, G., Blanchet, F., Kindt, R., Legendre, P., Minchin, P., O'hara, R., Solymos, P., Stevens, M., Szoecs, E., Wagner, H., Barbour, M., Bedward, M., Bolker, B., Borcard, D., Carvalho, G., Chirico, M., De Caceres, M., Durand, S., Evangelista, H., Fitzjohn, R., Friendly, M., Furneaux, B., Hannigan, G., Hill, M., Lahti, L., Mcglinn, D., Ouellette, M., Ribeiro, C. E., Smith, T., Stier, A., Ter Braak, C., and Weedon, J.: _vegan: Community Ecology Package_, 2025.

Olefeldt, D., Turetsky, M. R., Crill, P. M., and McGuire, A. D.: Environmental and physical controls on northern terrestrial methane emissions across permafrost zones, Glob. Chang. Biol., 19, 589–603, https://doi.org/10.1111/gcb.12071, 2013.

Olvmo, M., Holmer, B., Thorsson, S., Reese, H., and Lindberg, F.: Sub-arctic palsa degradation and the role of climatic drivers in the largest coherent palsa mire complex in Sweden (Vissátvuopmi), 1955–2016, Sci. Rep., 10, 8937, https://doi.org/10.1038/s41598-020-65719-1, 2020.

https://doi.org/10.5194/egusphere-2026-467
Preprint. Discussion started: 29 January 2026

Öquist, M. G. and Svensson, B. H.: Vascular plants as regulators of methane emissions from a subarctic mire ecosystem, Journal of Geophysical Research: Atmospheres, 107, ACL 10–1–ACL 10–10, https://doi.org/10.1029/2001JD001030, 2002.

Ouyang, W., Mueller, F., Hjelmare, M., Lundberg, E., and Zimmer, C.: ImJoy: an open-source computational platform for the deep learning era, Nat. Methods, 16, 1199–1200, https://doi.org/10.1038/s41592-019-0627-0, 2019.

Palace, M., Herrick, C., DelGreco, J., Finnell, D., Garnello, A. J., McCalley, C., McArthur, K., Sullivan, F., and Varner, R. K.: Determining subarctic peatland vegetation using an unmanned aerial system (UAS), Remote Sens. (Basel), 10, 1498, https://doi.org/10.3390/rs10091498, 2018.

Palace, M., Varner, R., Crill, P. M., Frolking, S., McCalley, C. K., Burke, S. A., Chanton, J. P., Holmes, M. E., IsoGenie Project Coordinators, and Saleska, S.: Stordalen Mire ground cover classifications, based on 2014 WorldView-2 satellite imagery 0145_Wv2-2014_GroundCoverClassifications (0.0.0), 2022.

Pan, Y., Cieraad, E., and van Bodegom, P. M.: Are ecophysiological adaptive traits decoupled from leaf economics traits in wetlands?, Funct. Ecol., 33, 1202–1210, https://doi.org/10.1111/1365-2435.13329, 2019.

Pastorello, G., Trotta, C., Canfora, E., Chu, H., Christianson, D., Cheah, Y.-W., Poindexter, C., Chen, J., Elbashandy, A., Humphrey, M., Isaac, P., Polidori, D., Reichstein, M., Ribeca, A., van Ingen, C., Vuichard, N., Zhang, L., Amiro, B., Ammann, C., Arain, M. A., Ardö, J., Arkebauer, T., Arndt, S. K., Arriga, N., Aubinet, M., Aurela, M., Baldocchi, D., Barr, A., Beamesderfer, E., Marchesini, L. B., Bergeron, O., Beringer, J., Bernhofer, C., Berveiller, D., Billesbach, D., Black, T. A., Blanken, P. D., Bohrer, G., Boike, J., Bolstad, P. V., Bonal, D., Bonnefond, J.-M., Bowling, D. R., Bracho, R., Brodeur, J., Brümmer, C., Buchmann, N., Burban, B., Burns, S. P., Buysse, P., Cale, P., Cavagna, M., Cellier, P., Chen, S., Chini, I., Christensen, T. R., Cleverly, J., Collalti, A., Consalvo, C., Cook, B. D., Cook, D., Coursolle, C., Cremonese, E., Curtis, P. S., D'Andrea, E., da Rocha, H., Dai, X., Davis, K. J., Cinti, B. D., Grandcourt, A. de, Ligne, A. D., De Oliveira, R. C., Delpierre, N., Desai, A. R., Di Bella, C. M., Tommasi, P. di, Dolman, H., Domingo, F., Dong, G., Dore, S., Duce, P., Dufrêne, E., Dunn, A., Dušek, J., Eamus, D., Eichelmann, U., ElKhidir, H. A. M., Eugster, W., Ewenz, C. M., Ewers, B., Famulari, D., Fares, S., Feigenwinter, I., Feitz, A., Fensholt, R., Filippa, G., Fischer, M., Frank, J., Galvagno, M., et al.: The FLUXNET2015 dataset and the ONEFlux processing pipeline for eddy covariance data, Sci. Data, 7, 225, https://doi.org/10.1038/s41597-020-0534-3, 2020.

Perryman, C. R., McCalley, C. K., Malhotra, A., Fahnestock, M. F., Kashi, N. N., Bryce, J. G., Giesler, R., and Varner, R. K.: Thaw transitions and redox conditions drive methane oxidation in a permafrost peatland, J. Geophys. Res. Biogeosci., 125, https://doi.org/10.1029/2019jg005526, 2020.

Phillips, R. P., Erlitz, Y., Bier, R., and Bernhardt, E. S.: New approach for capturing soluble root exudates in forest soils, Funct. Ecol., 22, 990–999, https://doi.org/10.1111/j.1365-2435.2008.01495.x, 2008.

Picon-Cochard, C., Pilon, R., Tarroux, E., Pagès, L., Robertson, J., and Dawson, L.: Effect of species, root branching order and season on the root traits of 13 perennial grass species, Plant Soil, 353, 47–57, https://doi.org/10.1007/s11104-011-1007-4, 2012.

Pinheiro, J. and Bates, D. M.: Mixed-effects models in S and S-PLUS, 1st ed., Springer, New York, NY, 528 pp., https://doi.org/10.1007/b98882, 2000.

Pinheiro J, Bates D, R Core Team: nlme: Linear and Nonlinear Mixed Effects Models, 2023.

Polarforskningssekretariatet and SMHI: Abisko Aut (ID 188790) Lufttemperatur (dygn) 1985-2025, 2025a.

Polarforskningssekretariatet and SMHI: Abisko Aut (ID 188790) Nederbördsmängd (dygn) 1985-2025, 2025b.

Purnobasuki, H. and Suzuki, M.: Aerenchyma formation and porosity in root of a mangrove plant, Sonneratia alba (Lythraceae), J. Plant Res., 117, 465–472, https://doi.org/10.1007/s10265-004-0181-3, 2004.

Putkinen, A., Larmola, T., Tuomivirta, T., Siljanen, H. M., Bodrossy, L., Tuittila, E.-S., and Fritze, H.: Peatland succession induces a shift in the community composition of Sphagnum-associated active methanotrophs, FEMS Microbiology Ecology, 88, 596–611, https://doi.org/10.1111/1574-6941.12327, 2014.

Raghoebarsing, A. A., Smolders, A. J. P., Schmid, M. C., Rijpstra, W. I. C., Wolters-Arts, M., Derksen, J., Jetten, M. S. M., Schouten, S., Sinninghe Damsté, J. S., Lamers, L. P. M., Roelofs, J. G. M., Op den Camp, H. J. M., and Strous, M.: Methanotrophic symbionts provide carbon for photosynthesis in peat bogs, Nature, 436, 1153–1156, https://doi.org/10.1038/nature03802, 2005.

Raivonen, M., Smolander, S., Backman, L., Susiluoto, J., Aalto, T., Markkanen, T., Mäkelä, J., Rinne, J., Peltola, O., Aurela, M., Lohila, A., Tomasic, M., Li, X., Larmola, T., Juutinen, S., Tuittila, E.-S., Heimann, M., Sevanto, S., Kleinen, T., Brovkin, V., and Vesala, T.: HIMMELI v1.0: HelsinkI Model of MEthane buiLd-up and emIssion for peatlands, Geosci. Model Dev., 10, 4665–4691, https://doi.org/10.5194/gmd-10-4665-2017, 2017.

https://doi.org/10.5194/egusphere-2026-467
Preprint. Discussion started: 29 January 2026

R Core Team: R: A Language and Environment for Statistical Computing. R Foundation for Statistical Computing, Vienna, Austria, 2024.

R Core Team: R: A Language and Environment for Statistical Computing, Vienna, Austria, 2025.

Reich, P. B., Walters, M. B., and Ellsworth, D. S.: From tropics to tundra: global convergence in plant functioning, Proc. Natl. Acad. Sci. U. S. A., 94, 13730–13734, https://doi.org/10.1073/pnas.94.25.13730, 1997.

Riutta, T., Laine, J., Aurela, M., Rinne, J., Vesala, T., Laurila, T., Haapanala, S., Pihlatie, M., and Tuittila, E.-S.: Spatial variation in plant community functions regulates carbon gas dynamics in a boreal fen ecosystem, Tellus B Chem. Phys. Meteorol., 59, 838, https://doi.org/10.1111/j.1600-0889.2007.00302.x, 2007.

Rose, L.: Pitfalls in root trait calculations: How ignoring diameter heterogeneity can lead to overestimation of functional traits, Front. Plant Sci., 8, 898, https://doi.org/10.3389/fpls.2017.00898, 2017.

Saarnio, S., Wittenmayer, L., and Merbach, W.: Rhizospheric exudation of Eriophorum vaginatum L. — Potential link to methanogenesis, Plant Soil, 267, 343–355, https://doi.org/10.1007/s11104-005-0140-3, 2004.

Schaefer, K., Lantuit, H., Romanovsky, V. E., Schuur, E. A. G., and Witt, R.: The impact of the permafrost carbon feedback on global climate, Environ. Res. Lett., 9, 085003, https://doi.org/10.1088/1748-9326/9/8/085003, 2014.

Scheffer, R. A. and Aerts, R.: Root decomposition and soil nutrient and carbon cycling in two temperate fen ecosystems, Oikos, 91, 541–549, https://doi.org/10.1034/j.1600-0706.2000.910316.x, 2000.

Schimel, J. P.: Plant transport and methane production as controls on methane flux from arctic wet meadow tundra, Biogeochemistry, 28, 183–200, https://doi.org/10.1007/BF02186458, 1995.

Schneider, C. A., Rasband, W. S., and Eliceiri, K. W.: NIH Image to ImageJ: 25 years of image analysis, Nat. Methods, 9, 671–675, https://doi.org/10.1038/nmeth.2089, 2012.

Schuur, E. A. G., Bockheim, J., Canadell, J. G., Euskirchen, E., Field, C. B., Goryachkin, S. V., Hagemann, S., Kuhry, P., Lafleur, P. M., Lee, H., Mazhitova, G., Nelson, F. E., Rinke, A., Romanovsky, V. E., Shiklomanov, N., Tarnocai, C., Venevsky, S., Vogel, J. G., and Zimov, S. A.: Vulnerability of permafrost carbon to climate change: Implications for the global carbon cycle, Bioscience, 58, 701–714, https://doi.org/10.1641/b580807, 2008.

https://doi.org/10.5194/egusphere-2026-467
Preprint. Discussion started: 29 January 2026

Shaver, G. R.: Ecology of roots and rhizomes in graminoid plants of the Alaskan coastal tundra, PhD thesis, Duke University, Durham, NC, USA, 1976.

Shaver, G. R. and Billings, W. D.: Root production and root turnover in a wet tundra ecosystem, barrow, Alaska, Ecology, 56, 401–409, https://doi.org/10.2307/1934970, 1975.

Shaver, G. R. and Billings, W. D.: Effects of daylength and temperature on root elongation in tundra graminoids, Oecologia, 28, 57–65, https://doi.org/10.1007/BF00346836, 1977.

Singleton, C. M., McCalley, C. K., Woodcroft, B. J., Boyd, J. A., Evans, P. N., Hodgkins, S. B., Chanton, J. P., Frolking, S., Crill, P. M., Saleska, S. R., Rich, V. I., and Tyson, G. W.: Methanotrophy across a natural permafrost thaw environment, ISME J., 12, 2544–2558, https://doi.org/10.1038/s41396-018-0065-5, 2018.

Smirnoff, N. and Crawford, R. M. M.: Variation in the structure and response to flooding of root aerenchyma in some wetland plants, Ann. Bot., 51, 237–249, https://doi.org/10.1093/oxfordjournals.aob.a086462, 1983.

Smith, B., Prentice, C., and Sykes, M. T.: Representation of vegetation dynamics in the modelling of terrestrial ecosystems: comparing two contrasting approaches within European climate space, Global Ecol. Biogeogr., 10, 621–637, https://doi.org/10.1046/j.1466-822X.2001.t01-1-00256.x, 2001.

Smith, B., Wårlind, D., Arneth, A., Hickler, T., Leadley, P., Siltberg, J., and Zaehle, S.: Implications of incorporating N cycling and N limitations on primary production in an individual-based dynamic vegetation model, Biogeosciences, 11, 2027–2054, https://doi.org/10.5194/bg-11-2027-2014, 2014.

Ström, L. and Christensen, T. R.: Below ground carbon turnover and greenhouse gas exchanges in a sub-arctic wetland, Soil Biol. Biochem., 39, 1689–1698, https://doi.org/10.1016/j.soilbio.2007.01.019, 2007.

Ström, L., Ekberg, A., Mastepanov, M., and Røjle Christensen, T.: The effect of vascular plants on carbon turnover and methane emissions from a tundra wetland, Glob. Chang. Biol., 9, 1185–1192, https://doi.org/10.1046/j.1365-2486.2003.00655.x, 2003.

Ström, L., Mastepanov, M., and Christensen, T. R.: Species-specific Effects of Vascular Plants on Carbon Turnover and Methane Emissions from Wetlands, Biogeochemistry, 75, 65–82, https://doi.org/10.1007/s10533-004-6124-1, 2005.

https://doi.org/10.5194/egusphere-2026-467
Preprint. Discussion started: 29 January 2026

Ström, L., Tagesson, T., Mastepanov, M., and Christensen, T. R.: Presence of Eriophorum scheuchzeri enhances substrate availability and methane emission in an Arctic wetland, Soil Biol. Biochem., 45, 61–70, https://doi.org/10.1016/j.soilbio.2011.09.005, 2012.

Swindles, G. T., Morris, P. J., Mullan, D., Watson, E. J., Turner, T. E., Roland, T. P., Amesbury, M. J., Kokfelt, U., Schoning, K., Pratte, S., Gallego-Sala, A., Charman, D. J., Sanderson, N., Garneau, M., Carrivick, J. L., Woulds, C., Holden, J., Parry, L., and Galloway, J. M.: The long-term fate of permafrost peatlands under rapid climate warming, Sci. Rep., 5, 17951, https://doi.org/10.1038/srep17951, 2015.

Turetsky, M. R., Kotowska, A., Bubier, J., Dise, N. B., Crill, P., Hornibrook, E. R. C., Minkkinen, K., Moore, T. R., Myers-Smith, I. H., Nykänen, H., Olefeldt, D., Rinne, J., Saarnio, S., Shurpali, N., Tuittila, E.-S., Waddington, J. M., White, J. R., Wickland, K. P., and Wilmking, M.: A synthesis of methane emissions from 71 northern, temperate, and subtropical wetlands, Glob. Chang. Biol., 20, 2183–2197, https://doi.org/10.1111/gcb.12580, 2014.

Vahsen, M. L., Blum, M. J., Megonigal, J. P., Emrich, S. J., Holmquist, J. R., Stiller, B., Todd-Brown, K. E. O., and McLachlan, J. S.: Rapid plant trait evolution can alter coastal wetland resilience to sea level rise, Science, 379, 393–398, https://doi.org/10.1126/science.abq0595, 2023.

Varner, R. K., Crill, P. M., Frolking, S., McCalley, C. K., Burke, S. A., Chanton, J. P., Holmes, M. E., Isogenie Project Coordinators, Saleska, S., and Palace, M. W.: Permafrost thaw driven changes in hydrology and vegetation cover increase trace gas emissions and climate forcing in Stordalen Mire from 1970 to 2014, Philos. Trans. A Math. Phys. Eng. Sci., 380, 20210022, https://doi.org/10.1098/rsta.2021.0022, 2022.

Violle, C., Reich, P. B., Pacala, S. W., Enquist, B. J., and Kattge, J.: The emergence and promise of functional biogeography, Proc. Natl. Acad. Sci. U. S. A., 111, 13690–13696, https://doi.org/10.1073/pnas.1415442111, 2014.

Visser, E. J. W., Bögemann, G. M., VAN DE Steeg, H. M., Pierik, R., and Blom, C. W. P. M.: Flooding tolerance of Carex species in relation to field distribution and aerenchyma formation: RESEARCH Flooding tolerance of Carex species, New Phytol., 148, 93–103, https://doi.org/10.1046/j.1469-8137.2000.00742.x, 2000.

Vroom, R. J. E., van den Berg, M., Pangala, S. R., van der Scheer, O. E., and Sorrell, B. K.: Physiological processes affecting methane transport by wetland vegetation – A review, Aquat. Bot., 182, 103547, https://doi.org/10.1016/j.aquabot.2022.103547, 2022.

https://doi.org/10.5194/egusphere-2026-467
Preprint. Discussion started: 29 January 2026

Waldo, N. B., Hunt, B. K., Fadely, E. C., Moran, J. J., and Neumann, R. B.: Plant root exudates increase methane emissions through direct and indirect pathways, Biogeochemistry, 145, 213–234, https://doi.org/10.1007/s10533-019-00600-6, 2019.

Wallén, B.: Above and below ground dry mass of the three main vascular plants on hummocks on a subarctic peat bog, Oikos, 46, 51, https://doi.org/10.2307/3565379, 1986.

Wang, P., Mommer, L., van Ruijven, J., Berendse, F., Maximov, T. C., and Heijmans, M. M. P. D.: Seasonal changes and vertical distribution of root standing biomass of graminoids and shrubs at a Siberian tundra site, Plant Soil, 407, 55–65, https://doi.org/10.1007/s11104-016-2858-5, 2016.

Wen, Z., White, P. J., Shen, J., and Lambers, H.: Linking root exudation to belowground economic traits for resource acquisition, New Phytol., 233, 1620–1635, https://doi.org/10.1111/nph.17854, 2022.

Whiting, G. J. and Chanton, J. P.: Primary production control of methane emission from wetlands, Nature, 364, 794–795, https://doi.org/10.1038/364794a0, 1993.

Wilson, D., Alm, J., Riutta, T., Laine, J., Byrne, K. A., Farrell, E. P., and Tuittila, E.-S.: A high resolution green area index for modelling the seasonal dynamics of CO2 exchange in peatland vascular plant communities, Plant Ecol., 190, 37–51, https://doi.org/10.1007/s11258-006-9189-1, 2007.

Wilson, R., Bosman, S., and Chanton, J.: CH_4 and DIC concentrations and $\delta^{13}C$ from porewater at Stordalen Mire, July 2023, Zenodo, https://doi.org/10.5281/zenodo.18363867, 2026.

Wilson, R. M., Hough, M. A., Verbeke, B. A., Hodgkins, S. B., IsoGenie Coordinators, Chanton, J. P., Saleska, S. D., Rich, V. I., and Tfaily, M. M.: Plant organic matter inputs exert a strong control on soil organic matter decomposition in a thawing permafrost peatland, Sci. Total Environ., 820, 152757, https://doi.org/10.1016/j.scitotenv.2021.152757, 2022.

Wood, S. N.: Fast stable restricted maximum likelihood and marginal likelihood estimation of semiparametric generalized linear models, J. R. Stat. Soc. Series B Stat. Methodol., 73, 3–36, https://doi.org/10.1111/j.1467-9868.2010.00749.x, 2011.

Wood, S. N.: Generalized additive models: An introduction with R, Chapman and Hall/CRC, https://doi.org/10.1201/9781315370279, 2017.

https://doi.org/10.5194/egusphere-2026-467
Preprint. Discussion started: 29 January 2026

Ye, Z. and Ryser, P.: Root porosity contributes to root trait space of wetland monocotyledons independently of economics traits, Plant Soil, 471, 301–314, https://doi.org/10.1007/s11104-021-05186-3, 2022.

Zhuang, Q., Melillo, J. M., Kicklighter, D. W., Prinn, R. G., McGuire, A. D., Steudler, P. A., Felzer, B. S., and Hu, S.: Methane fluxes between terrestrial ecosystems and the atmosphere at northern high latitudes during the past century: A retrospective analysis with a process-based biogeochemistry model, Global Biogeochem. Cycles, 18, https://doi.org/10.1029/2004gb002239, 2004.